
Version 7.0
April 2019

STIS Data Handbook



STScI | SPACE TELESCOPE
SCIENCE INSTITUTE

3700 San Martin Drive
Baltimore, Maryland 21218
help@stsci.edu

STIS Data Handbook

Version 7.0 - April 2019

[PDF version](#)

Space Telescope Imaging Spectrograph Data Handbook

Table of Contents

[Expand all](#) [Collapse all](#)

User Support

Please contact the HST Help Desk for assistance. We encourage users to access the new web portal where you can submit your questions directly to the appropriate team of experts.

- **Website:** <http://hsthhelp.stsci.edu>
- **E-mail:** help@stsci.edu

Additional Resources

Information and other resources are available on the STIS website:

- <http://www.stsci.edu/hst/instrumentation/stis>

Revision History

| Version | Date | Editor |
|----------------|---------------|---|
| 7.0 | April 2019 | S. Tony Sohn |
| 6.0 | May 2011 | K. Azalee Bostroem and Charles Proffitt |
| 5.0 | July 2007 | Linda Dressel, Sherie Holfeltz & Jessica Kim Quijano |
| 4.0 | January 2002 | Thomas M. Brown, STIS Editor Bahram Mobasher, Chief Editor |
| 3.1 | March 1998 | Tony Keyes |
| 3.0, Vol. II | October 1997 | Tony Keyes |
| 3.0, Vol. I | October 1997 | Mark Voit |
| 2.0 | December 1995 | Claus Leitherer |
| 1.0 | February 1994 | Stefi Baum |

Contributors

This document is written and maintained by the STIS Team in the Instruments Division of STScI with the assistance of associates in the Operations and Engineering Division. Contributions to the current edition were made by D. Branton, J. Carlberg, J. H. Debes, S. E. Deustua, S. Lockwood, M. Maclay, T. R. Monroe, A. Riley, P. G. Sonnentrucker, and D. E. Welty.

Citation

In publications, refer to this document as:


- Sohn, S. T., et al., 2019, “STIS Data Handbook”, Version 7.0, (Baltimore: STScI).

| | |
|--|-----|
| Preface | 2 |
| Handbook Structure | 3 |
| Typographic Conventions | 4 |
| Chapter 1: STIS Overview | 5 |
| 1.1 Instrument Capabilities and Design | 6 |
| 1.2 Basic Instrument Operations | 16 |
| 1.3 STIS Operations on Side-2 | 19 |
| 1.4 Failure of Side-2 | 21 |
| 1.5 STIS Closeout | 22 |
| 1.6 Post Servicing Mission 4 Operation | 24 |
| 1.7 STIS Operations and Calibration Timeline | 25 |
| Chapter 2: STIS Data Structure | 29 |
| 2.1 STIS Overview | 30 |
| 2.2 Types of STIS Files | 31 |
| 2.3 STIS File Structures | 38 |
| 2.4 Headers, Keywords, and Relationship to Phase II | 48 |
| 2.5 Error and Data Quality Array | 60 |
| 2.6 STIS Coordinate Systems | 63 |
| Chapter 3: STIS Calibration | 66 |
| 3.1 Pipeline Processing Overview | 67 |
| 3.2 Structure of calstis | 70 |
| 3.3 Data Flow Through calstis | 80 |
| 3.4 Descriptions of Calibration Steps | 88 |
| 3.5 Recalibration of STIS Data | 120 |
| 3.6 Updates to calstis | 132 |
| Chapter 4: STIS Error Sources | 133 |
| 4.1 Error Sources Associated with Pipeline Calibration Steps | 134 |
| 4.2 Summary of Accuracies | 148 |
| 4.3 Factors Limiting Flux and Wavelength Accuracy | 152 |
| Chapter 5: STIS Data Analysis | 156 |
| 5.1 Data Reduction and Analysis Applications | 157 |
| 5.2 Evaluating Target Acquisitions and Guiding | 162 |
| 5.3 Working with Imaging Data | 174 |
| 5.4 Working with Spectral Images | 176 |
| 5.5 Working with Extracted Spectra | 185 |
| 5.6 Working with TIME-TAG Data | 198 |

Preface

How to Use this Handbook

This handbook describes data from the Space Telescope Imaging Spectrograph (STIS) onboard the Hubble Space Telescope (*HST*), and how to manipulate, calibrate, and analyze those data. The current version of the *STIS Data Handbook* is presented as an independent and self-contained document, extensively built on the contents of version 6 of the *HST Data Handbook*. Users are referred to a companion volume, *Introduction to the HST Data Handbooks*, for more general information about the details of acquiring data from the *HST* archive, *HST* file formats, and general purpose software for displaying and processing *HST* data. For detailed information on the capabilities of the instrument, and how to plan observations, users should refer to the *STIS Instrument Handbook*. For further information and timely updates, users should consult the STIS web page (<http://www.stsci.edu/hst/instrumentation/stis>), and the [Document Archive link](#). In particular, the [STScI Analysis Newsletters](#) (STANs) highlight changes in code and calibration procedures and provide other instrument-related news. The [Instrument Science Reports](#) (ISRs) present in-depth characterizations of the instrument and detailed explanations of calibration code and procedures.

 *STSDAS and PyRAF are soon to be deprecated, and are now only recommended/supported where necessary. Most of the data processing described herein now uses Python available via the STScI [AstroConda channel website](#).*

Handbook Structure

The STIS Data Handbook is organized in five chapters, which discuss the following topics:

- [Chapter 1: STIS Overview](#) provides a brief overview of the instrument and its operational capabilities, and a summary of important changes in the state of the instrument and in the data archive. If you are not already familiar with the details of STIS, you should begin here.
- [Chapter 2: STIS Data Structure](#) describes the contents of STIS data files, the meanings of selected header keywords, and the relationship of the data products to the original Phase II proposal. If you are not familiar with the filenames, header keywords, or contents of the data files from STIS, you should read this chapter next.
- [Chapter 3: STIS Calibration](#) describes how the calibration pipeline processes your observation, how to determine if your data files need recalibration, and how to perform basic recalibration. If you are not familiar with the important characteristics of STIS data and the standard procedures for reducing them, or do not know how your data have been calibrated, you should read this chapter.
- [Chapter 4: STIS Error Sources](#) describes the sources of uncertainty and limiting accuracies of STIS data, with new in-depth discussions of instrumental phenomena and the creation of reference files that characterize those phenomena. STIS observers should read this chapter to acquaint themselves with the limitations of the data that remain after pipeline calibration.
- [Chapter 5: STIS Data Analysis](#) discusses software tools that can be applied to specific types of data and data formats, how to analyze target acquisitions and guide star tracking, and detailed instructions on how to work with imaging data, spectral images, extracted spectra, and TIME-TAG data. Many users will find this chapter useful when determining how they should reduce and analyze their data.

There are some important pieces of general information about *HST* data, the *HST* Archive, and the **IRAF** and **STSDAS** analysis software that are not specific to the STIS, and which are therefore not discussed here in the *STIS Data Handbook*. We refer the reader to the most recent version of the companion [Introduction to the HST Data Handbooks](#) for this information. Additional help with *HST* data is always available at STScI Help Desk at hsthhelp.stsci.edu.

Readers are advised to consult the STIS web pages (<http://www.stsci.edu/hst/instrumentation/stis>) for the latest news and updates on STIS performance.

Typographic Conventions

To help you understand the material in this Data Handbook, we will use a few consistent typographic conventions.


Visual Cues

The following typographic cues are used:

- **bold words** identify a **Python** library or function
- `typewriter-like` words identify a file name, system command, or response that is typed or displayed.
- *italic type* indicates a new term, an important point, a mathematical -variable, or a task parameter.
- SMALL CAPS identifies a header keyword.
- ALL CAPS identifies a table column.

Comments

Occasional side comments point out three types of information, each identified by an icon in the left margin.

 *Warning: You could corrupt data, produce incorrect results, or create some other kind of severe problem.*

 *Heads Up: Here is something that is often done incorrectly or that is not -obvious.*

 *Tip: No problems... just another way to do something or a suggestion that might make your life easier.*

 *Information especially likely to be updated on the STIS Web site is indicated by this symbol.*

Chapter 1: STIS Overview

1.1 Instrument Capabilities and Design

1.1.1 The STIS Detectors

1.1.2 STIS Physical Configuration

The [Space Telescope Imaging Spectrograph](#) (STIS) was built by Ball Aerospace Corporation for the NASA's Goddard Space Flight Center (GSFC) Laboratory for Astronomy and Solar Physics, under the direction of Bruce Woodgate, the Principal Investigator (PI). STIS performed very well upon its installation during the second *HST* servicing mission in February 1997. A basic description of the instrument and of its on-orbit performance through the first Servicing Mission Observatory Verification (SMOV) program is provided by Kimble et al. (1998, *ApJL*, 492, L83). We encourage all STIS users to reference this paper. The Early Release Observations are also presented in this special ApJ Letters issue.

STIS is a versatile instrument providing two-dimensional imaging and spectroscopic capabilities with three detectors operating from the ultraviolet to the near-infrared. The optics and detectors were designed to exploit the high spatial resolution of the *HST*. STIS has first-order gratings, designed for spatially resolved long slit spectroscopy over its entire spectral range, and echelle gratings, available only in the ultraviolet, that maximize the wavelength range covered in a single spectral observation of a point source. The STIS Flight Software supports on-board target acquisitions and peakups to center science targets on slits and coronagraphic bars.

STIS can be used to obtain:

- Spatially resolved, long slit or slitless spectroscopy from 1150–10300 Å at low to medium spectral resolution (R ~ 500–17000) in first order.
- Echelle spectroscopy at medium to high spectral resolution (R ~ 30000–110000), covering a broad instantaneous spectral range (~ 800 or 200 Å, respectively) in the ultraviolet (1150–3100 Å).

In addition to these two prime capabilities, STIS also provides:

- Modest imaging capability using: the solar-blind CsI far-ultraviolet Multi-Anode Micro-channel Array (MAMA) detector (1150–1700 Å); the solar-insensitive Cs₂Te near-ultraviolet MAMA

detector (1650–3100 Å); and the optical CCD (2000–11000 Å) through a small complement of narrow- and broad-band filters.

- Objective prism spectroscopy ($R \sim 500\text{--}10$) in the vacuum ultraviolet (1200–3100 Å).
- High time resolution ($t = 125$ microseconds) imaging and spectroscopy in the ultraviolet (1150–3100 Å) and moderate time resolution ($t \sim 20$ -seconds) CCD imaging and spectroscopy in the optical and near IR (2000–10300 Å).
- Coronagraphic imaging in the optical and near IR (2000–10300 Å), and bar-occulted spectroscopy over the entire spectral range (1150-10300 Å).

A complete list of gratings and filters are given in [Table 1.1](#) and [Table 1.2](#), respectively, with references to the *STIS Instrument Handbook* for more details.

Table 1.1: STIS Spectroscopic Capabilities; for more information, refer to [Section 13.3](#) of the *STIS Instrument Handbook*.

| Grating | Spectral Range (Å) | | Spectral Resolution | | No. Prime Tilts ² | Detector | Recommended Slits (apertures) ^{3,4,5,6,7,8,9,10} |
|--------------------------------------|--------------------|----------|---------------------|-----------------------------------|------------------------------|----------|--|
| | Complete | Per Tilt | Scale (Å per pixel) | Resolving Power ¹ (/2) | | | |
| <i>MAMA First-Order Spectroscopy</i> | | | | | | | |
| G140L | 1150–1730 | 590 | 0.60 | 960–1440 | 1 | FUV-MAMA | 52X0.05D1 , 52X0.1D1 |
| G140M | 1140–1740 | 55 | 0.05 | 11,400–17,400 | 12 | FUV-MAMA | 52X0.2D1 , 52X0.5D1 52X2D1 , 25MAMAD1 F25SRF2D1 , F25QTZD1 |
| | | | | | | | 52X0.05 52X0. |

| | | | | | | | | | |
|-------------------------------------|----------------------------|-------------|--------------|-----------------------|--------|------------|--|------------------------------|---|
| G230L | 1570–3180 | 1616 | 1.58 | 500–1010 | 1 | NUV-MAMA | | | 1 52X0. |
| G230M | 1640–3100 | 90 | 0.09 | 9110–17,220 | 18 | NUV-MAMA | | | 2 52X0. 5 52X2 52X0. 2F1 |
| CCD First-Order Spectroscopy | | | | | | | | | |
| G230LB | 1680–3060 | 1380 | 1.35 | 620–1130 | 1 | CCD | | 52X0. 05E1 | 0.2 X0.2 |
| G230MB | 1640–3190 | 156 | 0.15 | 5470–10,630 | 11 | CCD | | 52X0. 1E1 52X0. 2E1 | |
| G430L | 2900–5700 | 2800 | 2.73 | 530–1040 | 1 | CCD | | 52X0. 5E1 | |
| G430M | 3020–5610 | 286 | 0.28 | 5390–10,020 | 10 | CCD | | 52X2E1 | |
| G750L G750M | 5240-10,270 5450-10,140 | 5030 572 | 4.92 0.56 | 530-1040 4870-9050 | 1 9 | CCD CCD | 52X0. 2E2 52X0. 5E2 52X2E2 | | |
| MAMA Echelle Spectroscopy | | | | | | | | | |
| E140M | 1144–1710 | 567 | /91, 700 | 45,800 | 1 | FUV-MAMA | 0.2X0.2, 0.2 X0.06 | | |
| E140H | 1140–1700 | 210 | /228, 000 | 114,000 ¹¹ | 3 | FUV-MAMA | 0.2X0.2, 0.2 X0.09 | | |
| E230M | 1605–3110 | 800 | /60, 000 | 30,000 | 2 | NUV-MAMA | 0.2X0.2, 0.2 X0.06 | | |

| | | | | | | | | |
|---------------------------------------|---------------|------|--------------|-----------------------|---|--------------|---|--|
| E230H | 1620– 3150 | 267 | /228, 000 | 114,000 ¹² | 6 | NUV- MAMA | 0.2X0.2, 0.2 X0.09 | |
| <i>MAMA Prism Spectroscopy</i> | | | | | | | | |
| PRISM | 1150– 3620 | 2470 | 0.2 - 72 | 10-2500 | 1 | NUV- MAMA | 25MAMA, 52X0.05, 52X0. 1, 52X0.2, 52X0.5, 52X2 | |

¹ See "Line Spread Functions in [Section 13.6](#) of the *STIS Instrument Handbook* for detailed estimates.

² Number of exposures at distinct tilts needed to cover spectral range of grating with 10% wavelength overlap between adjacent settings.

³ For a complete list of supported and available-but-unsupported apertures for each grating, see [Appendix A](#) of the *STIS Instrument Handbook*.

⁴ Naming convention gives dimensions of slit in arcseconds. E.g., 52X0.1 indicates the slit is 52 arcsec long perpendicular to the dispersion direction and 0.1 arcsec wide in the dispersion direction. The F (e.g., in 52X0.2F1) indicates a fiducial bar to be used for coronagraphic spectroscopy.

⁵ For MAMA first-order modes, only ~ 25 arcsec of a long slit's length projects on the detector. (See also [Section 4.2.2](#) in the *STIS Instrument Handbook*.)

⁶ Full-aperture clear (50CCD or 25MAMA), longpass-filtered (F25QTZ or F25SRF2 in UV), and neutral-density-filtered slitless spectroscopy are also supported with the appropriate first-order and echelle gratings, as well as the PRISM.

⁷ The following slits are also supported for all echelle gratings. The 6X0.2 and 52X0.05 long slits are intended for use with extended emission line objects; order overlap must be considered when using these slits. Also the high S/N multi-slits 0.2X0.2FP(A-E) and 0.2X0.06FP(A-E) (see Chapter 12), the very narrow 0.1X0.03 slit for maximum spectral resolution, and the 0.2X0.05ND, 0.3X0.05ND, and 31X0.05ND(A-C) neutral density slits.

⁸ The 0.1X0.09 and 0.1X0.2 slits are supported with E230H only. F25MGII is supported with all NUV-MAMA gratings and the PRISM.

⁹ The 0.2X0.2 aperture is also supported with all first-order gratings. It is available-but-unsupported with the PRISM.

¹⁰ The F25SRF2 aperture can be used with the prism to filter out (geocoronal) Lyman- emission.

11 Resolution of 200,000 or greater is possible when used with the 0.1X0.03 slit and special observing and data reduction techniques.

12 Resolution of 200,000 or greater is possible when used with the 0.1X0.03 slit and special observing and data reduction techniques.

Table 1.2: STIS Imaging Capabilities; for more details refer to Section 14.3-14.5 of the *STIS Instrument Handbook*.

| Aperture Name | Filter | Central Wavelength (c in Å) | FWHM (in Å) | Field of View (arcsec) | Detector |
|--|------------------|-----------------------------|-------------|------------------------|----------|
| <i>Visible plate scale 0.05071 ± 0.00007 per pixel</i> | | | | | |
| 50CCD | Clear | 5850 | 4410 | 52 × 52 | STIS/CCD |
| F28X50LP | Optical longpass | 7230 | 2720 | 28 × 50 ¹ | STIS/CCD |
| F28X50OIII | [O III] | 5007 | 5 | 28 × 50 ¹ | STIS/CCD |
| F28X50OII | [O II] | 3740 | 80 | 28 × 50 ¹ | STIS/CCD |

| | | | | | |
|--|-------------------------------|--------------|-------------|---------|--------------------------------|
| 50CORON | Clear + coronographic fingers | 5850 | 4410 | 52 × 52 | STIS/CCD |
| 2 Ultraviolet plate scale ~0.0246 per pixel | | | | | |
| 25MAMA | Clear | 2220 1370 | 1200 320 | 25 × 25 | STIS/NUV-MAMA STIS/FUV-MAMA |
| F25QTZ | UV near longpass | 2320 1590 | 1010 220 | 25 × 25 | STIS/NUV-MAMA STIS/FUV-MAMA |
| F25SRF2 | UV far longpass | 2270 1480 | 1110 280 | 25 × 25 | STIS/NUV-MAMA STIS/FUV-MAMA |
| F25MGII | Mg II | 2800 | 70 | 25 × 25 | STIS/NUV-MAMA |
| F25CN270 | Continuum near 2700 Å | 2700 | 350 | 25 × 25 | STIS/NUV-MAMA |
| F25CIII | C III] | 1909 | 70 | 25 × 25 | STIS/NUV-MAMA |
| F25CN182 | Continuum near 1800 Å | 1820 | 350 | 25 × 25 | STIS/NUV-MAMA |
| F25LYA | Lyman- | 1216 | 85 | 25 × 25 | STIS/FUV-MAMA |
| Neutral-Density-Filtered Imaging | | | | | |

| | | | | |
|---------|--|--------------|---------|-----------|
| F25NDQ1 | ND=10 ⁻¹ | 1150–10300 Å | 12 × 12 | STIS/CCD |
| F25NDQ2 | ND=10 ⁻² | | 12 × 12 | STIS/NUV- |
| F25NDQ3 | ND=10 ⁻³ | | 12 × 12 | MAMA |
| F25NDQ4 | ND=10 ⁻⁴ | | 12 × 12 | STIS/FUV- |
| | | | | MAMA |
| F25ND3 | Neutral density filter, ND=10 ⁻³ | 1150–10300 Å | 25 × 25 | STIS/NUV- |
| | | | | MAMA |
| | | | | STIS/FUV- |
| | | | | MAMA |
| F25ND5 | ND=10 ⁻⁵ | 1150–10300 Å | 25 × 25 | STIS/NUV- |
| | | | | MAMA |
| | | | | STIS/FUV- |
| | | | | MAMA |

¹ The dimensions are 28 arcsec on AXIS2=Y and 50 arcsec on AXIS1=X. See [Figure 3.2](#) and [Figure 11.1](#) in the *STIS Instrument Handbook*.

² The MAMA plate scales differ by about 1% in the AXIS1 and AXIS2 directions, a factor that must be taken into account when trying to add together rotated images. Also, the FUV-MAMA uses a different mirror in the filtered and unfiltered modes. In the filtered mode, the plate scale is 0.3% larger (more arcsec/pixel). Further information on geometric distortions can be found in [Chapter 14](#) of the *STIS Instrument Handbook*.

1.1.1 The STIS Detectors

STIS uses three large format (1024 × 1024 pixel) detectors:

- A Scientific Image Technologies (SITE) CCD, called the STIS/CCD, with 0.05 arcsec square pixels, covering a nominal 52 × 52 arcsec square field of view (FOV), operating from ~2000 to 10300 Å.
- A Cs₂Te MAMA detector, called the STIS/NUV-MAMA, with 0.025 arcsec square pixels, and a nominal 25 × 25 arcsec square FOV, operating in the near-ultraviolet from 1650 to 3100 Å.
- A solar blind CsI MAMA, called the STIS/FUV-MAMA, with 0.025 arcsec -pixels, and a nominal 25 × 25 arcsec square FOV, operating in the far-ultraviolet from 1150–1700 Å.

The basic observational parameters of these detectors are summarized in [Table 1.1](#) and [Table 1.2](#).

The CCD: The CCD provides high quantum efficiency and good dynamic range in the near-ultraviolet through the near-infrared. It produces a time integrated image in the so called ACCUM data taking mode. As with all CCDs, there is noise (*read noise*) and time (*read time*) associated with reading out the detector. Time resolved work with this detector is done by taking a series of multiple short exposures. The minimum exposure time is 0.1 sec, and the minimum time between successive identical exposures is 45 sec for full frame readouts and 20 sec for subarray readouts. CCD detectors are capable of high dynamic range observations; for a single exposure taken with GAIN=4, the depth (the maximum amount of the charge or counts that can accumulate in any one pixel during any one exposure, without saturation) is limited by the CCD full well (roughly $\sim 144,000 e^-$), while for a single exposure taken with GAIN=1, the depth is limited by the gain amplifier saturation ($\sim 33,000 e^-$). Cosmic rays affect all CCD exposures, and observers will generally want to split up their observations into a number of multiple exposures of less than 1,000 sec each. This allows cosmic ray removal in post-observation data processing.

The MAMAs: The two MAMA detectors are *photon counting* detectors that provide a two-dimensional ultraviolet imaging capability. They can be operated either in ACCUM mode, to produce a time integrated image, or in TIME-TAG mode, to produce an event stream with high (125 sec) time resolution. Doppler correction for the spacecraft motion is applied automatically on-board for data taken in ACCUM high spectral resolution modes.

The STIS MAMA detectors are subject to both *performance* and *safety* brightness limits. At high local (>50 counts/sec/pixel) and global ($>285,000$ counts/sec) illumination rates, counting becomes nonlinear in a way that is not correctable. At only slightly higher illumination rates, the MAMA detectors are subject to damage. Specifically, charge is extracted from the micro-channel plate during UV observations, and over-illumination can cause decreased quantum efficiency (due to gain decline in the overexposed region) or catastrophic failure (high voltage arcing within the sealed tube due to excess gas generation from the plate). Thus, MAMA observations are subject to bright object checks.

Current information indicates that the pixel-to-pixel flat fields are stable at the 1% level, which is the signal-to-noise of the flats. Furthermore, these flats show no signs of DQE loss in regions where the detector has been heavily exposed.

A signal-to-noise of 50:1 per spectral resolution element is routinely obtained for extracted spectra of point sources when integrated over the observed aperture. Higher signal-to-noise values of 100-300 can be obtained by stepping the target along the slit in the first-order modes, or by use of FP-SPLIT slits with the echelles.

1.1.2 STIS Physical Configuration

The STIS optical design includes corrective optics to compensate for the spherical aberration of the *HST*, a focal plane slit wheel assembly, collimating optics, a grating selection mechanism, fixed optics, and focal plane detectors. An independent calibration lamp assembly can illuminate the focal plane with a range of continuum and emission line lamps.

The *slit wheel* contains apertures and slits for spectroscopic use and the clear, filtered, and coronagraphic apertures for imaging. The slit wheel positioning is repeatable to very high precision: ± 7.5 and ± 2.5 milliarcsec in the spatial and spectral directions, respectively.

The *grating wheel*, or Mode Selection Mechanism (MSM), contains the first-order gratings, the cross-disperser gratings used with the echelles, the prism, and the mirrors used for imaging. The MSM is a nutating wheel that can orient optical elements in three dimensions. It permits the selection of one of its 21 optical elements as well as adjustment of the tip and tilt angles of the selected grating or mirror. The grating wheel exhibits non-repeatability that is corrected in post-observation data processing using contemporaneously obtained comparison lamp exposures for wavelength calibrations.

For some gratings, only a portion of the spectral range of the grating falls on the detector in any one exposure. These gratings can be scanned (tilted by the MSM) so that different segments of the spectral range are moved onto the detector for different exposures. For these gratings a set of pre-specified central wavelengths, corresponding to specific MSM positions (i.e., grating tilts) have been defined.

STIS has two independent calibration subsystems, the Hole in the Mirror (HITM) system and the Insert Mechanism (IM) system. The HITM system contains two Pt-Cr/Ne line lamps, used to obtain wavelength comparison exposures and to illuminate the slit during target acquisitions. Light from the HITM lamps is projected through a hole in the second correction mirror (CM2). For wavecal data taken before 1998-Nov-9, light from the external sky fell on the detector when the HITM lamps were used, but for subsequent wavecal data, an external shutter is closed to block external sky light. The IM system contains flat fielding lamps (a tungsten lamp for CCD flats, a deuterium lamp for NUV-MAMA flats, and a Krypton lamp for FUV-MAMA flats) and a single Pt-Cr/Ne line comparison lamp. When the IM lamps are used, the Calibration Insert Mechanism (CIM) is inserted into the light path, blocking all external light. Observers will be relieved to know that the ground system will *automatically* choose the right subsystem and provide the necessary calibration exposures.

1.2 Basic Instrument Operations

1.2.1 Target Acquisitions and Peakups

1.2.2 Routine Wavecals

1.2.3 Data Storage and Transfer

1.2.4 Parallel Operations

1.2.1 Target Acquisitions and Peakups

Once the telescope acquires its guide stars, the target will be within 0.2-0.3 arcsec of the aperture center when using GSC-II positions. For science observations taken through apertures smaller than three arcsec in either dimension, and for observations involving the coronagraphic bars, a target acquisition exposure should be taken to center the target in the chosen science aperture. Furthermore, if either dimension of the aperture is 0.1 arcsec, the acquisition exposure should be followed by one or more peakup exposures to refine the target centering of point or point-like sources. The nominal accuracy of STIS point source ($V < 21$ mag) target acquisitions is 0.01 arcsec, with a peak-up accuracy of 5% of the slit width used.

Acquisition exposures always use the CCD, one of the filtered or unfiltered apertures for CCD imaging, and a mirror as the optical element in the grating wheel (as opposed to a dispersive element). Peakup exposures use a science slit or coronagraphic aperture, the CCD, and either a mirror or a spectroscopic element in the MSM.

1.2.2 Routine Wavecals

Each time the MSM is moved to select a new optical element or to tilt a grating, the resulting spectrum is projected onto the detector with an uncertainty of roughly ± 3 pixels. In addition, thermal effects cause the spectrum to drift slowly with time (typical drifts are 0.1 pixels per orbit, with extreme cases of forced large temperature swings as high as 0.35 pixels per orbit). An internal calibration lamp observation (*wavecal*) is automatically taken, following each use of a new grating element or new scan position (grating tilt) and every 40 minutes thereafter, in order to allow calibration of the zero point of the wavelength (dispersion) and spatial (cross-dispersion) axes in the spectroscopic science data during post-observation data processing. These routine, automatically occurring, wavecal observations provide sufficient wavelength zero point accuracy for the large majority of GO science. Only if your science requires particularly accurate tracking of the wavelength zero points do you need to insert additional wavecal observations in your exposure sequence.

1.2.3 Data Storage and Transfer

At the conclusion of each exposure, the science data are read out from the detector in use and placed in the STIS internal buffer memory, where they are stored until they can be transferred to the *HST* data recorder (and thereafter to the ground). This design makes for more efficient use of the instrument, as up to seven CCD or four MAMA full frame images can be stored in the internal buffer at any time. The frames can be transferred out of the internal buffer to the data recorder during subsequent exposures, as long as those exposures are longer than three minutes.

The STIS internal buffer stores the data in a 16-bit per pixel format. This format imposes a maximum of 65,536 data numbers per pixel. For the MAMA detectors, this number is equivalent to a limit on the total number of *photons* per pixel that can be accumulated in a single exposure. For a single exposure with the CCD, the gain amplifier saturation level (33,000 e^-) limits the total counts per pixel that can be sustained at GAIN=1, while the CCD full well (144,000 e^- or 36,000 DN) limits the total counts per pixel that can be sustained at GAIN=4.

1.2.4 Parallel Operations

The three STIS detectors do not operate in parallel; only one detector can be used at one time. Exposures with different STIS detectors can, however, be freely interleaved in an observing sequence, but incurs overheads associated with changes in grating and aperture. The three detectors, sharing the bulk of their optical paths, also share a common field of view of the sky. While the STIS CCD can *always* be used in parallel with any of the other science instruments on the *HST*, there are restrictions in the parallel use of the MAMA detectors.

1.3 STIS Operations on Side-2

STIS was built with two redundant sets of electronics. On 2001-May-16, the primary (Side-1) set of STIS electronics failed, and operations had to be resumed on the backup (Side-2) set. Although most operations on Side-2 are identical to those on Side-1, there are two important differences, both in regard to the CCD. First, the effective read noise through each of the four available CCD amplifiers has increased by approximately $1 \text{ e}^-/\text{pix}$ in the $\text{GAIN}=1$ setting (e.g., from $\sim 4.5 \text{ e}^-/\text{pix}$ to $5.5 \text{ e}^-/\text{pix}$ for the default D amplifier, which has the lowest read noise). This increase in noise is spatially correlated (i.e., pattern noise), although the pattern can sometimes be mitigated through filtering. See [STIS ISR 2001-05](#) for full details on the CCD pattern noise and filtering techniques. The current readout noise of amplifier D in the $\text{GAIN}=1$ setting as of Cycle 25 is $6.2 \text{ e}^-/\text{s}$. The second ramification of the switch to Side-2 was that some of the thermal control of the CCD has been lost, causing variations in the CCD dark rate.

On Side-1, a temperature sensor mounted on the CCD carrier provided closed-loop control of the current to the thermoelectric cooler (TEC), ensuring a stable detector temperature at the commanded set point (-83°C). Side-2 does not have a functioning temperature sensor, and so the TEC is run at a constant current. Thus, under Side-2 operations, the CCD temperature varies with that of the spacecraft environment, and these temperature changes are accompanied by changes in detector dark rate. Because the current to the TEC on Side-2 is fixed at a higher value than the typical value required to hold the -83°C set point on Side-1 (i.e., 3 A vs. 2.7 A), the detector often runs cooler on Side-2 than it did on Side-1. The result is that the median dark rate initially varied from 4 to 5 e^- per 1000 s on Side-2, as opposed to 4.6 to 5 e^- per 1000 s on Side-1. The dark rate as of Cycle 25 on the detector is closer to 19 e^- per 1000 s. Details of the temperature dependence of the STIS CCD dark rate are somewhat complicated, however, and they are fully explained in STIS ISRs [2001-03](#) and [2018-05](#).

Although no sensor is available to measure the temperature of the CCD itself, there is a sensor for the CCD housing temperature. The hot side of the TEC is bonded to the CCD housing baseplate; hence with fixed TEC current, the CCD housing should track closely the detector temperature under Side-2 operations, and this can be seen by the excellent correlation between the dark rate and the housing temperature ([STIS ISR 2001-03](#)). Note that the CCD housing is far hotter than the detector itself: the housing temperature is approximately 18°C during normal operations, while the detector runs at approximately -83°C. Starting in January 2002, the CCD housing temperature for each Side-2 observation was included in the science header (keyword OCCDHTAV) and applied to the dark reference file by the pipeline. Since January 2005, this information has instead been taken from _epc.fits files.

1.4 Failure of Side-2

STIS stopped science operations on 2004-Aug-03, due to the failure of a power supply within the Side-2 electronics. Between 2004 and the Servicing Mission 4 in 2009, STIS remained in safe mode: the instrument and its on-board computer were switched off but the heaters remained on to ensure a stable thermal environment.

The failed unit delivered power to all the mechanisms within STIS, including the aperture wheel, the Mode Select Mechanism, and the CCD shutter. At the time of the failure, STIS was in *idle mode*, in which the light path is completely blocked (a precaution to prevent over-illumination of the MAMA detectors). In the absence of a working power supply, the mechanisms could not be moved from their current positions. STIS therefore remained inoperable until Servicing Mission 4 (SM4).

1.5 STIS Closeout

Given the long hiatus in STIS operations after the power failure in August 2004, it was decided to do a closeout of existing STIS data. As part of this closeout effort, a substantial number of improvements were made in **calstis** pipeline software and reference files. Most notable among these are:

- Updated echelle flux calibration and blaze shift corrections. See [STIS ISR 2007-01](#) and Aloisi (2006).
- Updated flux calibration for first-order medium resolution spectra. See [STIS ISR 2006-04](#).
- Improved flux calibration for first-order spectra taken at E1 aperture positions or with narrow apertures. See Proffitt (2006).
- Improved algorithm to correct for charge transfer inefficiency (CTI) when extracting fluxes for first-order spectra. See [STIS ISR 2006-01](#) and Goudfrooij et al. (2006, *PASP*, 118, 1455).
- Improved spectral traces for the most commonly used first-order modes, including date-dependent rotation parameters. See the [Oct./Nov. 2006 STAN](#) article and Dressel (2006).
- Recommended fringe flat exposures are now delivered with most G750L and G750M data, and the name of this recommended fringe flat is put into the `FRNGFLAT` keyword in the data file header.
- Association of GO-specified wavecal. Normally wavelength calibration exposures are automatically inserted for all STIS external spectroscopic observations, and these are used by the calibration pipeline to determine the zero point offset for the dispersion solution. Without this measurement, wavelength and flux calibrated spectra cannot be produced. If observers turned off the auto-wavecal and substituted separate, user specified calibration lamp exposures (referred to as *GO wavecal*s), the calibration pipeline did not know how to associate these with the appropriate science observations. As part of the STIS calibration closeout, those science exposures that lack auto-wavecal, but for which GO wavecal are available, were identified, and the science data and lamp exposures were combined into associations that treat the GO wavecal in the same way as auto-wavecal.
- For a small number of spectroscopic data sets which were taken without either automatic or GO specified wavecal, a procedure was devised that allows fixed shift values to be read from a data base during calibration. For these data sets the `SHIFTA1` keyword in each sci extension header of the `_raw` file is set to a specified value, and the `WAVECORR` header keyword in the primary header of the `_raw` file is set to “COMPLETE”. This allows **calstis** to produce fully calibrated 1D and 2D spectra despite the lack of any wavecal observation. Users should remember, however, that the shifts in such cases are imposed rather than measured. Such data sets can be easily identified, as

they have the WAVECAL header keyword set to “N/A” and the WAVECORR keyword set to “COMPLETE”.

1.6 Post Servicing Mission 4 Operation

In May 2009, during the fourth space walk of the *HST* Servicing Mission 4 (SM4), the STIS Side-2 circuit board containing the failed low voltage power supply was replaced. This repair fully restored the STIS instrument to operation with capabilities similar to those it had before the Side-2 failure. Although the performance of STIS post SM4 is similar to its performance prior to the 2004 failure, there were some important differences. These include increases in the CCD readnoise, the NUV-MAMA dark current, the CCD dark current, the CCD Charge Transfer Inefficiency and modestly decreased sensitivity of all channels. More details on these changes can be found in the [STIS Instrument Handbook](#).

1.7 STIS Operations and Calibration Timeline

Here we summarize the milestones in STIS operations and innovations in calibration.

| Date | Event |
|---------------------|---|
| 1997- Feb- 14 | STIS installed on HST |
| 1997- Feb- 21 | Servicing Mission 2 programs started |
| 1997- Sep- 25 | Servicing Mission 2 programs finished |
| 1999- Mar- 15 | G140L and G140M moved from 3" above center to 3" below center to avoid repeller wire (see the <i>STIS Instrument Handbook</i> , Section 7.5 MAMA Spectral Offsetting) shadow |
| 1999- Dec- 14 | On-the-fly-calibration (OTFC) enabled |
| 1999- Dec- 27 | Servicing Mission 3A programs started |
| 2000- Feb- 06 | Servicing Mission 3A programs finished |
| 2000- Jul-03 | E1 pseudo-apertures (see the <i>STIS Instrument Handbook</i> , Section 7.2.7) implemented |

| | |
|---------------------|---|
| 2001- May- 01 | On-the-fly-recalibration (OTFR) enabled |
| 2001- May- 16 | Side-1 electronics failed, operations suspended |
| 2001- Jul-10 | Side-2 electronics enabled, operations resumed |
| 2002- Mar- 12 | Servicing Mission 3B programs started |
| 2002- May- 05 | Servicing Mission 3B programs finished |
| 2002- Sep- 05 | Time-dependent sensitivity correction implemented for MAMA data |
| 2002- Sep- 05 | Blaze shift correction for echelle data implemented |
| 2003- Aug- 04 | E2 and D1 pseudo-apertures implemented, E1 pseudo-apertures revised (see Section 4.3.2) |
| 2003- Nov- 13 | Time-dependent sensitivity correction implemented for CCD data |

| | |
|---------------------|--|
| 2003- Dec- 16 | Charge transfer inefficiency correction implemented for CCD data |
| 2004- Aug- 03 | Side-2 electronics failed, operations suspended |
| 2005- Dec- 13 | New combined grating/aperture correction implemented (see Section 3.4.13) |
| 2006- Nov- 03 | Echelle data flux calibration significantly improved, trace rotation implemented for commonly used first order modes |
| 2006- Nov- 22 | Full recalibration of archival STIS data started |
| 2009- May- 11 | Servicing Mission 4 program started |
| 2009- May- 17 | Side-2 electronics are repaired, operations resumed |
| 2009- May- 24 | Servicing Mission 4 program finished |
| 2011- Mar- 01 | Updated NUV-MAMA bad-pixel masks to include vignetted corners for different optical elements |

| | |
|---------------------|---|
| 2011- Nov- 08 | Consistent post-SM4 sensitivity curves implemented for all echelle modes. |
| 2015- Sep- 03 | Pixel-based CTE correction stand-alone tool released |
| 2016- May- 16 | BAR5 coronagraphic aperture location implemented |
| 2017- Jan- 20 | HST/STIS Target Acquisition Simulator Released |
| 2017- Jul-07 | FUV-MAMA geometric distortion correction implemented |
| 2017- Sep- 19 | STIS blaze fix tool released |

Chapter 2: STIS Data Structure

2.1 STIS Overview

Raw STIS data are calibrated through the STScI **calstis** pipeline. The pipeline unpacks the data bits from individual exposures, combines them into files containing raw, uncalibrated data, and performs image and spectroscopic reduction to produce output files that can be used directly for scientific analysis (see [Chapter 3](#) for a more detailed description of the STIS pipeline). Unlike previous *HST* pipelines, the STIS pipeline calibrates data from multiple science exposures and any contemporaneously obtained line lamp calibration exposures through the pipeline as a single unit. These multiple *associated* STIS exposures that are processed through the pipeline as a unit are combined into a single dataset, to allow easy identification and compact storage. See [Chapter 5](#) in the *Introduction to the HST Data Handbooks* for a general explanation of *HST* data associations.

To work effectively with your data you will need to understand:

- The nature of the individual files in your dataset. To understand the contents of each file, see [Section 2.2](#).
- The basic format in which the STIS data are stored, the information and nature of the data stored for each observation; see [Section 2.3](#).
- How to use the header keyword information to identify the principal parameters of your observation and to determine the calibration processing steps that were performed on your dataset; see [Section 2.4](#).
- The meanings of the error and data quality arrays, which are propagated through the pipeline for each STIS science observation; see [Section 2.5](#).

2.2 Types of STIS Files

[2.2.1 Trailer Files](#)

[2.2.2 Understanding Associations](#)

The naming convention for STIS files is `rootname_XXX.fits`, where `XXX` is a three-character file suffix. The suffix identifies the type of data within the file. [Table 2.1](#) lists the file suffixes for both uncalibrated and calibrated data files. Depending on the type of observation you have obtained, and therefore on the path it has taken through the calibration pipeline, you will find an appropriate subset of these files in your particular dataset. [Table 2.2](#) shows the datasets that are produced by the `calstis` pipeline for different types of datasets.

Table 2.1: Data File Naming Conventions

| Suffix | Type | Contents |
|----------------------------------|-------|--|
| Uncalibrated Science Data | | |
| <code>_raw</code> | image | Raw science ¹ |
| <code>_tag</code> | table | TIME-TAG event list |
| <code>_wav</code> | image | Associated wavecal exposure |
| Uncalibrated Support Data | | |
| <code>_asn</code> | table | Association file |
| <code>_epc</code> | table | CCD housing temperature at 1.26 s intervals |
| <code>_jif</code> | image | 2-D histogram of the <code>_jit</code> file |
| <code>_jit</code> | table | Spacecraft pointing data averaged over 3 s intervals |
| <code>_lrc</code> | image | Local rate check image |

| | | |
|------------------------|-------|--|
| _lsp | text | LRC support file (header) |
| _pdq | table | Post observation summary and Data Quality |
| _spt | image | Support, planning & telemetry information |
| _trl | table | Trailer file; historical record of generic conversion and pipeline processing |
| _wsp | image | The _spt file for _wav (wavecal) |
| Calibrated Data | | |
| _flt | image | Flat-fielded science |
| _crj | image | Cosmic ray rejected, flat-fielded science (CCD data only) |
| _sfl | image | Summed flat-fielded science (MAMA data only) |
| _x1d | table | 1-D extracted spectra for individual imsets: <ul style="list-style-type: none"> • Aperture extracted, background subtracted, flux and wavelength calibrated spectra |
| _x2d | image | 2-D spectral and direct images for individual imsets: <ul style="list-style-type: none"> • Rectified, wavelength and flux calibrated first order spectra or • Geometrically corrected imaging data. |
| _sx1 | table | 1-D extracted spectra from summed (REPEATOBS) or cosmic ray rejected (CRSPLIT) images. |
| _sx2 | image | 2-D rectified direct or spectral images from summed (REPEATOBS) or cosmic ray rejected (CRSPLIT) images. |

1 Raw data from non-automated GO wavecals, biases, darks, and flats, as well as from ACQs and ACQ/PEAKs, also have the _raw suffix.

Table 2.2: STIS Data File by Observation Type

| Data Type | Header Keywords Determining Number of Imsets | Uncalibrated Files | Calibrated Files Containing Individual Imsets | Calibrated Files Containing Combined Imsets ¹ |
|--|---|----------------------------------|---|--|
| ACQ, ACQ/PEAK | | raw | | |
| ACCUM: Single Imset Spectroscopic | | | | |
| CCD 1st order MAMA 1st order MAMA echelle | NRPTEXT=1 & CRSPLIT=1 NRPTEXT=1 NRPTEXT=1 | raw, wav raw, wav raw, wav | flt, x2d, x1d flt, x2d, x1d flt, ----, x1d | |
| ACCUM: Single Imset Imaging | | | | |
| CCD MAMA | NRPTEXT=1 & CRSPLIT=1 NRPTEXT=1 | raw raw | flt, x2d flt, x2d | |
| ACCUM: Multiple Imset Spectroscopic | | | | |
| CCD 1st order MAMA 1st order MAMA echelle | NRPTEXT>1 or CRSPLIT>1 NRPTEXT>1 NRPTEXT>1 | raw, wav raw, wav raw, wav | flt flt, x2d, x1d flt, ----, x1d | crj, sx2, sx1 sfl, sx2, ² sfl |
| ACCUM: Multiple Imset Imaging | | | | |

| | | | | | |
|--|--------------------------------------|--|--------------------------------|---------------------------------|----------------------|
| | CCD MAMA | NRPTEXT>1 or CRSPLIT>1 NRPTEXT>1 | raw raw | flt flt, x2d | crj, sx2 sfl, sx2 |
| TIME-TAG: Spectroscopic³ | | | | | |
| | MAMA 1st order MAMA echelle | | tag, raw, wav tag, raw, wav | flt, x2d, x1d flt, ----, x1d | |
| TIME-TAG: Imaging³ | | | | | |
| | MAMA | | tag, raw | flt, x2d | |

¹ Combined: summed if MAMA data, summed with cosmic ray rejection if CCD data.

² Note that, while the pipeline does not produce a summed sx1 file for MAMA multiple imset spectroscopic datasets, you can easily do so by running **x1d** on the sfl file.

³ A single raw image is generated from the tag file for TIME-TAG data. For other options, see [Section 5.6](#).

2.2.1 Trailer Files

Each task in the **calstis** package creates messages during processing which describe the progress of the calibration. These messages are quite relevant to understanding how the data was calibrated, and in some of the cases, to determining the accuracy of the products.

When the data is processed in the archive pipeline, the output messages from the conversion of the telemetry data and the different calibration steps done by the **calstis** software are stored in a text FITS file known as the trailer file, with extension `_trl`. Each time the archive processes data before retrieval, the old trailer file is erased and a new one created using the results of the most recent processing performed. This is not the case when **calstis** is run in a user's home environment. **Calstis** redirects the output of its many steps to the `STDOUT`, so when run on a personal machine, it will not override this `_trl` file but rather will direct the output to `STDOUT`.

The data on the telemetry conversion appears first in this table. In this section of the `_trl` file, there is also information relevant to the selection of the best reference files and the population of some of the header keywords. The second part of this file is the information on the calibration steps performed by the `calstis` pipeline, appearing in the order in which each step was performed. In this last section of the `_trl` file, the `calstis` steps are indicated by their module name (see [Table 3.1](#) of this document).

The **calstis** messages provide information on the input and output files for each step, the corrections performed, information regarding the reference files used, and in the case of spectroscopic data, messages about the location of the extracted spectrum or shift correction applied to the data. **Calstis** also gives warnings in the event of failures of the software to locate the spectrum or when the appropriate correction to the data could not be applied. For more detailed information on the calibration steps and structure of `calstis`, please refer to [Chapter 3](#).

2.2.2 Understanding Associations

An *association* is created when repeated exposures are obtained through CR-SPLITS or REPEATOBS, and when wavecal exposures are linked to science exposures. The repeated exposures in an association will appear in a single FITS file. You can recognize a file as part of an association because there will be a zero in the last position of the rootname (e.g., `o3tt01010_raw.fits`). The rootnames of the individual exposures in an association are contained in the association file, which has suffix `_asn` (e.g., `o3tt01010_asn.fits`). An association file holds a single binary table extension, which can be displayed with **astropy.table**. The information within an association table shows how the associated exposures are related. [Table 2.3](#) illustrates the contents of the association table for a `CRSPLIT=2` observation, with an associated wavecal.

Table 2.3: Contents of Association Table.

To display the association table for `o3tt01010_asn.fits`:

```
>>> from astropy.table import Table

>>> data_table = Table.read('o3tt01010_asn.fits', hdu='asn')
>>> print (data_table)
```

| MEMNAME | MEMTYPE | MEMPRSNT |
|-----------|---------|----------|
| O3TT01AVQ | CRSPLIT | True |
| O3TT01AWQ | CRSPLIT | True |
| O3TT01010 | PRODUCT | True |

The association table above tells the user that the product, or dataset, will have the rootname `o3tt01010`, that there will be two science exposures contained in the `o3tt01010_raw.fits` file that are `CR-SPLITS`, and that a `o3tt01010_wav.fits` file should exist containing the contemporaneously obtained automatic wavecal. The `o3tt01010_raw.fits` file will contain six image extensions, one triplet of {`SCI`, `ERR`, `DQ`} for each exposure (see [Section 2.3.1](#)). The pipeline will calibrate these data as a unit, producing, in the case of CCD data, a single cosmic ray rejected image (`rootname_crj.fits`), its data quality and error images, and rectified spectra. Similarly, for `REPEATOBS` observations, in which many identical exposures are taken to obtain a time series, all the science data will be stored in sequential triplet extensions of a single FITS file (`rootnameflt.fits`). These will be processed through the **calstis** pipeline as a unit, with each image extension individually calibrated. The set of images will also be combined to produce a total time-integrated calibrated image.

Originally, only automatically inserted wavecals were associated and used for wavelength calibration in the OTFR pipeline. Although GOs could specify additional lamp exposures with the `LINE`, `HITM1`, or `HITM2` lamps that could be used to supplement or replace the automatic wavecals, these were not used in the pipeline.

For a number of such spectroscopic datasets without auto-wavecals that were taken between STIS launch and the Side-2 failure in 2004, the associations were subsequently redefined to allow GO-specified wavecals to be used in place of the missing auto-wavecals. In these new associations, the GO-specified wavecal is treated in the same way as a standard auto-wavecal, although some parameters used for the exposure (e.g., aperture, exposure time, lamp, or lamp current) may differ from the default values that would have been used by the automatic wavecal.

It was also decided that it would be desirable to “associate” STIS IR fringe flats taken using the tungsten calibration lamp with the `G750M` or `G750L` science exposures for which they were taken. Instead of creating a formal association between such datasets, the name of the recommended fringe flat is placed in the `FRNGFLAT` header keyword in the extension header of the science data, and all tungsten lamp images taken contiguously with the science data (i.e., no `MSM` motion between exposures) are automatically delivered to the user whenever data are requested from the archive.

When suitable fringe flats are available, the recommended flat is chosen based on the aperture used for the fringe flat with the order of preference being 52X0.1, 52X0.05, 52X0.2, 52X0.5, 52X2, 0.3X0.09, and then any other. Should there be multiple suitable fringe flats taken using the same aperture, the one taken closest in time to the science exposure is preferred.

[Chapter 3](#) of this document gives more information about the pipeline processing.

2.3 STIS File Structures

[2.3.1 STIS FITS Image Extension Files](#)

[2.3.2 STIS FITS Table Extension Files](#)

All STIS data products are FITS files. Images and two-dimensional spectroscopic data are stored in FITS image extension files, which can be directly manipulated, without conversion, in the **AstroConda** environment. These FITS image extension files allow an associated set of STIS science exposures, processed through calibration as a single unit, to be packaged into a single file. The **fits.info** function in **astropy.io.fits** can be used to list the complete set of the primary and extension headers of the data files.

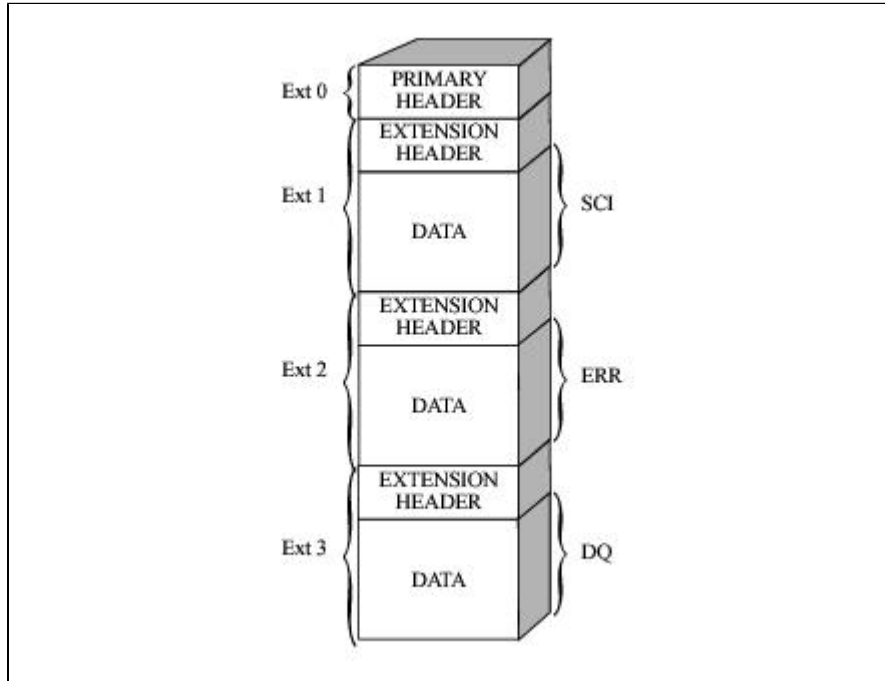
Tabular STIS information, such as extracted one-dimensional spectra or the TIME-TAG mode event series, are stored as three-dimensional FITS binary tables.

2.3.1 STIS FITS Image Extension Files

[Figure 2.1](#) illustrates the structure of a STIS FITS image extension file, which contains:

- A primary header that stores keyword information describing the global properties of all of the exposures in the file (e.g., the target name, target coordinates, total summed exposure time of all exposures in the file, optical element, aperture, detector, calibration switches, reference files used).
- A series of image extensions, each containing header keywords with information specific to the given exposure (e.g., exposure time, world coordinate system) and a data array.

Figure 2.1: FITS Image Extension File for STIS



All uncalibrated and calibrated ACCUM mode science data (with the exception of the extracted one-dimensional spectra and TIME-TAG data, see below) are stored in FITS image extension files with the particular format shown in [Figure 2.1](#). Each STIS readout generates three FITS images or extensions (SCI, ERR and DQ) as explained below:

- The first, of extension type SCI, stores the science values.
- The second, of extension type ERR, contains the statistical errors, which are propagated through the calibration process. It is unpopulated in raw data files.
- The third, of extension type DQ, stores the data quality values, which flag suspect pixels in the corresponding SCI data. It is unpopulated in raw data files.

The error arrays and data quality values are described in more detail in [Section 2.5](#). Each of these extensions can contain one of several different data types, including images, binary tables and ASCII text tables. The value of the `XTENSION` keyword in the extension's header identifies the type of data the extension contains; the value of this keyword may be determined using the `fits.info` function in **astropy.io.fits**.

Acquisition Images: Almost all STIS spectroscopic science exposures will have been preceded by an acquisition (and possibly an acquisition/peakup) exposure to place the target in the slit. Keywords in the header of spectroscopic data identify the dataset name of the acquisition (in the `ACQNAME` keyword). An acquisition exposure produces a raw data file (`rootname_raw.fits`) containing three science image extension corresponding to the three stages of the acquisition procedure:

- `[SCI,1]` is a subarray image (100×100 pixels) for point source acquisitions; larger for diffuse acquisitions) of the target area obtained after the initial blind pointing.
- `[SCI,2]` is a sub-array image of the same size after the coarse centering phase of the acquisition.
- `[SCI,3]` is a sub-array image (32×32 pixels) of the lamp viewed through the 0.2×0.2 aperture (to identify the location of the aperture on the detector).

Acquisition/Peakup Images: An acquisition/peakup exposure will produce a single raw data file for a spiral search peakup, and one for each linear search peakup; that is, if you have performed a peakup that requires `SEARCH=LINEARAXIS1` and `SEARCH=LINEARAXIS2` scans, then two datasets will be produced: one for each scan. Keywords `ACQPEAK1` and `ACQPEAK2` in the header of STIS data identify the dataset name of the acquisition/peakup images. The `_raw` data file produced for an `ACQ/PEAK` exposure contains one science image extension:

- `[SCI,1]` is the confirmation image of the target, taken at the *end* of the peakup, after the final move which places the target in the slit.

To examine the flux values of the individual steps in the ACQ/PEAK, relative to the lowest flux, which has been set to 0, list the entries of the fourth extension, i.e., `rootname_raw.fits[4]`. Extensions [2] and [3] are the unpopulated ERR and DQ arrays that accompany extension [1]; recall that [1] = [SCI,1].

Direct and Spectral Imaging Data: The intermediate calibrated output product for CCD direct and spectral imaging data is the `_flt` or `_crj` file, and the intermediate calibrated product for MAMA data is the `_flt` or `_sfl` file, depending on whether the file contains single or multiple imsets (see [Table 2.2](#)). The units of the data in these files are counts per pixel. The conversion of the counts to flux (or magnitude) is explained in [Section 5.3.1](#).

The `_x2d` and `_sx2` files hold the geometric distortion corrected imaging data or the flux and wavelength calibrated two-dimensional spectra for long slit first order observations. These are stored as FITS images, as are the raw and calibrated imaging data. The units of the data in the direct images and two dimensional spectra are counts sec^{-1} and $\text{ergs sec}^{-1} \text{cm}^{-2} \text{\AA}^{-1} \text{arcsec}^{-2}$, respectively. The procedure to derive flux information from these data is described in [Section 5.3.1](#) and [Section 5.4.1](#), respectively. Discussion of the one-dimensional extracted spectra is presented in [Section 2.3.2](#) and [Section 5.5](#).

2.3.2 STIS FITS Table Extension Files

All the `TIME-TAG` and one-dimensional STIS spectra are stored in binary tables, as described below.

Time-Tag: `TIME-TAG` mode is used for high time resolution spectroscopy and imaging in the UV (with the MAMA detectors only). `TIME-TAG` event data (`rootname_tag.fits`) are contained in a binary table extension. [Figure 2.2](#) shows the format of `TIME-TAG` tables. The first extension contains the events table, in which each row of the table corresponds to a single event in the data stream and the columns of the table contain scalar quantities that describe the event, as shown in [Table 2.4](#). The second extension contains the good time intervals information, where an uninterrupted period of time is considered as one good time interval. Interruptions in the data taking due to memory overflow or corrupted fine times could result in more than one GTI (see [STIS ISR 2000-02](#)).

Figure 2.2: FITS File Format For TIME-TAG Tables

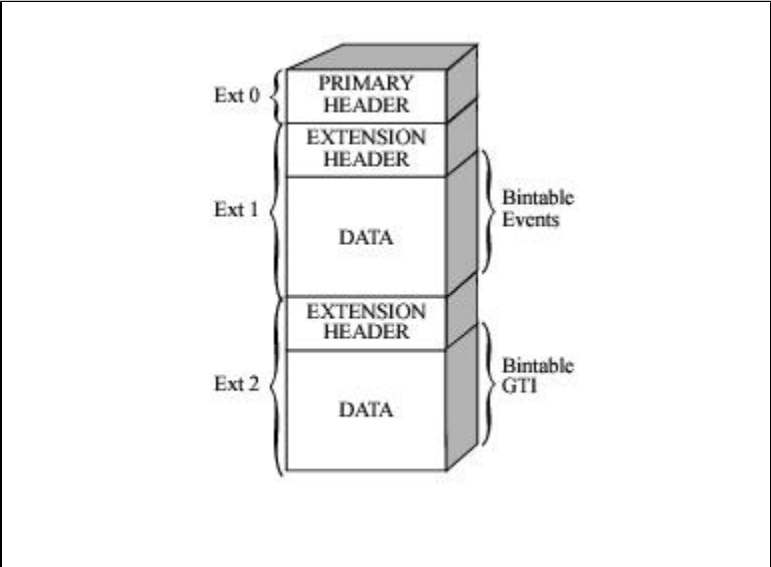


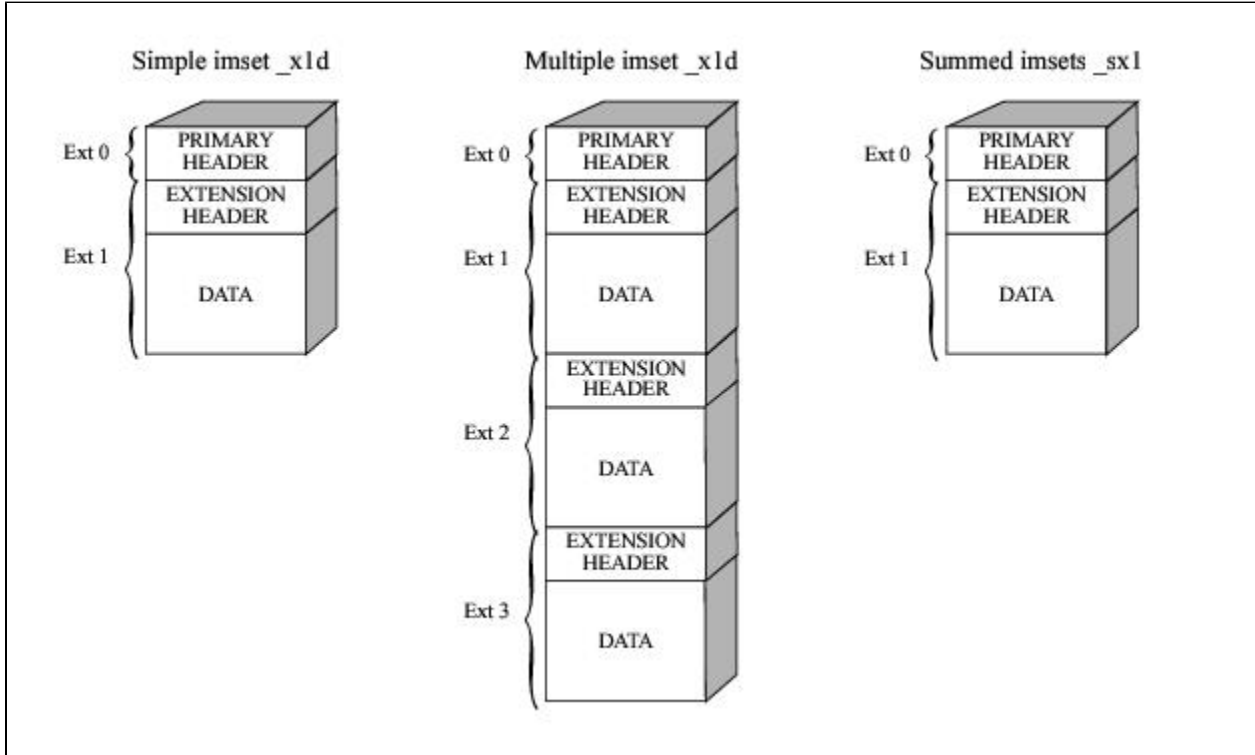
Table 2.4: Columns of a TIME-TAG Data Table

| Extension 1 | | |
|--------------------|--------------|---|
| Column Name | Units | Description |
| TIME | sec | Elapsed time in seconds since the exposure start time |
| AXIS1 | pixel | Pixel coordinate along the spectral axis, with Doppler correction |
| AXIS2 | pixel | Pixel coordinate along the spatial axis, no Doppler correction |
| DETAXIS1 | pixel | Pixel coordinate along the spectral axis, prior to Doppler correction |
| Extension 2 | | |
| Column Name | Units | Description |
| START | sec | Start good time interval |
| STOP | sec | End good time interval |

The STIS pipeline collapses a TIME-TAG event series into a single time-integrated image and processes it as if it were an ACCUM mode image. Outside of the pipeline the raw TIME-TAG event stream can be manipulated to produce two-dimensional images which are integrated over user-specified times or manipulated directly (see [Section 5.6](#)).

One-Dimensional Extracted Spectra: The STIS pipeline produces aperture extracted one-dimensional spectra and stores them in binary tables (rootname_x1d.fits or rootname_sx1.fits). [Figure 2.3](#) shows the format of the 1-D extracted spectra table. For a single first order spectroscopic observation, the calibrated spectrum is stored in the first row of the first extension of the _x1d file. Each column of the table contains a particular quantity, such as WAVELENGTH or FLUX. [Table 2.5](#) shows the contents of the different columns in a STIS extracted spectrum table. Each table cell can contain either a scalar value or an array of values. The SPORDER column value is equal to 1 for first order spectral data. There will be a separate table extension for each associated exposure in an associated set. For example, if you specified Number_of_Iterations=2 in your Phase II proposal, you will find the extracted spectrum from the second exposure in the second table extension. The _sx2 file, on the other hand, contains one single spectra that is derived from the flat-fielded, co-added, individual repeat observations file rootname_sfl.fits.

Figure 2.3: FITS File Format For 1-D Extracted Spectra Table



For echelle data, each spectral order is extracted from the image and a fully calibrated spectrum of that order is stored in a separate row of the first extension of the binary table. The number of orders (and ultimately the number of rows in the table) in the SPORDER column in this case will be anywhere between 24 and 70 depending on the echelle grating being used.

For more information on how to handle STIS BINTABLE files please refer to the [Introduction to the HST Data Handbooks](#).

Table 2.5: Columns of a STIS Extracted Spectrum Table

| Column Name | Contents | Units | Description |
|-------------|----------|-------|-------------|
|-------------|----------|-------|-------------|

| | | | |
|------------|--------|--|---|
| SPORDER | scalar | | Spectral order number |
| NELEM | scalar | | Number of valid elements in each array |
| WAVELENGTH | array | Å | Wavelengths corresponding to fluxes |
| GROSS | array | counts s ⁻¹ | Extracted spectrum before subtracting BACKGROUND |
| BACKGROUND | array | counts s ⁻¹ | Background that was subtracted to obtain NET |
| NET | array | counts s ⁻¹ | Difference of GROSS and BACKGROUND arrays |
| FLUX | array | erg s ⁻¹ cm ⁻² Å ⁻¹ | Flux calibrated NET spectrum |
| ERROR | array | erg s ⁻¹ cm ⁻² Å ⁻¹ | Internal error estimate |
| DQ | array | | Data quality flags |
| A2CENTER | scalar | pixel | Nominal spectrum location |
| EXTRSIZE | scalar | pixel | Extraction box size |
| MAXSRCH | scalar | pixel | Maximum search box for spectrum |
| BK1SIZE | scalar | pixel | Size of background box 1 |
| BK2SIZE | scalar | pixel | Size of background box 2 |
| BK1OFFST | scalar | pixel | Offset location of background box 1 from A2CENTER |
| BK2OFFST | scalar | pixel | Offset location of background box 2 from A2CENTER |
| EXTRLOCY | array | pixel | Extraction location from _flt, _sfl, or _crj file |

| | | | |
|--------|--------|-------|------------------------------|
| OFFSET | scalar | pixel | Offset from nominal A2CENTER |
|--------|--------|-------|------------------------------|

2.4 Headers, Keywords, and Relationship to Phase II

As with previous *HST* instruments, the FITS header keywords in STIS data files store important information characterizing the observations and telemetry received during the observations, and describe the post-observation processing of your dataset. Each keyword follows FITS conventions and is no longer than eight characters. Values of keywords can be integer, real (floating-point), or character string. Many are *HST* and STIS specific. Knowledge of the keywords and where to find them is an important first step in understanding your data. By examining your file headers, using the various functions in **astropy.io.fits**, you will find detailed information about your data including:

- Target name, coordinates, proposal ID, and other proposal level information.
- Observation and exposure time information such as observation start and duration.
- Instrument configuration information such as detector, grating, central wavelength setting, and filter.
- Readout definition parameters such as binning, gain, and subarray parameters.
- Exposure-specific information such as more detailed timing, world coordinate system information, and fine guidance sensor identification.
- Calibration information such as the calibration switches and reference files used by the pipeline and parameters derived from the calibration, such as image statistics and wavelength shifts.

STIS takes CCD and MAMA spectroscopic and imaging data, as well as acquisitions and ACQ/peakups. The keywords relevant for one of these data types will not necessarily be relevant to another. Accordingly, you will find that the header on your particular file contains a unique combination of keywords appropriate for your type of observation. Long definitions for the keywords can also be accessed from the following Web page, which provides detailed explanations of the contents and algorithm for populating the keywords. This site also provides sample headers for different STIS file types: http://archive.stsci.edu/keyword/cgi-bin/kdct-header_form.cgi?db=Operational#STIS.

Keywords that deal with a particular topic, such as the instrument configuration, are grouped together logically throughout the headers. [Table 2.6](#) lists a useful subset of these groups of keywords, indicates the name of the grouping, and where applicable, shows their relationship to the corresponding information from the Phase II proposal.

Table 2.7 summarizes the possible calibration switch keywords, and indicates whether they are present for a particular observation; it also indicates the reference file keyword corresponding to the particular calibration step. A calibration switch keyword is populated with values of OMIT, COMPLETE, or PERFORM. Similarly, Table 2.8 summarizes the reference file group of keywords that identify the files used by the pipeline during calibration (see Chapter 3 for a detailed description of pipeline processing).

Table 2.6: Selected Header Keywords and Relationship to Phase II Parameters

| Header Keyword | Phase II Equivalent | Description |
|--|----------------------------------|---|
| NEXTEND | | Number of image extensions in the file. |
| Target Information (Primary Header) | | |
| TARGNAME | Target_Name | Name of target. |
| RA_TARG | RA | Right ascension of the target (deg) (J2000). |
| DEC_TARG | DEC | Declination of the target (deg) (J2000). |
| PROPOSID | | 4 or 5 digit proposal number. |
| LINENUM | Visit_Number, Exposure_Number | Indicates the visit and exposure number from the Phase II proposal: Visit_Number.Exposure_Number. |
| Summary Exposure Information (Primary Header) | | |
| TDATEOBS | | UT date of start of first exposure in file (a character string, yyyy-mm-dd). |
| TTIMEOBS | | UT start time of first exposure in file (a character string, hh:mm:ss). |

| | | |
|--|---|--|
| TEXPSTRT | | Start time (MJD) of first exposure in file (a real number). |
| TEXPEND | | End time (MJD) of last exposure in the file (a real number). |
| TEXPTIME | Number_of_Iterations × Time_per_Exposure | Total of science exposure times in an association. |
| Science Instrument Configuration (Primary Header) | | |
| OBSTYPE | | Observation type (IMAGING or SPECTROSCOPIC). |
| OBSMODE | Opmode | Operating mode (ACQ, ACQ/PEAK, ACCUM, TIME-TAG). |
| DETECTOR | Config | Detector in use (NUV-MAMA, FUV-MAMA, or CCD). |
| OPT_ELEM | Sp_Element | Optical element in use (grating name or mirror). |
| CENWAVE | Wavelength | Central wavelength for grating settings. |
| APERTURE | Aperture | Aperture name. |
| PROPAPER | Aperture | Proposed aperture name. |
| FILTER | Aperture | Filter in use. |
| APER_FOV | | Aperture field of view. |
| PLATESC | | Nominal plate scale (arcsec/pixel); see Section 3.4.14 . |
| SCLAMP | | Lamp status (NONE or name of lamp which is on). |

| | | |
|--|---|---|
| LAMPSET | | Spectral cal lamp current value (milliamps). |
| NRPTXP | Number_of_Iterations | Number of repeat exposures in dataset (for MAMA data only): Default = 1. ASN_MTYP=REPEATOBS. |
| SUBARRAY | | Data from a subarray (T) or full frame (F). |
| CRSPLIT | CR-SPLIT (optional parameter) | Number of split exposures for cosmic ray removal in CCD data. ASN_MTYP=CRSPLIT. |
| TARGNAME | WAVECAL=NO & Target_Name = WAVELINE or Target_Name = WAVEHITM | Turn off automated wavecal exposures. Note: This is not a default or recommended setting and is listed here for informational purposes only. |
| Readout Definition Parameters | | |
| SIZAXIS1 | SIZEAXIS1 | Subarray axis 1 size in unbinned detector pixels. |
| SIZAXIS2 | SIZEAXIS2 | Subarray axis 2 size in unbinned detector pixels. |
| BINAXIS1 | BINAXIS1 | Axis 1 data bin size in unbinned detector pixels. |
| BINAXIS2 | BINAXIS2 | Axis 2 data bin size in unbinned detector pixels. |
| Engineering Parameters | | |
| CCDAMP | AMP (optional engineering parameter) | CCD amplifier read out (A, B, C, D). |
| CCDGAIN | GAIN (optional parameter) | Commanded gain of CCD. |
| Exposure Information (in Extension header 1 or greater) | | |

| | | |
|-------------------|---|--|
| DATE-OBS | | UT date of start of observation (yyyy-mm-dd). |
| TIME-OBS | | UT time of start of observation (hh:mm:ss). |
| PA_APER | | Position angle of reference aperture. |
| ORIENTAT | | Position angle of image y-axis. |
| CRPIX1, CRPIX2 | | X and Y coordinates of reference pixel. |
| DGESTAR | | Dominant guide star ID // FGS ID (F1,F2,F3); (_spt file) e. g., DGESTAR = 0087900462F3. |
| EXPTIME | Time_per_Exposure /CR-SPLIT or Time_per_Exposure (if not CR-SPLIT) | Exposure time of an individual exposure in a CR-SPLIT or REPEATOBS series, in seconds (a real number). |
| EXPSTART | | Exposure start time (Modified Julian Date). |
| EXPEND | | Exposure end time (Modified Julian Date). |

Table 2.7: Calibration Switch Keywords

| Header Keywords | Explanation | Spectra | Images | CCD | MAMA |
|-----------------|-------------|---------|--------|-----|------|
| | | | | | |

| Calibration Switch | Reference File | | | | | |
|--------------------|----------------|--|---|---|---|---|
| ATODCORR | ATODTAB | A-to-D correction | • | • | • | |
| BACKCORR | ADDSTAB | Subtract spectral background | • | | • | • |
| BIASCORR | BIASFILE | Bias image (structure) correction | • | • | • | |
| BLEVCORR | N/A | Correct for CCD bias level (trim overscan) | • | • | • | |
| CRCORR | CRREJTAB | Cosmic ray subtraction | • | • | • | |
| CTECORR | CCDTAB | Correct flux for CTE losses | • | | • | |
| DARKCORR | DARKFILE | Dark image correction | • | • | • | • |
| | CCDTAB | CCD Parameters | • | • | • | • |
| DISPCORR | DISPTAB | Apply dispersion solution | • | | • | • |
| | INANGTAB | Incident angle correction | • | | • | • |
| | MOFFTAB | MAMA offset correction | • | | | • |
| DOPPCORR | N/A | Doppler correction | • | | | • |
| DQICORR | BPIXTAB | Initialize data quality image | • | • | • | • |

| | | | | | | |
|----------|----------|--|---|---|---|---|
| EXPSCORR | N/A | Process individual observations after CRCORR | • | • | • | |
| FLATCORR | LFLTFILE | Flat field corrections | • | • | | • |
| | PFLTFILE | Pixel-to-pixel flat | | | | |
| | DFLTFILE | (Not done) | | | | |
| FLUXCORR | APERTAB | Convert to absolute flux | • | | • | • |
| | PCTAB | Photometry correction | | | | |
| | PHOTTAB | Photometric conversion | | | | |
| | TDSTAB | Time dependent sensitivity correction | | | | |
| GEOCORR | IDCTAB | Geometric correction | | • | • | • |
| GLINCORR | MLINTAB | Global detector non-linearities | • | • | | • |
| HELCORR | N/A | Convert to heliocentric wavelengths | • | | • | • |
| LFLGCORR | HLINTAB | Flag pixels for local and global non-linearities | • | • | | • |
| LORSCORR | N/A | Convert MAMA image to low-res | • | • | | • |

| | | | | | | |
|----------|----------|---------------------------------------|---|---|---|---|
| PHOTCORR | PHOTTAB | Populate header photometric keywords | | • | • | • |
| | APERTAB | Aperture throughput | | • | • | • |
| | CCDTAB | CCD parameters | | • | • | • |
| | IMPHTTAB | Photometry keywords | • | • | • | • |
| | TDSTAB | Time dependent sensitivity correction | | • | • | • |
| RPTCORR | N/A | Add individual repeat observations | • | • | | • |
| SC2DCORR | CDSTAB | 2-D scattered light correction | • | | | • |
| | ECHSCTAB | Echelle scattering | | | | |
| | EXSTAB | Echelle cross-dispersion scattering | | | | |
| | RIPTAB | Echelle ripple | | | | |
| | HALOTAB | Detector halo | | | | |
| | TELTAB | Telescope point spread function | | | | |
| | SRWTAB | Scattering reference wavelengths | | | | |

| | | | | | | |
|----------|----------|--|---|---|---|---|
| SGEOCORR | SDSTFILE | Small-scale distortion correction (not done) | • | • | | • |
| SHADCORR | SHADFILE | Shutter shading correction (not done) | • | • | • | |
| STATFLAG | N/A | Calculate image statistics | • | • | • | • |
| WAVECORR | WAVECAL | Use wavecal to adjust wavelength zero point | • | | • | • |
| | LAMPTAB | Template calibration lamp spectra | | | | |
| | APDESTAB | Aperture descriptions | | | | |
| X1DCORR | SPTRCTAB | Extract 1-D spectrum | • | | • | • |
| | XTRACTAB | 1-D extraction parameters | • | | • | • |
| | GACTAB | Grating-aperture correction | • | | • | |
| X2DCORR | SDCTAB | Rectify 2-D spectral image | • | | • | • |
| | APDESTAB | Aperture descriptions | | | | |
| | SPTRCTAB | 1-D spectrum trace | | | | |

Table 2.8: Reference File Keywords

| Header Keyword | File Suffix | Format | Explanation | Spectra | Images | CCD | MAMA |
|----------------|-------------|--------|-------------------------------------|---------|--------|-----|------|
| APDESTAB | _apd | Table | Aperture descriptions | • | | • | • |
| APERTAB | _apt | Table | Aperture throughput | • | • | • | • |
| ATODTAB | _a2d | Table | A-to-D correction | • | • | • | |
| BIASFILE | _bia | Image | Bias (structure) | • | • | • | |
| BPIXTAB | _bpx | Table | Bad pixel | • | • | • | • |
| CCDTAB | _ccd | Table | CCD parameters | • | • | • | |
| CDSTAB | _cds | Table | Cross-disperser scattering | • | | | • |
| CRREJTAB | _crr | Table | Cosmic ray rejection parameters | • | • | • | |
| DARKFILE | _drk | Image | Dark current | • | • | • | • |
| DFLTFILE | _dfl | Image | Delta-flat (not available) | • | • | • | • |
| DISPTAB | _dsp | Table | Dispersion coefficients | • | | • | • |
| ECHSCTAB | _ech | Table | Echelle scattering | • | | | • |
| EXSTAB | _exs | Table | Echelle cross-dispersion scattering | • | | | • |

| | | | | | | | |
|----------|------|-------|---|---|---|---|---|
| GACTAB | _gac | Table | Grating-aperture correction | • | | • | |
| HALOTAB | _hal | Table | Detector halo | • | | | • |
| IDCTAB | _idc | Table | Image distortion correction | | • | • | • |
| INANGTAB | _iac | Table | Incident angle correction | • | | • | • |
| LAMPTAB | _lmp | Table | Template CAL lamp spectra | • | | • | • |
| LFLTFILE | _lfl | Image | Low-order flat | • | • | • | • |
| MLINTAB | _lin | Table | Flux linearity | • | • | | • |
| MOFFTAB | _moc | Table | MAMA offset correction | • | | | • |
| PCTAB | _pct | Table | Photometry correction | • | | • | • |
| PFLTFILE | _pfl | Image | Pixel-to-pixel flat | • | • | • | • |
| PHOTTAB | _pht | Table | Photometric conversion | • | • | • | • |
| RIPTAB | _rip | Table | Echelle ripple | • | • | | • |
| SDCTAB | _sdc | Table | 2-D spectrum distortion correction | • | | • | • |
| SDSTFILE | _ssd | Image | Small-scale distortion correction (not available) | • | • | | • |

| | | | | | | | |
|----------|------|-------|--|---|---|---|---|
| SHADFILE | _ssc | Image | Shutter shading correction (not available) | • | • | • | |
| SPTRCTAB | _1dt | Table | 1-D spectrum trace | • | | • | • |
| SRWTAB | _srw | Table | Scattering reference wavelengths | • | | | • |
| TDCTAB | _tdc | Table | NUV dark correction | • | • | | • |
| TDSTAB | _tds | Table | Time dependent sensitivity correction | • | • | • | • |
| TELTAB | _tel | Table | Telescope point spread function | • | | | • |
| WAVECAL | _wav | Image | Wavelength calibration | • | | • | • |
| WCPTAB | _wcp | Table | Wavecal parameters | • | | • | • |
| XTRACTAB | _1dx | Table | 1-D extraction parameters | • | | • | • |

2.5 Error and Data Quality Array

2.5.1 The Error Array

2.5.2 Data Quality Flagging

The STIS pipeline propagates both statistical errors and data quality flags throughout the calibration process. These are then combined from both the science data and the reference file data to produce triplets of {SCI, ERR and DQ} in the calibrated direct and spectral imaging data.

Note that both the error and data quality image extensions may be represented with a null array (i.e., NAXIS=0 following STScI conventions) if all the values are identically zero (see [Table 2.9](#) and [STIS ISR 95-06](#)).

2.5.1 The Error Array

The error array contains an estimate of the statistical error at each pixel. In the raw file, the error array is empty. The first step of **calstis** is to calculate the error array for the input data. This raw data error is simply given as:

$$\sigma_{\text{DN}} = \frac{\sqrt{\sigma_c^2 + R \cdot g}}{g}$$

where:

- R is the observed data number (counts) minus the electronic bias of the pixel; note that the electronic bias is zero for the MAMA.
- g is the gain factor; note that the gain is unity for MAMA observations.
- σ_c is the read noise in electrons for CCD observations (it is set to zero for MAMA observations).

The bias, gain factor, and read noise are read from the CCD parameters reference file for CCD data (a `_ccd` file specified by keyword `CCDTAB`). As the data are calibrated through the **calstis** pipeline, the statistical errors are propagated through, reflecting both the science and reference file errors (see [STIS ISR 98-26](#) Section 6 for details).

2.5.2 Data Quality Flagging

Data quality flags are assigned to each pixel in the data quality extension. Each flag has a true (set) or false (unset) state. Flagged conditions are set as specific bits in a 16-bit integer word. For a single pixel, this allows for up to 15 data quality conditions to be flagged simultaneously, using the bitwise logical OR operation. Note that the data quality flags cannot be interpreted simply as integers but must be converted to base-2 and interpreted as flags. [Table 2.9](#) gives the specific conditions that are flagged, depending on the states of different bits (i.e., being on or off).

The raw data quality files will be filled only when there are missing (data lost) or dubious (software error) data. If no such errors exist, initialization will produce an empty data quality file whose header has NAXIS=0.

These flags are set and used during the course of calibration, and may likewise be interpreted and used by downstream analysis applications.

Table 2.9: STIS Data Quality Flags

| FLAG Value | Bit Setting ¹ | Quality Condition Indicated |
|------------|--------------------------|--|
| 1 | 0000 0000 0000 0001 | Error in the Reed-Solomon decoding (an algorithm for error correction in digital communications). |
| 2 | 0000 0000 0000 0010 | Lost data replaced by fill values. |
| 4 | 0000 0000 0000 0100 | Bad detector pixel (e.g., bad column or row, mixed science and bias for overscan, or beyond aperture). |
| 8 | 0000 0000 0000 1000 | Data masked by occulting bar. |
| 16 | 0000 0000 0001 0000 | Pixel having dark rate > 5 times the median dark level. |

| | | |
|-------|-------------------------|--|
| 32 | 0000 0000 001 0 0000 | Large blemish, depth > 40% of the normalized p-flat (repeller wire). |
| 64 | 0000 0000 01 00 0000 | Vignetted pixel |
| 128 | 0000 0000 1 000 0000 | Pixel in the overscan region. |
| 256 | 0000 0001 0000 0000 | Saturated pixel, count rate at 90% of max possible—local non-linearity turns over and is multi-valued; pixels within 10% of turnover and all pixels within 4 pixels of that pixel are flagged. |
| 512 | 0000 001 0 0000 0000 | Bad pixel in reference file. |
| 1024 | 0000 01 00 0000 0000 | Small blemish, depth between 40% and 70% of the normalized flat. Applies to MAMA and CCD p-flats. |
| 2048 | 0000 1 000 0000 0000 | >30% of background pixels rejected by sigma-clip, or flagged, during 1-D spectral extraction. |
| 4096 | 0001 0000 0000 0000 | Extracted flux affected by bad input data. |
| 8192 | 001 0 0000 0000 0000 | Data rejected in input pixel during image combination for cosmic ray rejection. |
| 16384 | 01 00 0000 0000 0000 | Extracted flux not CTI corrected because gross counts are 0. |

1 The most significant bit is on the left in this representation.

2.6 STIS Coordinate Systems

[2.6.1 Spacecraft, User, and Aperture Frames](#)

[2.6.2 CCD Binned Pixel and Sub-array Coordinates](#)

2.6.1 Spacecraft, User, and Aperture Frames

References to multiple coordinate systems appear in the headers of STIS data, tied to the spacecraft frame, the user frame, and the aperture frame. We briefly explain here the relationships among these coordinate systems.

The three coordinate systems of interest are the:

- Vehicle Frame (V_1, V_2, V_3): The right-handed coordinate system for the telescope, with V_1 pointing in the direction the telescope is looking.
- User Frame ($X_{\text{user}}, Y_{\text{user}}$): This is the user frame, aligned with the detector.
- Aperture Frame ($X_{\text{aperture}}, Y_{\text{aperture}}$): This frame is aligned with the slit. POS-TARG movements are aligned with the aperture frame.

The angles associated with these frames that appear in the headers of STIS data files are:

- PA_V3: The position angle of the V_3 axis; the angle from North, towards East, to V_3 , measured at the center of the *HST* focal plane (in the `_spt` header).
- ROLL_AVG: The average angle from North towards East to V_3 , measured at the position of the STIS field in the *HST* focal plane (in the `_jit` header, computed).
- PA_APER: The angle from North through East to Y_{aperture} measured at the aperture reference (in the science header). PA_V3 - PA_APER is either 225 or -135 degrees, with small variations (a few tenths of a degree).
- ORIENTAT: The angle from North through East to Y_{user} measured at the aperture reference (in science header). It can differ from PA_APER by up to ~1.5 degrees (e.g., for the long slits with offset occulting bars). Note that this is not the same angle as the ORIENT specified in Phase II, which gives the position angle of the U_3 axis, where $U_3 = -V_3$. For further information on slit

orientation while planning STIS observations, see [Figure 3.2](#) and “Fixing Orientation on the Sky” in [Chapter 11](#) of the *STIS Instrument Handbook*.

2.6.2 CCD Binned Pixel and Sub-array Coordinates

The STIS CCD detector supports on-chip binning by factors of 2 and 4 in each dimension. This option was often used early in the operational life of the instrument to increase the signal-to-noise for faint targets, but became less favorable as the number of hot pixels increased over time. The readout of subarrays, with less than the full dimension in Y, is also supported to reduce the readout time. These modes are discussed in [Section 11.1.1](#) of the *STIS Instrument Handbook*.

Reference files for the CCD use unbinned full-frame coordinates $(X_{\text{ref}}, Y_{\text{ref}})$ after overscan trimming. The coordinates in a trimmed science image (X, Y) are related to these reference coordinates by values given in keywords in the primary header:

$$\begin{aligned} X &= (X_{\text{ref}} \times \text{LTM1_1}) + \text{LTV1} \\ Y &= (Y_{\text{ref}} \times \text{LTM2_2}) + \text{LTV2} \end{aligned}$$

[Table 2.10](#) gives examples of coordinates and conversion parameters for datasets with different binnings (BINAXIS1, BINAXIS2) and array size (NAXIS1, NAXIS2). The image coordinates of the reference pixel (CRPIX1, CRPIX2) are near the center of the image.

Table 2.10: Coordinates and Conversion Parameters for Binned Data

| Image Type: File | NAXIS1 | CRPIX1 | BINAXIS1 | LTM1_1 | LTV1 |
|--|---------------|------------------|-----------------|---------------|--------------------|
| 1x1 full array: o8sv05010_fit | 1024 | 517.90 | 1 | 1.00 | 0.00 |
| 2x1 full array: o4an07020_fit | 511 | 258.70 | 2 | 0.50 | -0.25 |
| 1x1 subarray: o5f1020g0_fit o8ma92030_fit | 1024 1024 | 517.90 517.90 | 1 1 | 1.00 1.00 | 0.00 0.00 |
| Image Type: File | NAXIS2 | CRPIX2 | BINAXIS2 | LTM2_2 | LTV2 |
| 1x1 full array: o8sv05010_fit | 1024 | 516.67 | 1 | 1.00 | 0.00 |
| 2x1 full array: o4an07020_fit | 1024 | 516.67 | 1 | 1.00 | 0.00 |
| 1x1 subarray: o5f1020g0_fit o8ma92030_fit | 512 400 | 256.67 200.67 | 1 1 | 1.00 1.00 | -260.00 -316.00 |

Chapter 3: STIS Calibration

3.1 Pipeline Processing Overview

During operation, telemetry containing STIS science data is downlinked through a TDRSS satellite to a ground station in White Sands, NM. From there it is sent to Goddard Space Flight Center where the PACOR data capture facility collects the downlinked science data into telemetry “pod files”. These pod files are then transmitted to STScI where they are saved to a permanent storage medium. The STScI ingest pipeline then unpacks the data, extracts keywords from the telemetry stream, reformats the data, and repackages them into raw, uncalibrated, but scientifically interpretable data files. These raw files are then processed by the **calstis** software to produce a variety of calibrated data files. The results of these procedures are then used to populate the databases that form the searchable archive catalog describing the individual instrument exposures.

The STIS calibration pipeline, **calstis**, performs the calibration of STIS science data and is available to the community in the **AstroConda** package **stistools**. Most **calstis** modules were written in the C programming language, and may be called with Python wrapper interfaces, which are documented at <https://stistools.readthedocs.io/>, and are explained further in [Chapter 5](#). Previously, STIS data taken prior to the 2004 Side-2 electronics failure were statically archived, and calibrated data products did not benefit from updates to **calstis** routines. However, those pre-SM4 data have now been recalibrated with the most recent version of **calstis** and will now be automatically reprocessed whenever relevant updates to the pipeline are implemented.

Conceptually, **calstis** is several pipelines in one, reflecting the complexity and diversity of STIS observing modes. Your STIS data will have been calibrated to different levels, depending on their nature:

- ACQs and ACQ/PEAKs are not calibrated by **calstis**; you will get only the raw data from observations taken in these modes.
- All other science data are processed through basic two-dimensional image reduction (available as **basic2d** in **stistools**), which includes such things as bias subtraction, dark subtraction, flat fielding, and linearity correction. In the case of CCD CR-SPLIT or REPEATOBS data, your data will also be passed through cosmic ray rejection (available as **ocrreject** in **stistools**).
- Data taken in TIME-TAG mode are available from the archive as both event streams (rootname_tag.fits binary tables), and as raw images equivalent to those produced for ACCUM mode observations. For TIME-TAG data, the accumulation into an image is done by the ground system, rather than onboard the spacecraft as is the case for ACCUM mode data. The **calstis** software as run in the

pipeline uses these raw image files as input in either case, and does not distinguish between TIME-TAG and ACCUM mode data. The **calstis** pipeline software does not operate on the `_tag` event files; (see [Section 5.6](#) for a discussion of how to analyze these files).

- For MAMA data, the input raw data format is 2048×2048 (so called *high-res* pixels), while the calibrated data are binned by the pipeline to 1024×1024 native format pixels (see [Section 3.4.17](#)).
- Spectral data that were taken using a sufficiently small aperture, and which were also taken together with a wavelength calibration spectrum, are then passed through spectroscopic reduction to produce flux and wavelength calibrated science data. For first order spectra modes, a two-dimensional rectified spectral image is produced, and for both echelle and first order modes, a one-dimensional, background subtracted spectrum is also produced. For first order spectral observations where the target was behind the fiducial bars of one of the long slits, only two-dimensional rectified spectra are produced.
- Spectral data taken with very large apertures are treated as slitless observations. For such data, as well as for data taken without contemporaneous wavecal observations, the presumption is that the target location along the dispersion direction is too uncertain to assign a reliable wavelength scale. No flux or wavelength calibrated spectra are produced by the pipeline for such observations. The definition of which apertures are treated as slitless varies depending on the grating in use.

See [Chapter 2](#) for the naming conventions of the various input, intermediate, and output calibrated files.

As with the calibration pipelines for the other *HST* instruments, the specific operations that are performed during calibrations are controlled by *calibration switches*, which are stored in the image headers as `KEYWORD=VALUE` pairs. Any given step in the calibration process may require the application of zero, one, or more *calibration reference files*, the names of which are also found in the image header. The names of the keywords containing the switches and reference file names were introduced in the previous chapter; [Section 3.3](#) will outline the role these keywords play in the data reduction, and description of the calibration steps are given in [Section 3.4](#). The path your data files take through the pipeline is determined by the calibration switches set in the primary header of the `_raw` data, which in turn depends directly on the type of data you have.

A few other general comments are in order. It is important to note that some of the STIS calibration reference data are obtained contemporaneously with the science observations. These data may be used to refine the calibration process (as with the automatic wavecal), or may require you to replace a default calibration reference file with a contemporaneously obtained one, as in the case of a CCD near infrared (NIR) fringe flat. The details of how these contemporaneous calibration files are used in calstis can be found in [Section 3.4](#). The STIS pipeline is also unusual in that they are *re-entrant*. That is, a user running **calstis** off-line may choose to reprocess STIS data partially, performing one or more of the intermediate steps without re-exercising the complete **calstis** pipeline, for instance to perform cosmic ray rejection or one dimensional spectral extraction. Refer to [Section 3.5](#) for the mechanics (and restrictions) of this kind of processing. Finally, as with other *HST* pipelines, **calstis** propagates statistical errors and tracks data quality flags throughout the calibration process.

3.2 Structure of calstis

Calstis consists of a series of individual modules that:

- Orchestrate the flow through the pipeline.
- Perform the preliminary tasks of basic two-dimensional image reduction (e.g., overscan subtraction, bias subtraction).
- Reject cosmic rays from CCD data.
- Perform the remaining tasks of basic two-dimensional image reduction (e.g., dark subtraction, flat fielding).
- Process the contemporaneously obtained wavecal data to obtain the zero point shifts in the spectral and spatial directions.
- Perform spectroscopic wavelength and flux calibration.
- Sum any REPEATOBS exposures.

[Table 3.1](#) describes in more detail the individual modules in **calstis** and what they do. The **stistools** task that can be used to run a particular segment of the pipeline independently is also provided (see [Section 3.5.2](#)).

Table 3.1

| stistools task | Description of Processing Modules | Module 1 |
|------------------------------------|---|-----------------|
| Full Pipeline | | |
| calstis | “Wrapper” program calls each of the calstis tasks as needed , according to the switches set in the <i>primary header</i> of the input file. The calstis constituent tasks can instead be executed independently when recalibrating. | <i>calstis0</i> |
| Initial 2-D Image Reduction | | |

| | | |
|---|--|------------------|
| basic2d | Fundamental steps of 2-D image reduction. This module is called to initialize the data quality array from the bad pixel table, to trim the overscan regions and subtract the bias level, and to subtract the bias image (before cosmic ray rejection for CCD data), then to subtract the dark image and perform flat fielding (after cosmic ray rejection). It assigns values to the error arrays and computes some simple statistics. | <i>calstis1</i> |
| ocrreject | Detect and remove cosmic rays in CCD data. This module identifies cosmic rays (by optionally flagging them in the input file) for multiple images taken at the same pointing. The input images are then co-added, resulting in an image with cosmic rays removed. | <i>calstis2</i> |
| Contemporaneous Wavecal Processing | | |
| wavecal | Determine MSM offset from wavecal. This step is used in conjunction with <i>calstis7</i> , <i>calstis11</i> , and <i>calstis12</i> . Its purpose is to find the offset of the spectrum from the expected location, owing to nonrepeatability of the mode select mechanism. The shift is written into the SCI extension header of the input wavecal image. | <i>calstis4</i> |
| | Subtract science image from wavecal. For CCD wavecal observations taken with the HITM system prior to 1998-Nov-9, the detector is exposed to both the wavecal and the science target (after this date, the external shutter would be closed). This task reads both the wavecal and science files and subtracts the science data from the wavecal. Following this step, <i>calstis4</i> can be used to determine the spectral shift. | <i>calstis11</i> |
| | Write spectral shift value to science header. A series of science images (i.e., CR-SPLIT or REPEATOBS) and wavecals may have been taken, with the wavecals interspersed in time among the science images. For each image in the science file, this task linearly interpolates the wavecals to the time of the science image, and then writes the keyword values <i>SHIFTA1</i> , <i>SHIFTA2</i> for the spectral and spatial shifts, respectively, to the science header. | <i>calstis12</i> |
| Spectroscopic Calibration, Extraction, and Rectification | | |

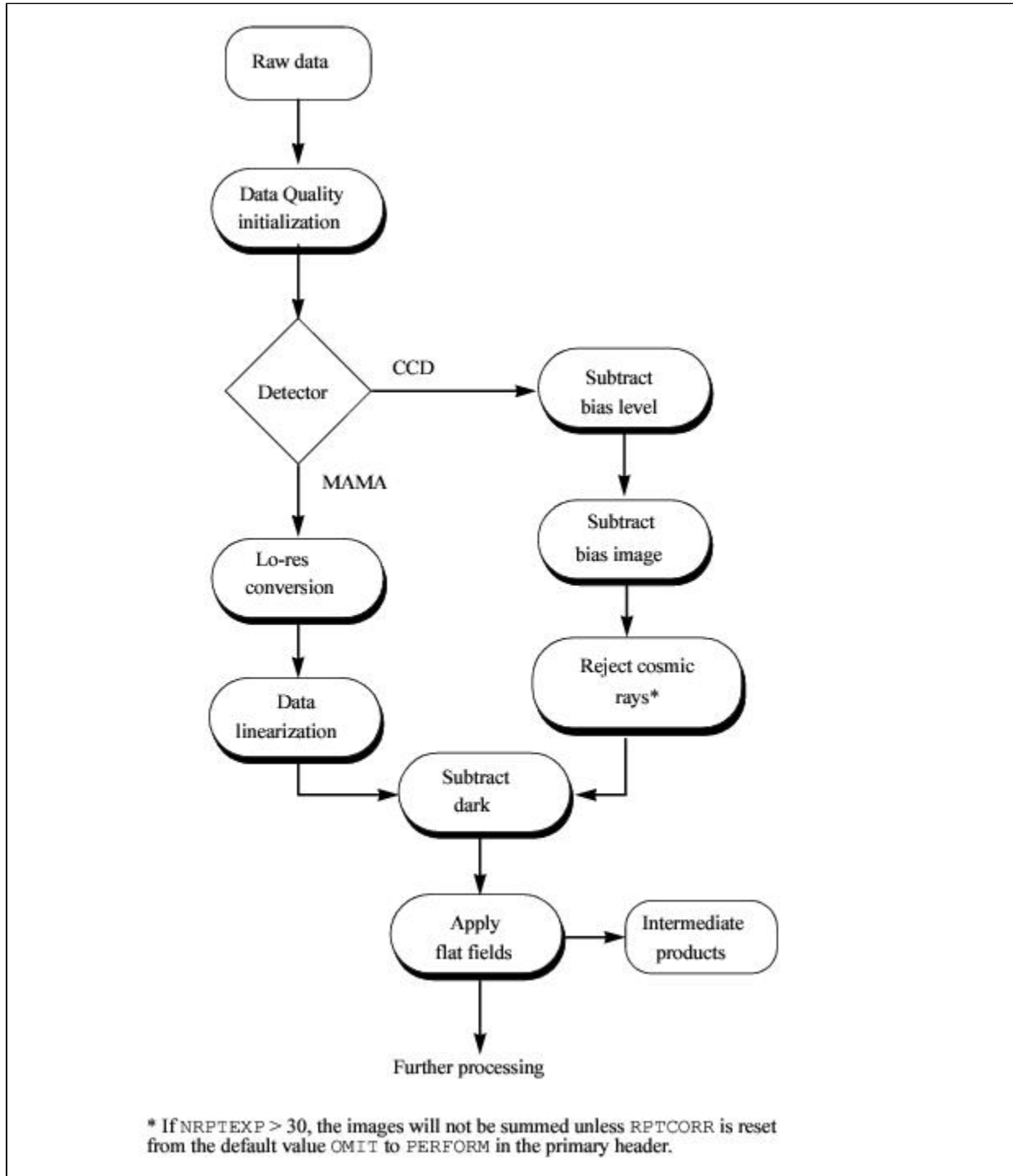
| | | |
|-------------------|---|-----------------|
| x1d | 1-D spectral extraction. This task is most appropriate for observations of a point source. A spectrum is extracted along a narrow band, summed over the cross-dispersion direction and background values subtracted to produce a 1-D array of fluxes for each spectral order. An array of wavelengths is generated, with each output spectrum written to a separate row of a FITS binary table, together with the arrays of the gross, net, and background count rates. One output table is generated for each image in a series of REPEATOBS data. For echelle observations, x1d and the echelle scattered light correction routine are called iteratively, to calculate the echelle background. | <i>calstis6</i> |
| x2d | 2-D rectification. This task performs geometric correction for direct imaging or long slit spectroscopic data. For the latter, it produces a spectral image that is linear in both wavelength and spatial directions. | <i>calstis7</i> |
| Sum Images | | |
| | Sum REPEATOBS data. This task adds together (pixel by pixel) multiple MAMA images, and combines them into one FITS file. This would not normally be used for CCD data because they would already have been combined for cosmic ray rejection. | <i>calstis8</i> |

¹ Referenced in the trailer file.

Below, we present a series of flow charts that provide a more complete overview of the processing of data through the **calstis** pipeline, starting with the fundamental steps of two-dimensional image reduction.

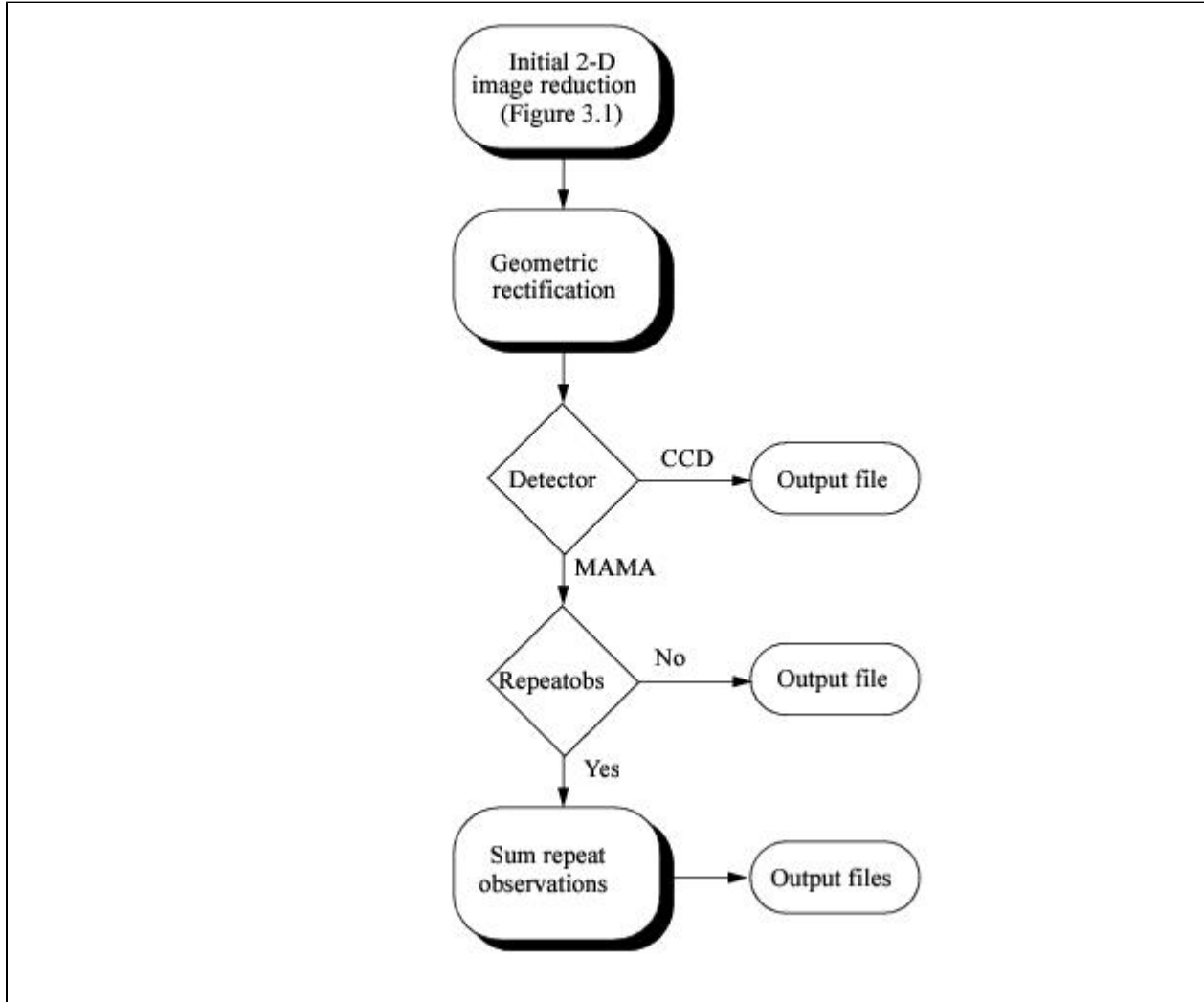
[Figure 3.1](#) shows the initial steps in the routes taken by CCD data and by MAMA data.

Figure 3.1: Initial 2-D Image Reduction (First Step in Subsequent Flowcharts)



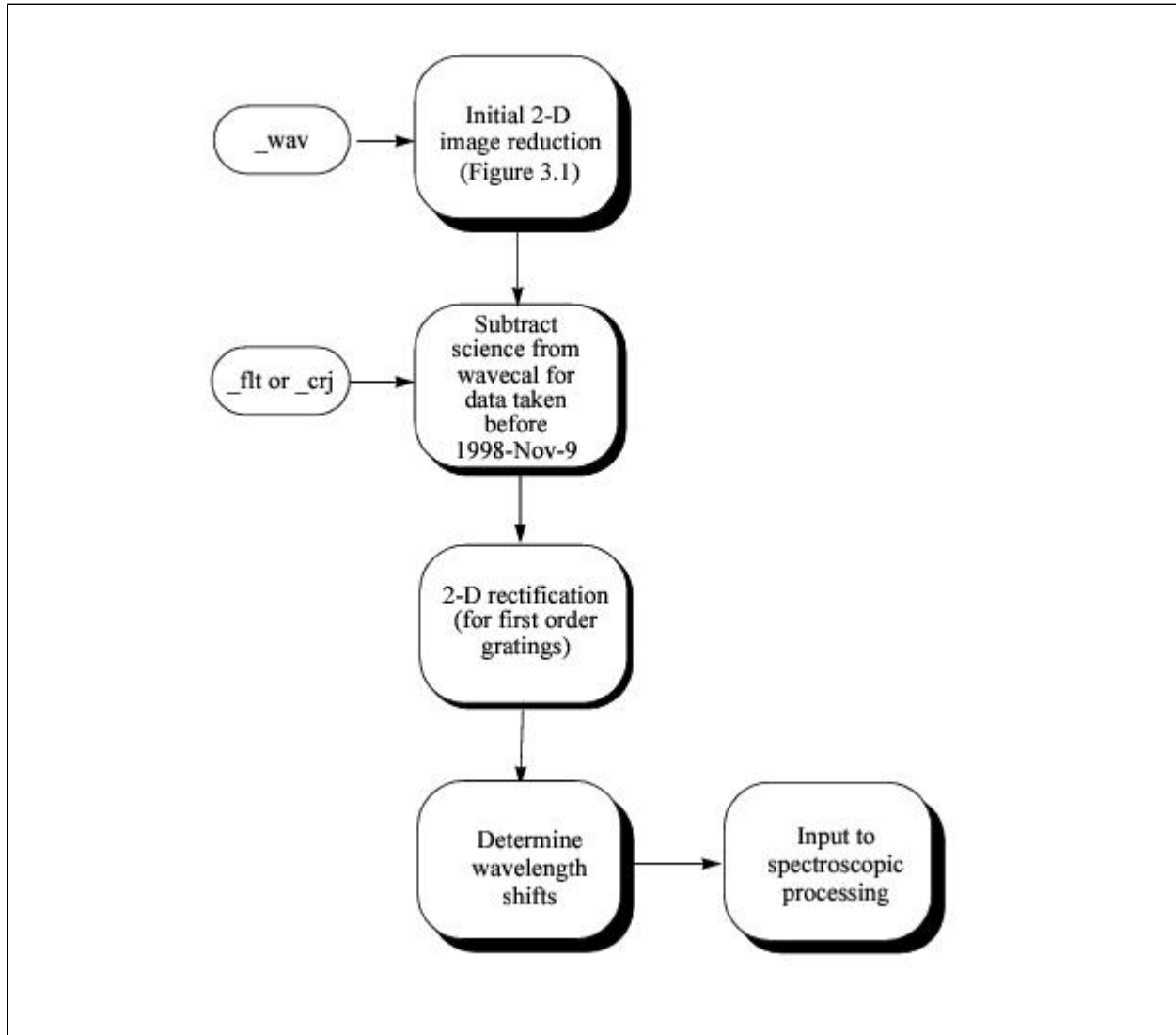
The calibration beyond the initial 2-D image processing depends upon whether the data are obtained in imaging or spectroscopic mode. For imaging modes, for example, ([Figure 3.2](#)), the primary operations in **calstis** are geometric distortion correction and photometric calibration, and a summation of multiple MAMA exposures if `NRPTEXP > 1`. The output is a geometrically rectified image with suffix `_x2d` or `_sx2`, and header keywords that specify the photometric calibration. When geometric correction is not applied, the output will be flat-fielded data with suffix `_crj`, `_flt`, or `_sfl`.

Figure 3.2: Schematic of calstis for Secondary Image Processing



For spectroscopic exposures, **calstis** will process the associated wavelength calibration exposure (wavecal; [Figure 3.3](#)) to determine the zero point offsets (SHIFTA1 , SHIFTA2) in the dispersion and cross-dispersion directions, thereby correcting for the lack of repeatability of the mode select mechanism (MSM) or for thermal drift. These keywords are written into the science header of the flat-fielded (MAMA or single exposure CCD) or cosmic ray rejected (CCD) image.

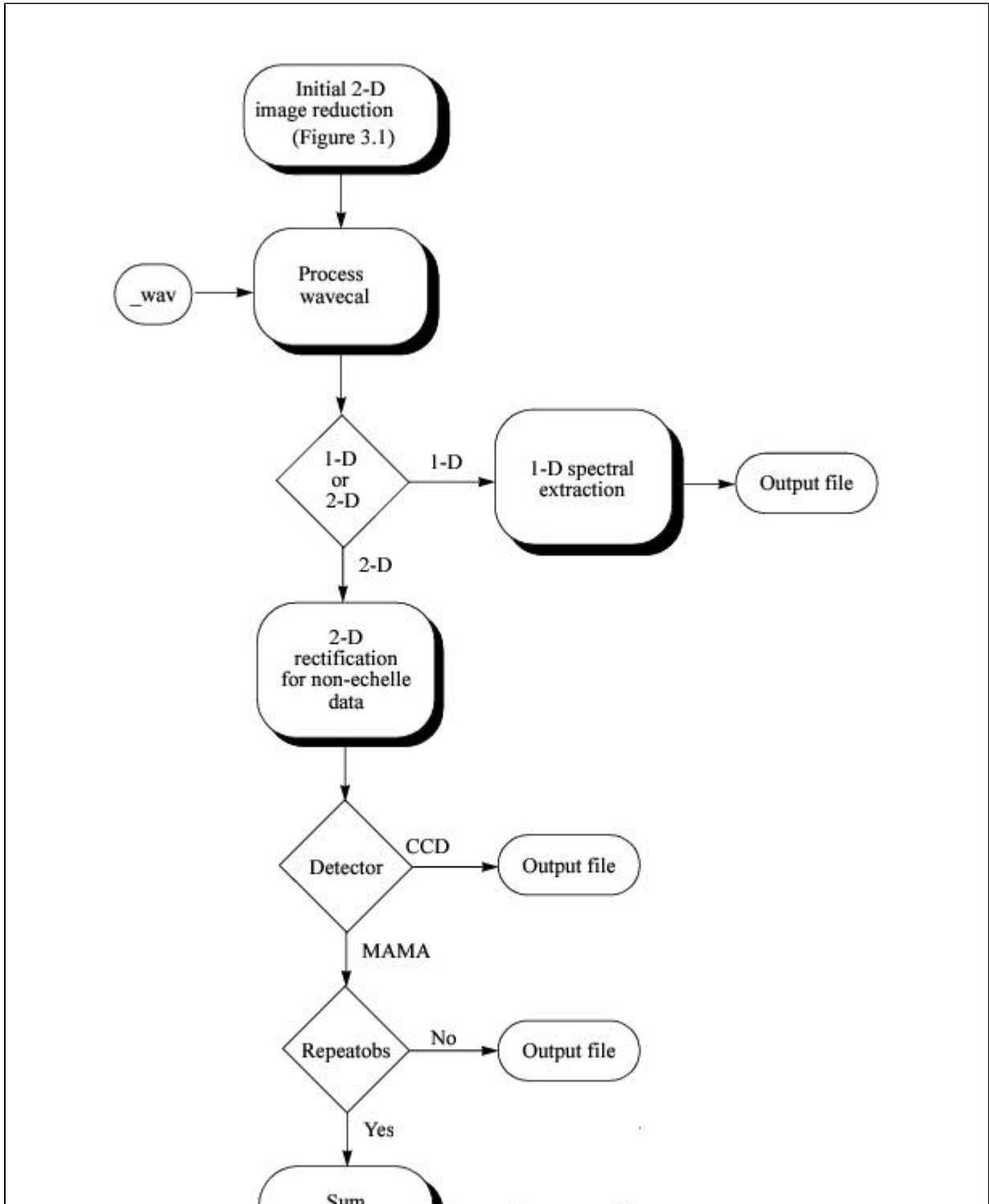
Figure 3.3: Schematic of calstis for Contemporaneous Wavecals



Two-dimensional spectral processing (Figure 3.4) produces a flux calibrated, rectified spectroscopic image with distance along the slit running linearly along the y-axis and dispersion running linearly along the x-axis.

One-dimensional spectral extraction produces a one-dimensional spectrum of flux versus wavelength (in the `_x1d` or `_sx1` file), uninterpolated in wavelength space, but integrated across an extraction aperture in the spatial direction. Figure

3.4: Schematic of calstisfor Spectroscopic Data





3.3 Data Flow Through calstis

This section details the data flow through the calstis pipeline for each calibrated operating mode, showing the switches, the reference file inputs, the science file inputs, and the output products. These details are shown as flow charts in [Figure 3.5](#) through [Figure 3.11](#). The following section describes the tasks corresponding to the various calibration switches.



Note that some tasks are not implemented at this time. These appear in grey text in the flow charts, and are noted in the descriptions given in the subsequent section.

Figure 3.5: 2-D CCD Data Reduction Common to Imaging and Spectroscopy

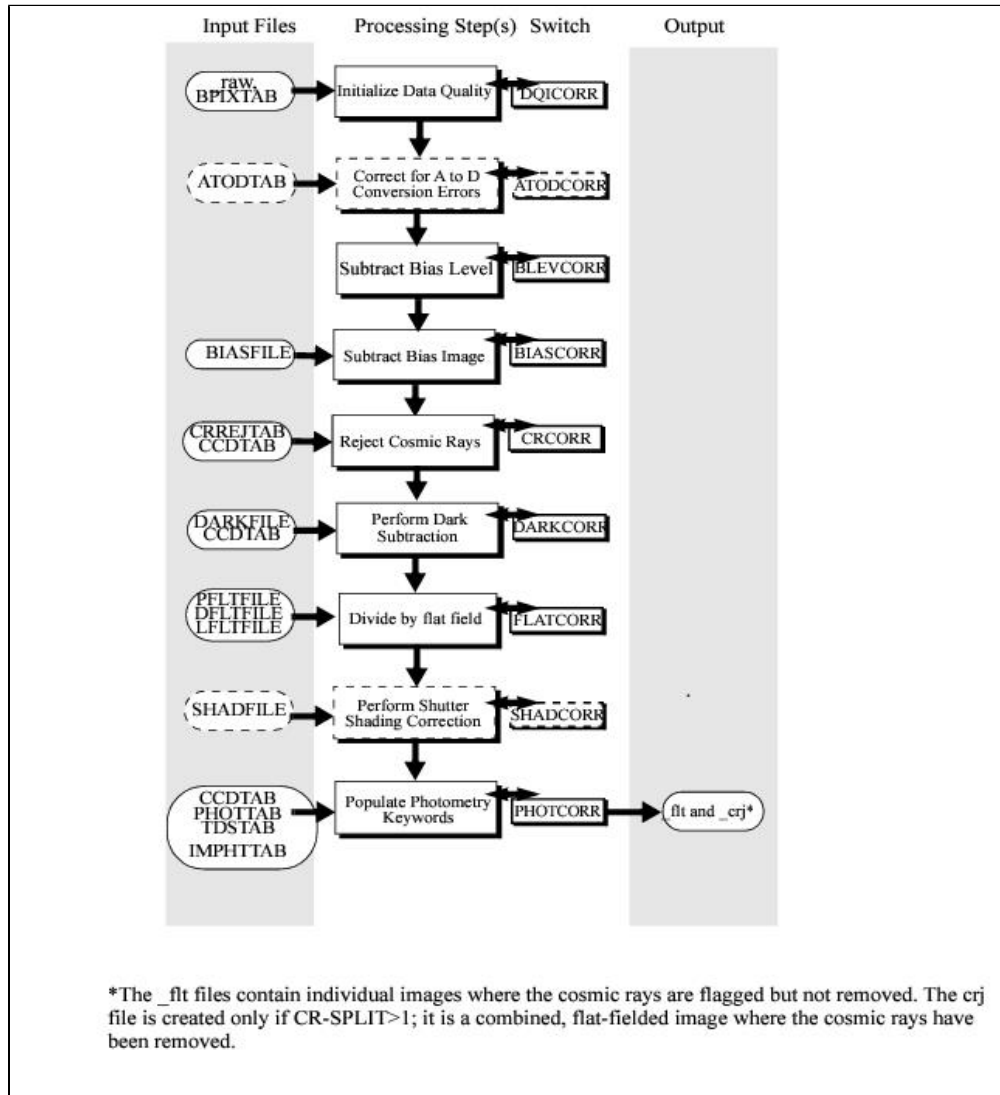


Figure 3.6: 2-D MAMA Data Reduction Common to Imaging and Spectroscopy

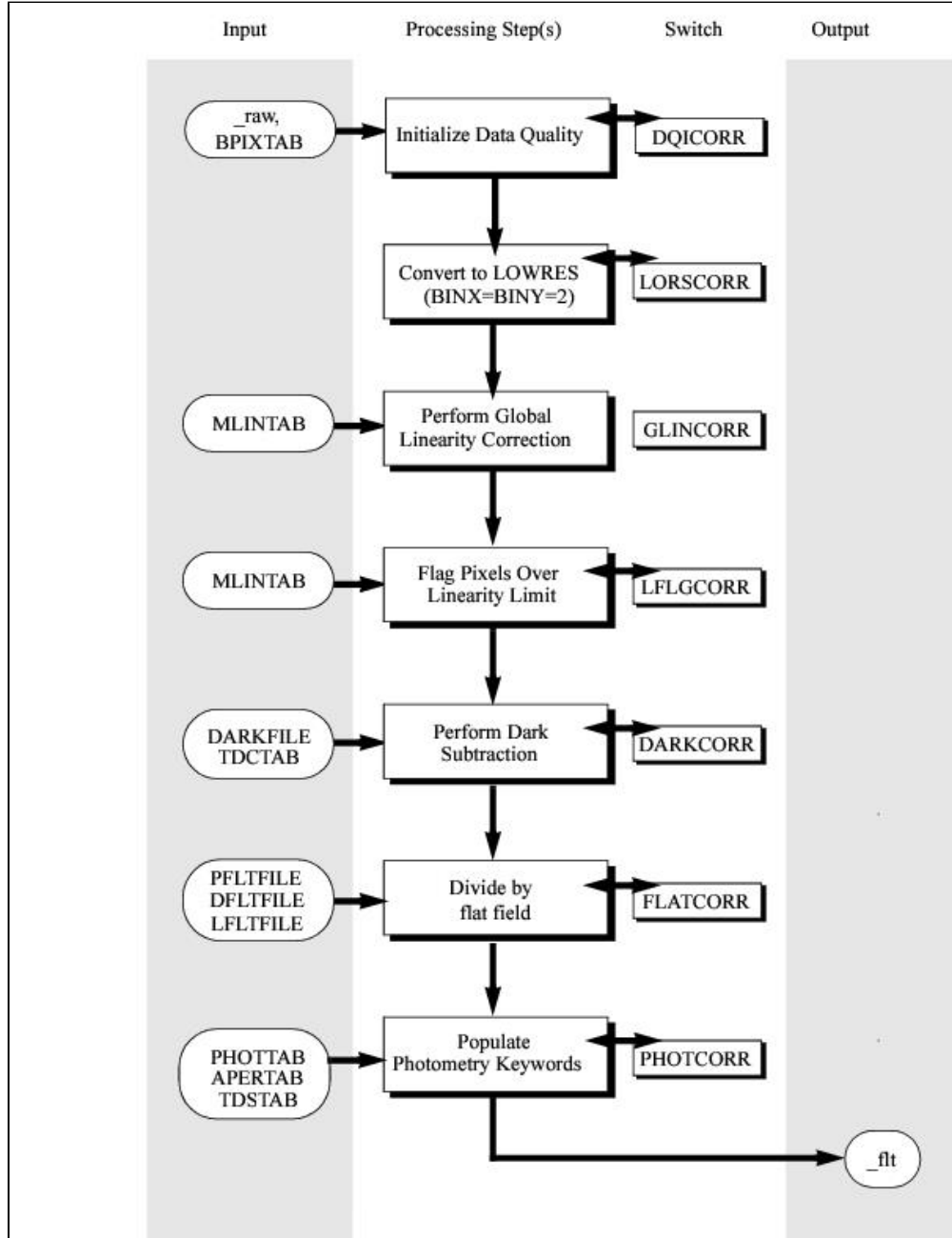


Figure 3.7: Flow of Imaging Data through Calstis-7, 2-D Rectification

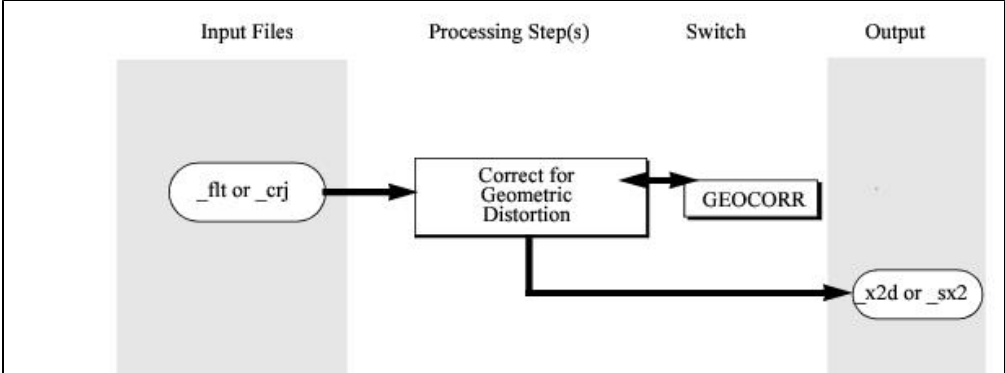


Figure 3.8: Flow of Spectroscopic Data through Calstis-4, wavecal Processing

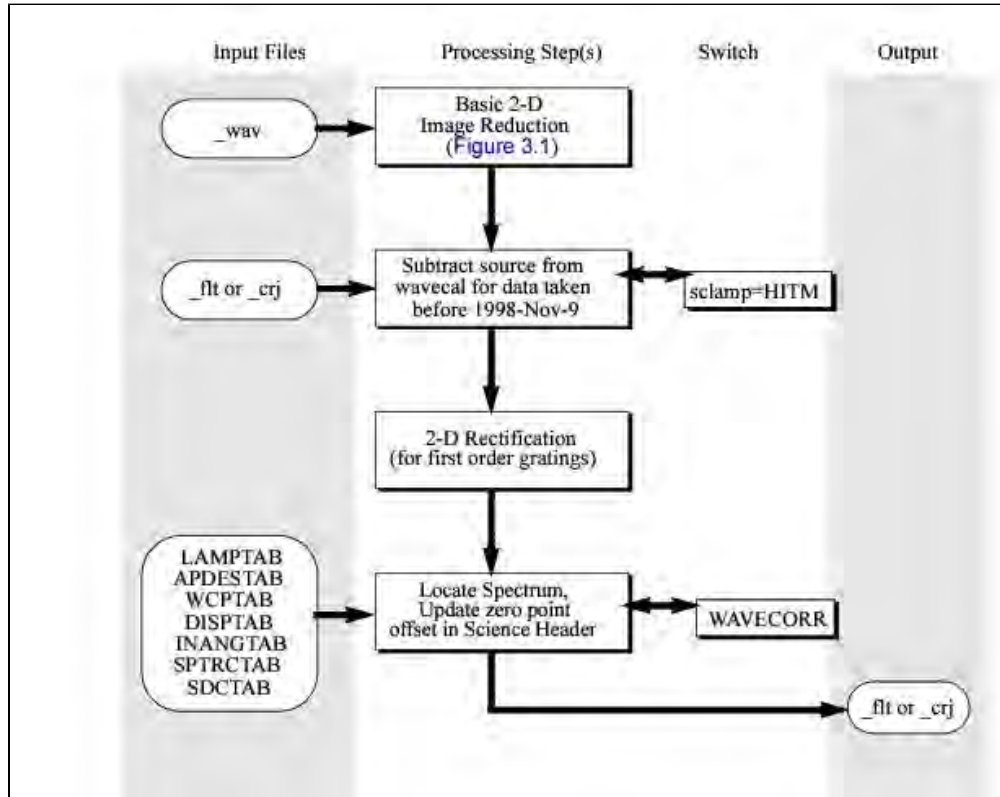


Figure 3.9: Flow of Spectroscopic Data through calstis-6, 1-D Extraction

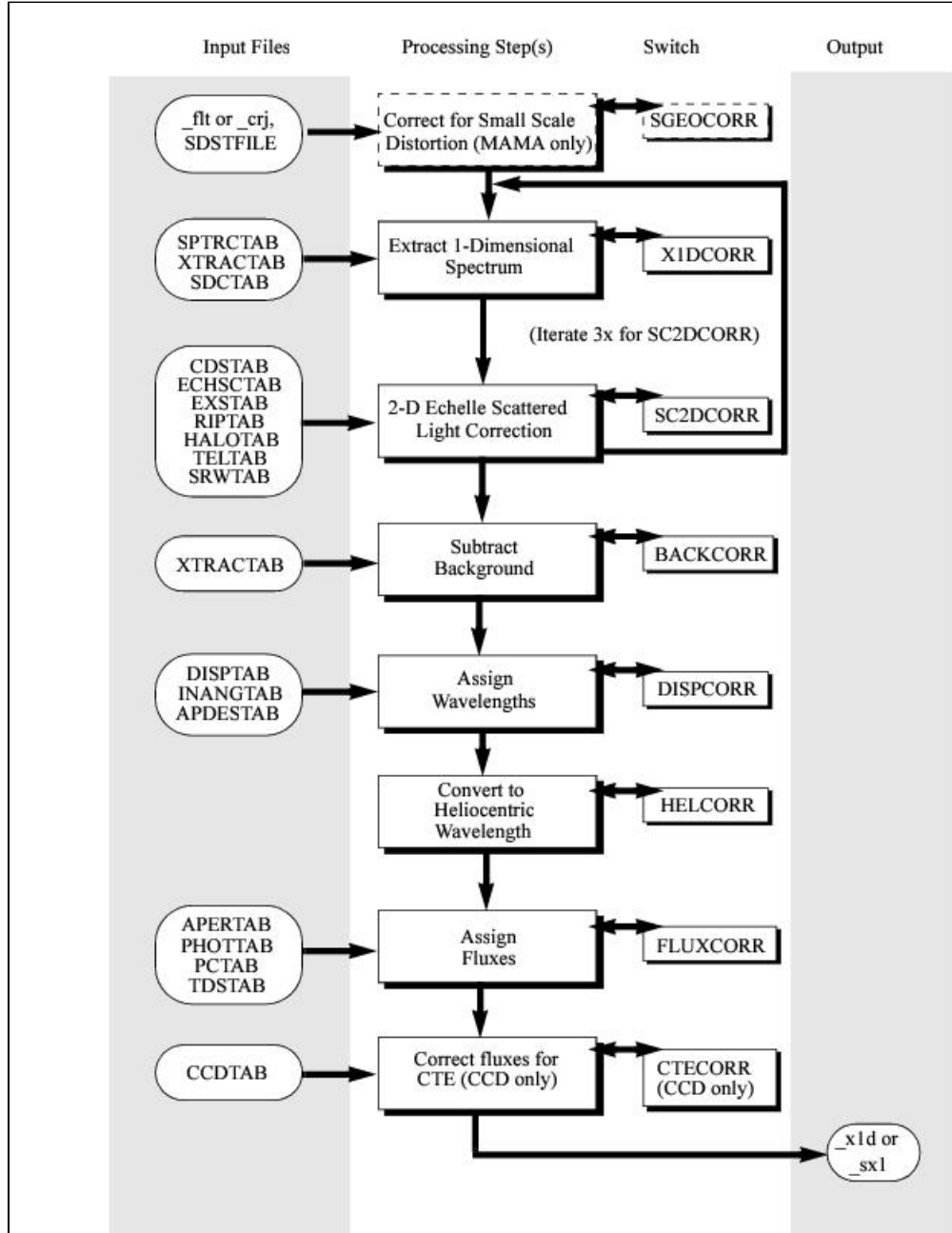


Figure 3.10: Flow of Spectroscopic Data through calstis-7, 2-D Rectification

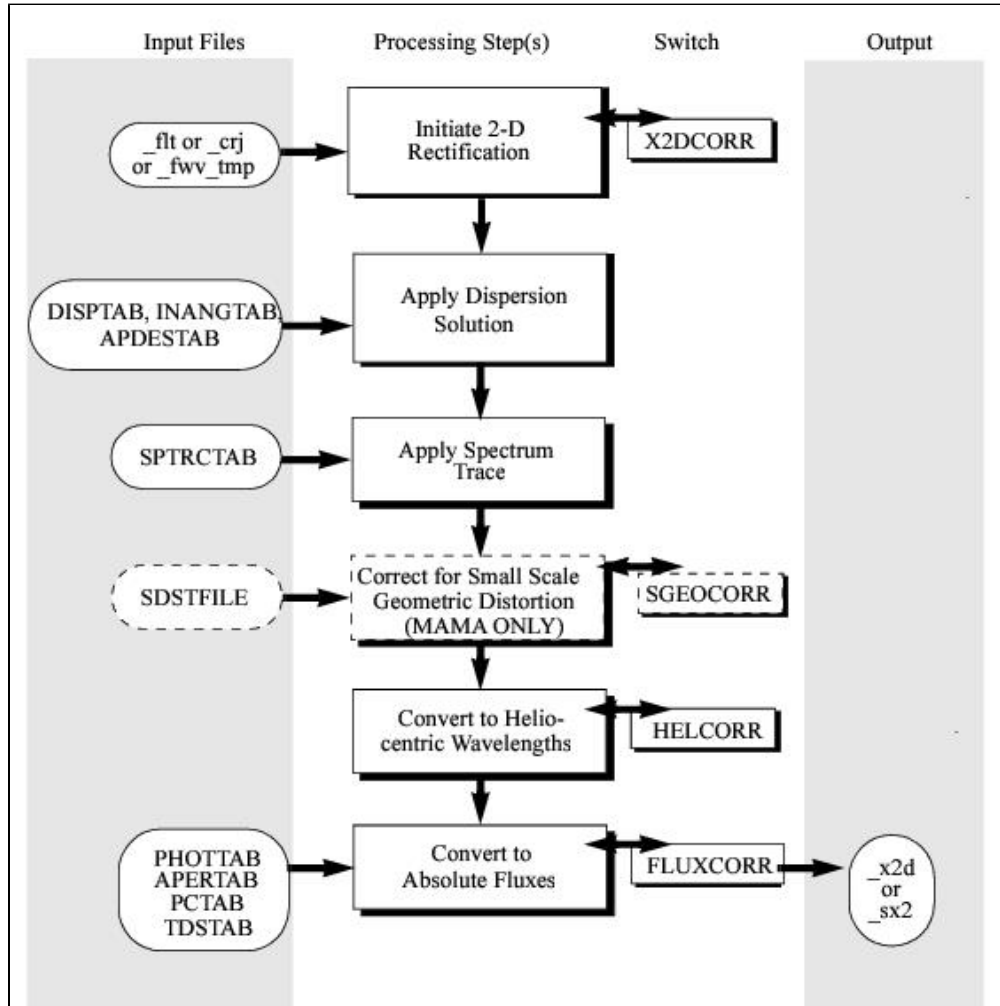
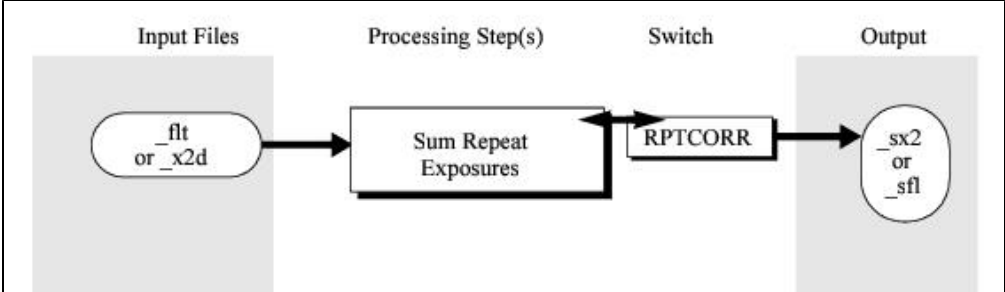


Figure 3.11: Flow through calstis-8, Summing MAMA REPEATOBS Exposures



3.4 Descriptions of Calibration Steps

- 3.4.1 ATODCORR: Analog to Digital Conversion Correction
- 3.4.2 BACKCORR: 1-D Spectral Background Subtraction
- 3.4.3 BIASCORR: Small Scale Bias Subtraction
- 3.4.4 BLEVCORR: Large Scale Bias & Overscan Subtraction
- 3.4.5 CRCORR: Cosmic Ray Correction
- 3.4.6 CTECORR: Correction for Charge Transfer Inefficiency Losses
- 3.4.7 DARKCORR: Dark Signal Subtraction
- 3.4.8 DISPCORR: Apply Dispersion Solution
- 3.4.9 DOPPCORR: Correct Reference Files for Doppler Shift
- 3.4.10 DQICORR: Initialize Data Quality File
- 3.4.11 EXPSCORR: Retain Individual CR-SPLIT Exposures
- 3.4.12 FLATCORR: Flat Field Correction
- 3.4.13 FLUXCORR: Conversion to cgs Flux
- 3.4.14 GEOCORR: Geometric Distortion Correction
- 3.4.15 GLINCORR and LFLGCORR: Nonlinearity Corrections
- 3.4.16 HELCORR: Correction to Heliocentric Reference Frame
- 3.4.17 LORSCORR: Conversion to Native Format MAMA Pixels
- 3.4.18 PHOTCORR: Populate Photometry Header Keywords
- 3.4.19 RPTCORR: Sum Repeated MAMA Observations
- 3.4.20 SC2DCORR: Echelle Scattered Light Correction
- 3.4.21 SGEOCORR: Small Scale Distortion Correction
- 3.4.22 SHADCORR: CCD Shading Correction
- 3.4.23 WAVECORR: Wavecal Correction
- 3.4.24 X1DCORR: Locate and Extract 1-D Spectrum
- 3.4.25 X2DCORR: Produce Rectified 2-D Spectral Image

In this section we provide a more detailed description of the algorithms applied by **calstis**. As always, a given step will be performed on your data if the corresponding calibration switch in the global header of the input data was set to `PERFORM` (see [Chapter 2](#)). The algorithms below are described according to the major component of the **calstis** pipeline in which they are used, namely:

- Two-dimensional image reduction, including basic 2-D reduction, cosmic ray rejection and image co-addition.
- Processing of the contemporaneously obtained wavecal.
- Two-dimensional rectification and one-dimensional spectral extraction, with flux and wavelength calibration.

Within each component, the individual steps are listed alphabetically, because the order in which they are performed can change for different types of data (e.g., CCD or MAMA, spectroscopic or imaging, CR-SPLIT or not).

More detailed descriptions can be found in a series of *Instrument Science Reports (ISRs)* that discuss the pipeline. Be aware, however, that while these reports describe the original design of the pipeline and the associated algorithms in detail, they do not always contain information concerning later modifications.

3.4.1 ATODCORR: Analog to Digital Conversion Correction

- Reference file: ATODTAB

This step is part of 2-D image reduction and applies only to CCD data. *Ground test results show that this correction is not currently needed, so the ATODCORR switch and the ATODTAB reference file keywords are omitted from FITS file headers.* An analog to digital correction would be applied if the CCD electronic circuitry that performs the analog to digital conversion were biased toward the assignment of certain DN (data number) values.

3.4.2 BACKCORR: 1-D Spectral Background Subtraction

- Reference file: XTRACTAB

This step is a part of spectral extraction and applies to one-dimensional extraction only. If the calibration switch BACKCORR is PERFORM, the background is calculated and subtracted from the extracted spectrum. The background is extracted from regions above and below the spectrum on the detector. The size and offsets of these two background regions are specified by the BK1OFFST, BK2OFFST, BK1SIZE, and BK2SIZE columns in the XTRACTAB reference table.

For most first order spectral modes, the default background parameters, as implemented in the XTRACTAB reference table, specify background regions 5 pixels wide located ± 300 pixels away from the center of the spectral extraction region. Exceptions are made for special aperture positions. For the E1 and E2 positions which are located at row 900 of the CCD, both background regions are offset below the spectral trace. For the FUV MAMA D1 aperture positions, which are located near the bottom of the FUV MAMA detector, below the region of enhanced dark current, (see [Section 4.1.3](#)), the background regions are only ± 30 pixels from the trace. The assumption is that most observations specifying the D1 position will be of very faint point source targets, where measuring an accurate local background is critical. See [Table 3.1](#) for a summary of the default background extraction parameters implemented in the XTRACTAB reference table.

Table 3.1: Default Background Parameters

| Spectral Mode | BK1SIZE, BK2SIZE | BK1OFFST | BK2OFFST | BACKORD |
|---------------------------|---------------------|-----------------------------|-----------------------------|---------|
| CCD E1/E2 positions | 5 | -300 | -320 | 0 |
| Other CCD positions | 5 | -300 | 300 | 0 |
| MAMA D1 positions | 5 | -30 | 30 | 0 |
| MAMA echelle spectra | 5 | varies by spectral order | varies by spectral order | 0 |
| All other MAMA spectra | 5 | -300 | 300 | 0 |

The background extraction is done one column at a time, with the average background values (in counts /sec/pixel) calculated (with 3 clipping) from each background bin, accounting for fractional pixel contributions. The background in each region is then smoothed with an algorithm that depends on the mode in use.

For CCD data, the raw background, after 1-D extraction, is smoothed by a running window low-pass filter (i.e. boxcar smoothing) with a 9 pixel window, then fitted by an nth degree polynomial. The value of the *bksmode* parameter defines the boxcar smoothing function to be either a median or average within the running window. The polynomial degree is defined by the *bksorder* task parameter. The default value for the *bksorder* parameter is 3, and this is what is used in the pipeline.

For MAMA first order data, the 1-D extracted background is fitted by an nth degree polynomial, and the background is replaced by the fitted curve. The data are not filtered before the polynomial fit, and so for MAMA first order data, the result is the same whether *bksmode* is set to *median* or *average*. The polynomial degree is defined by the *bksorder* task parameter. For the G140L/M first order gratings, the regions around Lyman and the 1300 Angstrom O I line are not smoothed.

The background vectors for the two background regions are then combined, either by simply taking the average value at each wavelength (*backord=0*), or by linear interpolation between the upper and lower regions values (*backord=1*). The parameter *backord* is read from the XTRACTAB reference table. The total background at each pixel in the output spectrum is then written to the output data table.

In general, the background or sky is not aligned with the detector pixels. To accommodate this misalignment, the definition of the background extraction apertures includes not only a length and offset (center-to-center) but also a linear tilt to assist in properly subtracting the background. This tilt is taken into account when calculating the average background in the background extraction boxes. The coefficients describing this tilt are given in the BKTcoeff column of the XTRACTAB table.

For echelle data, the default is to determine the background as part of the SC2DCORR calibration step. However, the background can optionally be determined by direct measurement in a background region by setting SC2DCORR to OMIT, and this simpler background subtraction is needed in any case in the early stages of the SC2DCORR procedure. When the background subtraction is done in this way for echelle observations, the measured background is smoothed twice with a 31 pixel wide boxcar window.

3.4.3 BIASCORR: Small Scale Bias Subtraction

- Reference file: BIASFILE

This step is part of basic 2-D image reduction and is performed only for CCD data, removing any two-dimensional additive stationary pattern in the electronic zero point of each CCD readout. To remove this pattern, a bias reference image is subtracted. The bias reference file is a full format *superbias* image created from many bias frames to assure low noise. Separate bias files are used for different values of binning and for different values of gain. The bias image has an associated data quality image extension; bad pixels in the bias image are flagged in the science data quality image.

3.4.4 BLEVCORR: Large Scale Bias & Overscan Subtraction

- Reference file: none

This step is part of basic 2-D image reduction and is performed only for CCD data. This step subtracts the electronic bias level for each line of the CCD image and trims the overscan regions off of the input image, leaving only the exposed portions of the image. Thus, the BLEVCORR corrects the large scale bias (a plane), while BIASCORR corrects the small scale (pixel by pixel) bias.

Because the electronic bias level can vary with time and temperature, its value is determined from the overscan region in the particular exposure being processed. A raw STIS CCD image taken in full frame unbinned mode will have 20 rows of virtual parallel overscan in the AXIS2 (image y) direction, which is created by over-clocking the readout of each line past its physical extent, and 19 leading and trailing columns of serial physical overscan in the AXIS1 (image x) direction, which arise from unilluminated pixels on the CCD. Thus the size of the uncalibrated and unbinned full frame CCD image is 1062 (serial) \times 1044 (parallel) pixels, with 1024 \times 1024 exposed science pixels.

The virtual overscan region is screened to identify and reject outliers that may be caused by hot columns. The median of those values in the virtual overscan region, but not in the parallel overscan region is taken. Then the quantity *MAD* is defined to be the median of the absolute values of the deviations from the median, and *sigma* is defined to be the square root of the sum of the squares of the differences between values and the median, ignoring any value that differs from the median by more than $4.5 * MAD$. The value *blev_clip* is the value taken from the appropriate row of the CCD parameters table. An outlier is then taken to be any value that is greater than $median + blev_clip * sigma$. These outliers are then replaced with the median of the values in the same row that are within ± 10 pixels of the outlier, although if an outlier is closer than 10 pixels to the left (or right) edge, then the median of the 21 values adjacent to the right (or left) edge is taken instead.

Both the serial (physical) and virtual (parallel) overscans are used for the overscan bias level determination. A line-by-line subtraction is performed in the following way. An initial value of the electronic bias level, or overscan, is determined for each line of the image, using the serial and parallel overscans, and a function, currently a straight line, is fit to these values as a function of image line. This determines the slope of the bias level across the image at each line. The actual overscan value subtracted from an image line is the value of the linear fit at that image line. The initial value for each line is found by taking the median of a predetermined subset of the trailing serial overscan pixels. Currently, that region includes most of the trailing overscan region, however the first pixel and last three pixels are skipped, as they have been shown to be subject to problems; pixels flagged as bad in the input data quality flag are also skipped. The region used changes as a function of the binning or sub-array (see [Table 3.2](#)). The mean value of all overscan levels is computed and the mean is written to the output SCI extension header as MEANBLEV.

In addition to subtracting the electronic bias level, the BLEVCORR step also trims the image of overscan. The sizes of the overscan regions depend on binning and whether the image is full frame or a subimage. The locations of the overscan regions depend on which amplifier was used for readout. The number of pixels to trim off each side of the image (before accounting for readout amplifier) is given in [Table 3.3](#). The values of NAXIS1, NAXIS2, BINAXIS1, and BINAXIS2 are obtained from image header keywords. Because the binning factor does not divide evenly into 19 and 1062, when on-chip pixel binning is used the raw image produced will contain both pure overscan pixels, overscan plus science pixels, and science pixels. The calstispipeline will only calibrate pixel binnings of 1, 2, and 4 in either AXIS1 or AXIS2.

The keywords CRPIX_i (giving the pixel coordinates of the reference pixel) and LTV_i (giving the pixel coordinates of the subsection start) are updated in the output. These depend on the offset due to removal of the overscan.

Table 3.2: Raw Image Pixels Used to Determine Line by Line Bias Level

| Columns in Raw Image | Binning |
|----------------------|------------------------------|
| 2 through 16 | Unbinned |
| 2 through 8 | All other supported binnings |

Table 3.3: Pixels Trimmed During CCD Bias Level Correction for Amp D

| Side | Full Image | Sub-array Images | Binned Images |
|--------|------------|------------------|---|
| Right | 19 | 18 | $(19 + 1) / \text{BINAXIS1}$ |
| Left | 19 | 18 | $\text{NAXIS1} - (1024 / \text{BINAXIS1} - 1) - \text{Right}$ |
| Top | 0 | 0 | 0 |
| Bottom | 20 | 0 | $\text{NAXIS2} - 1024 / \text{BINAXIS2}$ |

3.4.5 CRCORR: Cosmic Ray Correction

- Reference files: CRREJTAB & CCDTAB

CRCORR step is applicable only to CCD data: it is applied by the **ocreject** task partway through the basic 2-D reduction process as described at the beginning of [Section 3.2](#). For STIS, the recommended procedure for observations longer than several minutes is to obtain two or more identical exposures so that an anti-coincidence technique can be used in the data calibration pipeline. For this reason, the CCD exposures are split into multiple associated exposures, specified by the number of iterations NRPTXP or CRSPLIT parameters, with roughly the same exposure times. The CRCORR step sums the individual CRSPLIT exposures in an associated dataset, producing a single cosmic ray rejected file (rootname_crj.fits).

The CRCORR contains the following steps:

- Forms a stack of images to be combined (the CRSPLIT or NRPTXP exposures in the input file).
- Forms an initial guess image (minimum or median).
- Forms a summed CR-rejected image, using the guess image to reject high and low values in the stack, based on sigma and the radius parameter that signifies whether to reject pixels neighboring cosmic ray impacts.
- Iterates, using different (usually decreasing) rejection thresholds to produce a new guess image at each iteration.

- Produces a final cosmic ray rejected image (`_crj`), including science, data quality, and error extensions, which is the sum of the input images. Then updates various header keywords.
- Flags the data quality arrays of the individual (non-CR-rejected) input files to indicate where an outlier has been found (pixels that were rejected because of cosmic ray hits can be identified by looking for data quality bit = 14 in the `_flt` file).

Note that the `_crj` image is the sum of the input CR-SPLIT images. For each pixel in the `_crj` image, the sum has been scaled to reflect any cosmic ray rejections in the individual images contributing to that sum; thus, the counts in every `_crj` pixel correctly reflect the total exposure time (`TEXPTIME`) of the CR-SPLIT images. For example, if `CRSPLIT=3`, and one of the 3 input pixels contributing to a given pixel in the `_crj` file is rejected during `CRCORR`, that pixel in the `_crj` file will be the sum of the 2 good input pixels, scaled by $3/2$.

If `skysub=mode`, a sky value is calculated as the mode in all pixels for each input image and subtracted from each pixel value prior to the identification of cosmic rays; afterwards, it is restored. If `sky=none`, no background is subtracted.

The method for forming the initial guess image is controlled through the parameter `initguess`, which takes the median or minimum pixel value to indicate which of these in the stack, at each pixel, is to be used. Only input pixels whose data quality flags are not set to the `badinpdq` parameter are used to form the guess. The bad pixel masking takes place prior to forming the initial guess image, which prevents bad data in a single input image from contaminating the output product.

The cosmic ray rejected image is created by setting the value at each pixel to the sum of the values of all good pixels in the stack whose values are within $\pm crsigmas * NOISE$ of the initial guess image. Deviant (out of range) stack pixels are flagged as cosmic ray impacted by setting their stack data quality flags to $2^{13} = 8192$ in the input file.

The value of `NOISE` (in DN) is computed as:

$$NOISE = \sqrt{\left(\frac{READNSE}{ATODGAIN}\right)^2 + \left(\frac{DN}{ATODGAIN}\right) + (scalense \times 0.01 \times DN)^2}$$

where:

- `DN` = the data number of the stack pixel value in counts.

- *READNSE* is the read noise in electrons, read from the value of the primary header keyword *READNSE*.
- *ATODGAIN* is the calibrated conversion from electrons to DN, read from the primary header keyword *ATODGAIN*.
- *scalense* is an input parameter, read from the *CRREJTAB* -calibration -reference file.

The *crsigmas* parameter is a string, e.g., *crsigmas* = "4,3", read from the *CRREJTAB* calibration reference file. The number of entries in the string dictates the number of iterations to be performed (in this example two) and the values in the string indicate the value of *crsigmas* for each iteration. In this example, stack values that deviate from the guess image value by more than $4*NOISE$ in the first iteration are considered to be outliers and are excluded from the average on the first iteration when an improved guess image is formed. A second iteration is then performed in which *crsigmas* is set to 3 and good stack values disperse by more than $\pm 3*NOISE$ from the guess image are excluded when determining the average. In each iteration, if *cradius* is not *INDEF*, then pixels neighboring rejected pixels will be subjected to a more stringent rejection test. Most CR impacts affect more than one pixel. For this reason, the mechanism is designed to permit neighboring pixels to be examined as separate cases with more stringent rejection thresholds to exclude cosmic rays (see [STIS ISR 98-11](#)).

The *scalense* parameter is a string containing a multiplicative factor in the noise relation, linearly proportional to the signal level. This allows for the treatment of extra noise due to other factors, such as image motion (e.g., a bright star in one pixel moving to the next could erroneously get flagged as a CR). If *scalense* = "2.0", then the term $0.02*value$ is added in quadrature to the noise. This term accounts for multiplicative effects that would be expected if this rejection were applied to flat-fielded data. The *scalense* parameter allows well exposed regions to be used (such as the centers of stars, where jitter from the telescope may slightly change the pointing from image to image), rather than incorrectly rejecting such regions as cosmic rays.

The combination of the individual *CRSPLIT* or *NRPTXP* exposures into a single cosmic ray rejected frame is performed early in the **calstis** flow. The cosmic ray rejection is performed after each exposure has had its data quality file initialized (*DQICORR*), the overscan bias level subtracted (*BLEVCORR*), and the bias frame subtracted (*BIASCORR*), but prior to subtraction of a dark frame (*DARKCORR*) and flat fielding (*FLATCORR*). The CR-rejected image is then passed through the remainder of the two-dimensional image

reduction to produce a flat-fielded, CR-rejected image (rootname_crj.fits). This CR-rejected flat-fielded image is then passed through the subsequent processing steps in **calstis**. If **EXPSCORR** is set to **PERFORM** (see below), then the individual flat-fielded but not cosmic ray rejected exposures are also produced.

The strategy for optimizing the CR rejection parameters for the STIS pipeline is explained in detail in [STIS ISR 98-22](#).

3.4.6 CTECORR: Correction for Charge Transfer Inefficiency Losses

- Reference files: CCDTAB & PCTAB

Extracted one-dimensional fluxes for first order CCD spectra are corrected for losses due to imperfect charge transfer efficiency (CTE) using an empirical algorithm described in [STIS ISR 2006-03](#) and Goudfrooij et al. (2006, PASP, 118, 1455). The CTECORR processing is done only for STIS CCD spectra, and only as part of the FLUXCORR step in the **x1d** (calstis6) task. A separate CTECORR flag is available that allows this correction to be turned off when FLUXCORR is set to PERFORM. No CTE correction is applied to the flux calibration for two-dimensional rectified spectra (**x2d** task or calstis7). This empirical correction algorithm was designed to be used with full frame CCD data, and so for data taken using sub-arrays, the pipeline sets CTECORR to OMIT, although users recalibrating spectral data themselves may choose to apply the CTE correction; in this case, the CTE calculation is done by treating the sub-array as the appropriate piece of a full frame image. The correction also assumes that the standard 7 pixel high extraction box for CCD first order spectra is used, and that standard background regions were specified. If the gross flux in a pixel in an **_x1d** or **_sx1** table is 0, then the CTE correction is not applied to that flux and the DQ value for that pixel includes the value 16384.

The CTE correction factor applied to the flux is $1/(1-CTI)^{(1025-Y)}$, where Y is the position on the detector of the center of the spectrum at that wavelength, and CTI is the fractional charge loss per transfer. The CTI (charge transfer inefficiency) is calculated separately for each wavelength bin of the detector.

The formula for the CTI is

$$CTI = CTINORM \cdot G^{-CTIGPOWER} \cdot \left(\frac{((EXPSTART - CTIREFMJD/365.25) \cdot CTITIMFAC + 1) \cdot \exp(CTIBGFAC \cdot ((B' + HALOFAC \cdot HALOPAR)/G)^{CTIBGPOWER})}{1} \right)$$

where:

G = Gross electrons per pixel per exposure in the extraction region for that wavelength bin,

B' = Total background in electrons per pixel per exposure ($DARK + SKY + SPURCHARGE$).

If $B' < 0$, then the factor $\exp(CTIBGFAC \cdot ((B' + HALOFAC \cdot HALOPAR)/G)^{CTIBGPOWER})$ is replaced by unity.

The coefficients $CTINORM$, $CTIGPOWER$, $CTIREFMJD$, $CTITIMFAC$, $CTIBGFAC$, $HALOFAC$, and $CTIBGPOWER$ are taken from the CCDTAB. EXPSTART is the exposure start time from the extension header.

The SKY is the background in electrons per exposure per pixel as measured by the BACKCORR procedure, while the $DARK$ is taken from the MEANDARK keyword, put into the extension header by the DARKCORR calibration step, multiplied by the gain to convert to units of electrons. The spurious charge is taken from the SPURCHARGE column of the CCDTAB reference table.

For gratings other than G750L and G750M, $HALOPAR$ is defined to be zero. For G750L and G750M,

$$HALOPAR = MAX(0.0, (FRACHALO - HALOMINFRAC)) \cdot NET.$$

The encircled energy fractions tabulated in the PCTAB reference table are used to compute $FRACHALO$, which is defined to be the fraction of the PSF above the default extraction box of 7 pixels. The value of $HALOMINFRAC$ is taken from the CCDTAB, and the NET is the net electrons per exposure in each individual wavelength bin.

A stand-alone pixel-based CTI correction script has been developed to model the detector level physics of CTI effects, and then correct each pixel to the proper counts. The script can be found at: <http://www.stsci.edu/hst/instrumentation/stis/data-analysis-and-software-tools/pixel-based-cti>. The pixel-based algorithm iteratively relocates counts on the detector to nearby pixels and has been demonstrated to help remove trails and other artifacts caused by CTI effects on the CCD detector (see [STIS ISRs 2015-04](#) and [2015-05](#) for details). Please note that only one type of CTE correction should be applied to an image, i.e., if the pixel-based correction will be used, then the empirical correction should be turned off by setting the CTECORR flag to OMIT.

3.4.7 DARKCORR: Dark Signal Subtraction

- Reference files: DARKFILE & CCDTAB

The DARKCORR step is part of basic 2-D image reduction and removes the dark signal (count rate created in the detector in the absence of photons from the sky) from the uncalibrated science image. If the science image is a sub-array or was binned, the relevant section of the dark reference image must be selected and binned to match the science image. If the Doppler correction was applied onboard for the science data (i. e., if DOPPON = T, or, in the case of TIME-TAG data, if DOPPON = F and DOPPMAG > 0), the Doppler smearing function is computed and convolved with the dark image (if DOPPCORR=PERFORM) to account for the contributions of various detector pixels to a particular image pixel. This is done before binning the dark image and applies only to MAMA data taken with the first order medium resolution gratings or in the echelle gratings. The science data quality file is updated for bad pixels in the dark reference file.

The mean of the dark values subtracted is written to the SCI extension header with the keyword MEANDARK. For CCD data, the dark image is multiplied by the exposure time and divided by the ATODGAIN (from the CCD parameters table) before subtracting.

CCD Darks

After the failure of the primary (Side-1) STIS electronics in July 2001, STIS began operating using the redundant Side-2 electronics. Side-2 does not have a functioning temperature sensor for the CCD, and so a constant current is applied to the CCD thermoelectric cooler. This leads to variations in the detector temperature and corresponding variations in the dark current. Although the temperature of the CCD itself can no longer be measured directly, there is a sensor that can measure the temperature of the CCD housing, and this appears to be a good surrogate for tracking the CCD temperature and dark current variations. The dark current is typically observed to increase by about 7% per degree C for the average pixel, however, there have been minor fluctuations in this value over the history of Side-2 observing. See [STIS ISR 2001-03](#) and [2018-05](#) for further details.

Before being subtracted from the science data, Side-2 CCD darks are scaled by the factor $1 + \text{DRK_VS_T} \cdot (\text{OCCDHTAV} - \text{REF_TEMP})$, where OCCDHTAV is the average CCD housing temperature in degrees Celsius, DRK_VS_T is the slope of the dark scaling relation given as a keyword in the dark reference file header, and REF_TEMP is the reference temperature used to derive that slope, also found as a keyword in the dark reference file header.

For some Side-2 CCD observations, _epc (Engineering Parameter Calibration) files are available from the archive which tabulate the housing temperature values as a function of time during the observation. If

_epc files are available for the observation being processed, the values tabulated in the _epc file are evaluated to give the appropriate time average temperature for each exposure. The average temperature from the _epc file is used to update the OCCDHTAV header keyword prior to scaling the darks.

Hot pixels, caused by radiation damage, also occur in the STIS CCD. Annealing of hot pixels is performed by raising the temperature of the CCD from its normal operating temperature (-83 °C) to the ambient value of 5 °C. Analysis of the on-orbit data has shown that this process is successful in removing 73.1% of the transient pixels hotter than 0.1 e⁻/sec/pix for Side-1 and 49.1% of the transient pixels hotter than 0.1 e⁻/sec/pix for Side-2. While post-pipeline calibration using appropriate STIS reference superdarks allows one to subtract most hot pixels correctly, the best way to eliminate all hot pixels is by dithering (making pixel-scale positional offsets between individual exposures).

MAMA Darks

The NUV dark current is believed to be primarily due to phosphorescent glow from impurities in the detector window. Over short time scales, this glow varies exponentially with detector temperature, as the metastable states responsible are more easily de-excited at higher temperatures. Over longer time scales the behavior becomes more complex, as the population of these metastable states changes over time in response to both the previous thermal history and the incident high energy particle flux.

To correct for the dark current changes, the NUV dark reference image specified in the DARKFILE keyword is scaled by a factor based on the NUV dark time correction table (TDCTAB) reference file. For NUV-MAMA data obtained prior to the *HST* Servicing Mission 4 (SM4) on May 2009, the scale factor is

$$SCALE \cdot NORM \cdot \exp(-THERMCST/T_{Dark} + 273.155)/1190.3435$$

where $T_{Dark} = MAX(OM2CAT, T_{MIN})$. OM2CAT is the NUV-MAMA detector amplifier temperature in units of degrees Celsius; it appears as a keyword in the science extension header of each image. SCALE, NORM, T_MIN, and THERMCST are tabulated as a function of observation date in the NUVTDCTAB. In practice, only NORM and T_MIN change as a function of time. SCALE = 1.805 × 10²⁰ and THERMCST = 12211.8 K for all entries. T_MIN varies between 31.5 C and 35.2 C, and NORM is of order unity.

For NUV-MAMA data obtained after the SM4, an updated relation has been derived to account for both long-term and short-term variations (see [STIS ISR 2013-01](#) for details). The average dark count rate at a given date and detector temperature is estimated as

$$count_rate = A1 \cdot \exp(-(D - DATE0)/D1) + A2 \cdot \exp(-(D - DATE0)/D2) \\ + TA + TB \cdot (OM2CAT - TEMP0) + T \cdot (OM2CAT - TEMP0)^2$$

where D is the Julian date of the observation, $DATE0$ is the Julian starting date of each “segment” (the currently used TDCTAB is divided into three segments with starting dates of Aug 6, 2009, Sep 9, 2009, and Nov 16, 2010), and $TEMP0$ is the reference temperature set to 38 C. A_1 , A_2 , $D1$, $D2$, TA , TB , and TC are the fit parameters that are listed in the TDCTAB along with $DATE0$ and $TEMP0$. Once the $count_rate$ is calculated for a given exposure using the equation above, the scale factor is determined by dividing $count_rate$ by the mean dark rate of the dark reference image (DARKFILE). The resulting scale factor is then applied to the DARKFILE before the dark subtraction is performed.

3.4.8 DISPCORR: Apply Dispersion Solution

- Reference files: DISPTAB, INANGTAB, & APDESTAB

This step is a part of spectral extraction or rectification. Wavelengths are assigned to pixels in extracted spectra using dispersion coefficients from the reference table DISPTAB when the calibration switch DISPCORR is PERFORM; if DISPCORR is OMIT, no wavelengths are assigned. The pipeline performs DISPCORR for _x2d files whether or not DISPCORR is set to PERFORM, using interpolation to produce a linear wavelength scale. More details on the DISPCORR calibration step are given in [STIS ISR 99-03](#) (for **x1d**) and [STIS ISR 98-13](#) (for **x2d**).

The DISPTAB table contains dispersion solutions for a defined reference aperture. For L and M modes and the PRISM, solutions are given at numerous Y positions that span the detector. For the L, M, and E modes, the dispersion solution has the following form:

$$s = A_0 + A_1 m\lambda + A_2 (m\lambda)^2 + A_3 m + A_4 \lambda + A_5 m^2 \lambda + A_6 m\lambda^2 + A_7 (m\lambda)^3$$

where

- λ is the vacuum wavelength in Angstroms.
- s is the detector AXIS1 position.
- m is the spectral order.
- A_i are the dispersion coefficients.

For the PRISM, used with the NUV-MAMA detector, the dispersion relation gives wavelength as a function of pixel position as follows:

$$\lambda = A_1 + \frac{A_2}{s - A_0} + \frac{A_3}{(s - A_0)^2} + \frac{A_4}{(s - A_0)^3} + \frac{A_5}{(s - A_0)^4}$$

Offsets introduced by using apertures other than the reference aperture are removed using coefficients (IAC_COEFF) in the INANGTAB reference table. The A_0 parameter in the dispersion relation is modified as follows: $A'_0 = A_0 + IAC_COEFF \times \Delta x$, where Δx is the x offset between the apertures in pixels, determined from the APDESTAB.

Offsets due to MSM shift determined from wavecal exposures are corrected for by applying a linear offset after all other corrections have been made. For all modes, small offsets occur because of non-repeatability in the positioning of the MSM and thermal drift (see [Section 3.4.23](#)). Additionally, for MAMA L and M modes, and for echelle modes until August 2002, offsets of the projection of the spectrum onto the detector in both the spectral and spatial directions have been deliberately introduced by offsetting the Mode Select Mechanism (grating wheel) tilts. This has been done approximately monthly to assure a more uniform charge extraction from the micro-channel plate over time. Determination of these induced offsets is included in the wavecal processing, and they are subtracted along with the random MSM offset.

In **x1d**, for grating spectra, the Newton-Raphson method is applied to the first dispersion relation given above to solve for the wavelength, while for PRISM data the wavelength is computed directly from the second dispersion relation. The **x2d** task linearizes the wavelength scale and solves for pixel number as a function of wavelength (and spectral order). For grating spectra, the first equation is evaluated directly, and for prism data the pixel number from the second equation is found using binary search.

3.4.9 DOPPCORR: Correct Reference Files for Doppler Shift

- Reference files: none

This step is part of basic 2-D image reduction and is performed only for spectroscopic data taken with the MAMA detectors (the correction is not significant for CCD spectroscopy, which is at lower resolution). When MAMA data are taken in ACCUM mode in the first order medium (M) gratings or the echelle modes, the MAMA flight software corrects the location of each photon for the Doppler shift induced by the spacecraft motion, prior to updating the counter in the ACCUM mode image being produced. In this case, the flat field and dark reference files should be convolved with the Doppler smearing function,

because the counts on a single image pixel were actually detected at different (Doppler shifted) detector pixel locations. Therefore, during basic two-dimensional image reduction of the MAMA data, the darks and flats must be processed with the same Doppler smoothing as the science data prior to application of the reference image. Because this is not an independent routine, but a modifier for the steps DQICORR, DARKCORR and FLATCORR, the DOPPCOR flag is never set to COMPLETE.

The first step is to compute an array containing the Doppler smearing function. The expression below gives the computed Doppler shift, where the time t begins with the value of the header keyword EXPSTART and is incremented in one second intervals up to EXPSTART + EXPTIME inclusive. At each of these times, the Doppler shift in unbinned pixels is computed as:

$$shift = -DOPPMAG \times \sin(2\pi(t - DOPPZERO)/ORBITPER)$$

where *DOPPMAG* is the Doppler shift amplitude in high res pixels, *DOPPZERO* is the time when the Doppler shift was zero and was increasing (i.e., near when the *HST* was closest to the target) and *ORBITPER* is the orbital period of the *HST* in seconds. DOPPMAG, DOPPZERO and ORBITPER are all SCI extension header keywords. If a photon hits detector location (X,Y), then pixel (X+shift,Y) in the image would have been incremented. Therefore, a positive shift means that the reference files (dark and flat) should be shifted to the right before being applied. The value of *shift*, estimated from the above equation, is rounded to the nearest integer.

In TIME-TAG mode with the medium or high resolution echelles, this correction is not applied onboard, but is done by Generic Conversion when making an ACCUM image from the TIME-TAG table. The Doppler corrected coordinates are then written in a new column in the TIME-TAG table (rootname_tag.fits). When the TIME-TAG data are integrated in time (in Generic Conversion or by using **inttag**) to produce an uncalibrated accumulated science image (rootname_raw.fits), it is the Doppler corrected positions that are used.

3.4.10 DQICORR: Initialize Data Quality File

- Reference file:

The DQICORR step is part of basic 2-D image reduction. This routine takes the initial data quality file output for the science data and performs a bitwise OR with the values in the bad pixel reference file table (

BPIXTAB) to initialize the science data quality file for propagation through subsequent steps in **calstis**. If DOPPCORR=PEFORM, **calstis** will combine data quality information from neighboring pixels to accommodate Doppler smearing prior to performing the OR operation with the (unsmeared) science input data quality image. The DQICORR step also appropriately combines data quality flags in neighboring pixels if the images are binned.

For CCD data, this step also includes a check on saturation, comparing the science data values with the saturation level read from the CCD parameters table (CCDTAB). It also flags the regions of the CCD beyond the edge of the aperture to prevent problems with sky level computation and cosmic ray rejection. When a large fraction of the image is not illuminated, the computation of the sky level can be seriously affected. The aperture size is read from the APER_FOV keyword.

3.4.11 EXPSCORR: Retain Individual CR-SPLIT Exposures

- Reference file: none

The EXPSCORR step is a part of basic 2-D image reduction, for CCD data only. If the EXPSCORR calibration switch in the header is set to PERFORM, the pipeline will also process the SCI extensions in the _raw files as individual exposures through **calstis**, outputting an intermediate product, rootname_flat.fits. This file contains the individual flat-fielded CRSPLIT exposures in successive imsets of a single file. This file will not be passed through the subsequent calibration steps (e.g., spectroscopic reduction), but will be retained as an intermediate data product, to allow users to see exactly which pixels were excluded from the summed, cosmic ray rejected image.

3.4.12 FLATCORR: Flat Field Correction

- Reference files: PFLTFIELD, DFLTFIELD, & LFLTFIELD

The FLATCORR step is part of basic 2-D image reduction and corrects for pixel-to-pixel and large scale sensitivity gradients across the detector by dividing the data by a flat field image. The flat field image used to correct the data is created from three flat field reference files:

- PFLTFIELD - This flat is a configuration (grating, central wavelength and detector) dependent pixel-to-pixel flat field image, from which any large scale sensitivity variations have been removed (i.e., it

will have a local mean value of unity across its entirety). Such configuration dependent flats are produced infrequently.

- `DFLTFILE` - This file is a *delta flat* that gives the changes in the small scale flat field response relative to the pixel-to-pixel flat (`PFLTFILE`). *Delta flats are not currently used.*
- `LFLTFILE` - This flat is a subsampled image containing the large scale sensitivity variation across the detector. It is usually grating- and central wavelength-dependent (for spectroscopic data) and aperture (filter) dependent for imaging data.

To flat field science data, **calstis** creates a single flat field image from these three files^[1] as described below and then divides the science image by the flat so created. The pixels of the science data quality file are updated to reflect bad pixels in the input reference files, and the errors in the science data are updated to reflect the application of the flat. Blank and “N/A” values of `PFLTFILE`, `DFLTFILE`, or `LFLTFILE` in the science data’s header indicate that type of flat is not to be used.

To create the single combined flat field file, **calstis** first expands the large scale sensitivity flat (`LFLTFILE`) to full format, using bilinear interpolation. The pixel-to-pixel flat, delta flat, and expanded low order flat are then multiplied together. For MAMA data, the product of the flat field images will be convolved with the Doppler smoothing function if `DOPPCORR=PERFORM`. If a sub-array or binning was used, after taking the product of all the flat fields that were specified, a subset is taken and binned if necessary to match the uncalibrated image, and the uncalibrated data are then divided by the binned subset.


The error and data quality arrays in the calibrated file are updated to reflect the error and data quality from the flat field (i.e., the errors are rescaled by the flat field, and the errors associated with the flat field are added in quadrature). If Doppler convolution is applied, a correction is also applied for the loss of counts at the image edges due to flight software’s “effective sub-array” (see [STIS ISR 98-05](#) for details).

3.4.13 FLUXCORR: Conversion to cgs Flux

- Reference files: `APERTAB`, `GACTAB`, `PHOTTAB`, `PCTAB` & `TDSTAB`

This step is part of spectral extraction (`X1DCORR`) and spectral image rectification (`X2DCORR`) if `FLUXCORR` is `PERFORM`. (See also [Section 3.4.6](#) for `CTECORR`, which is used in the extraction of point sources from full frame CCD spectral images.) Counts in `_flt` or `_crj` images are corrected to flux ($\text{erg cm}^{-2} \text{sec}^{-1} \text{\AA}^{-1}$) in the `_x1d` file or to surface brightness ($\text{erg cm}^{-2} \text{sec}^{-1} \text{\AA}^{-1} \text{arcsec}^{-2}$) in the `_x2d` file. The flux

calibration used in one-dimensional extraction is correct for a point source only, since it applies slit width and extraction height corrections appropriate for a point source. The surface brightness calibration used in the production of rectified spectral images is appropriate for diffuse sources, since no correction is made for slit losses.

 See [Section 5.4.1](#) for a discussion of the surface brightness calibration of rectified spectral images, and for an alternate method of computing the fluxes of point sources embedded in those images.

Execution of this calibration step requires that wavelengths have been assigned previously by DISPCORR. Corrections for vignetting and echelle blaze are handled within the PHOTTAB reference files.

The conversion to absolute flux for a point source is calculated as:

$$F_{\lambda} = \frac{10^8 \cdot h \cdot c \cdot g \cdot H \cdot C_{\lambda}}{A_{HST} \cdot R_{\lambda} \cdot T_{\lambda} \cdot \lambda \cdot \Delta\lambda \cdot f_{TDS} \cdot f_T \cdot f_{GAC}}$$

where:

- F_{λ} is the calibrated flux at a particular wavelength. This quantity is also multiplied by the ATODGAIN if the data were obtained with the CCD.
- h is Planck's constant.
- c is the speed of light.
- g is the detector gain, which is unity for MAMA observations. For the CCD, this is the conversion from counts to electrons, the value of which is given in the header keyword ATODGAIN.
- H is a correction factor accounting for the finite extraction box height (EXTRSIZE) used to extract the spectra; it is the ratio of throughput for an infinite extraction box height divided by the throughput for the extraction box height used to extract the spectrum, where the throughputs are taken from the PCTAB (*_pct.fits) reference table. Note that in the PCTAB, the throughput vector for the default extraction box size of a given mode is defined to be unity at all wavelengths, while the infinite extraction box throughput curve (labeled as extraction height = 600 in the PCTAB) will have throughput greater than unity at all wavelengths. So when an extraction is done using the default extraction box, the correction applied will be greater than unity, even though the PCTAB row for the default extraction box itself is equal to 1 at all wavelengths.
- C_{λ} is the net count rate (counts/sec) at a particular wavelength.

- A_{HST} is the area of the unobstructed HST primary mirror (45238.93416 cm²).
- R_λ is the wavelength dependent integrated system throughput, given in the PHOTTAB for individual optical elements.
- T_λ is the aperture throughput at a particular wavelength.
- λ is the wavelength in Angstroms, which is converted to cm by the factor of 10^8 in the numerator.
- $\Delta\lambda$ is the dispersion (Å/pixel) at a particular wavelength.
- f_{TDS} is the correction for time-dependent sensitivity (given in TDSTAB).
- f_T is the correction for temperature-dependent sensitivity (given in TDSTAB).
- f_{GAC} is the grating/aperture (GACTAB) throughput correction.

The FLUXCORR step includes corrections for time dependent sensitivity (TDS) changes. The coefficients to calculate these corrections are taken from the TDSTAB reference file. The coefficients specify the rate of change of the sensitivity with time (units of %/year), over a grid of time and wavelength values. These slopes are used to construct a piece wise linear throughput correction factor as a function of time at each wavelength. This is interpolated to each wavelength of the observation and used to correct the final flux. TDS corrections are applied to the final flux values for both one- and two-dimensional spectra (**calstis6** and **calstis7**). For imaging modes, the TDS calculation is used to correct the throughput curve before calculating the photometric keywords. In practice, for each detector, the TDS trends measured with the low dispersion modes are assumed to apply to all modes (See [STIS ISR 2004-04](#) and [STIS ISR 2017-06](#) for descriptions of how these trends were measured). The one exception to this is the NUV-MAMA PRISM, which has its own TDS determination ([STIS ISR 2005-01](#)).

Temperature-dependent corrections to the sensitivity are also made using two columns in the TDS file. The column REFTEMP contains a single value for each optical element. The column TEMPSSENS uses the same wavelength grid as already defined by the TDS corrections so that the temperature correction can be allowed to vary as a function of wavelength. The correction factor to the extracted flux is $(1 + \text{TEMPSSENS} * (T - \text{REFTEMP}))$, where T is given by the science extension header keywords: OM1CAT for the FUV-MAMA detector, OM2CAT for the NUV-MAMA detector, and OCCDHTAV for side-2 electronics CCD data. No correction is made for Side-1 electronics CCD data, since the detector temperature was stable under Side-1 operations.

The STIS spectroscopic flux calibration was set up under the assumption that the grating and aperture throughputs could be determined independently and then simply multiplied together. This turns out not to be true, especially for G430L and G750L modes, which contain a Lyot stop. The GACTAB reference file contains the needed correction vector (THROUGHPUT) at the nominal position of the aperture as a

function of wavelength for given OPT_ELEM/APERTURE/CENWAVE combinations. e.g., a vector for aperture 52X0.1E1 is appropriate for a target centered at the E1 aperture position, high on the CCD detector. The correction vector for a 52X2 observation at the standard central position is assumed to have a value of unity. The correction vector for a given mode is applied when a spectrum is extracted.

Blaze Shift

For echelle data, the flux correction also includes a blaze shift correction. The blaze functions are known to shift with respect to the wavelength scale depending on the time of observation and the location of the spectrum on the detector. This shift is necessary because depending on the location and time of the observation, the blaze function shifts differently compared to the wavelength scale. The shift is calculated as a linear function of location (x and y) on the detector (SHIFTA1 and SHIFTA2) and as a function of time. In particular, it has been found that the coefficients of the “spatial” component of the blaze shift only depend on the grating, while the coefficients of the “temporal” component and zero point depend on the grating, order, and side of operation (Side-1 or Side-2).

The blaze shift corrections have been updated and recalibrated multiple times during STIS's history, including when the monthly offsets of the Mode Select Mechanism were still being routinely performed for echelle data (see [Section 7.6.2](#) of the *STIS Instrument Handbook*). Because of this, not all of the echelle orders currently falling on the detector for a given grating/cenwave combination have well-calibrated blaze shift corrections. These echelle orders do not have entries in the PHOTTAB and RIPTAB reference files and will not be present in the resulting _x1d files when FLUXCORR is set to PERFORM. [STIS ISRs 2007-01](#) and [2012-01](#) document which echelle orders are affected.

3.4.14 GEOCORR: Geometric Distortion Correction

- Reference files: IDCTAB

Geometric correction is part of secondary 2-D image reduction and is applicable to all ACCUM and TIME-TAG mode imaging data. The method used is similar to 2-D rectification of spectroscopic data (see [Section 3.4.25](#)). For each pixel in the output rectified image, the corresponding point is found in the input distorted image. Bi-linear interpolation in the input image is used to get the data value to assign to the output. The output pixel value is the weighted sum of the values of the four nearest pixels in the input image. The weights depend on distances of that particular pixel from each of the four pixels, with the sum of the weights normalized to unity (see [STIS ISR 98-13](#)). Note that such distances are determined from the

centers of the pixels. Mapping from an output pixel back into the input images is specified by a two-dimensional power series polynomial. The distortion coefficients and their implementation in the IDCTAB are fully described in [ACS ISR 2000-11](#). The errors are interpolated using the same weights as for the science data, except that the errors are combined in quadrature. The distortion coefficients for the STIS detectors are given in [STIS ISRs 2001-02](#), [2004-02](#) and [2018-02](#). The plate scale of the geometrically corrected output image is given in the SCALE column of the IDCTAB.

3.4.15 GLINCORR and LFLGCORR: Nonlinearity Corrections

- Reference file: MLINTAB

These steps are part of basic 2-D image reduction and are performed only for the MAMA detectors. The MAMAs are photon counting detectors. At high photon (pulse) rates, the MAMA response becomes nonlinear due to four effects:

- Pore paralysis in the micro-channel plates arises when charge cannot flow rapidly enough to replenish channels whose electrons have been depleted due to high local photon rates. This depletion produces a *local* non-linearity. The local count rate is roughly linear up to ~200 counts/sec/pixel and then turns directly over, showing an inverted V shape. Thus, it is not possible to reliably correct for or flag pixels that have exceeded the local linearity limit in the pipeline (because the relation is bi-valued).
- The electronic processing circuitry has a dead time of roughly 350 nano seconds between pulses; thus at global count rates (across the detector) of 300,000 counts (pulses) per second, the electronic circuitry counts roughly 90% of the pulses.
- The MAMA Interface Electronics (MIE) and flight software can process at most 300,000 pulses per second (i.e., it is matched to the expected global count rate performance of the electronic circuitry). At count rates higher than this, the MIE will still count only 300,000 pulses per second—this represents a hard cutoff beyond which no information is available to allow correction to the true count rate. In practice, at count rates approaching 270,000 counts/sec the flight software begins losing counts due to the structure of its data buffers.
- For sub-arrays, the hard cutoff limit of the MIE electronics and software will differ from that for full frame processing, but will still be dependent on the total global rate in addition to the rate within the sub-array.

The local and global count rates that lead to nonlinearity are both above the screening limits for MAMA observations, so under normal circumstances, these nonlinearities are unimportant. However, if a brighter than allowed target is inadvertently observed without shuttering the detector, these linearity corrections are important.

The global count rate (across the entire detector) is determined as part of the bright object protection sequence and is passed down with the exposure as a header keyword, GLOBRATE, in the science header. **Calstis** also computes GLOBRATE and updates the value in the header. If either GLINCORR or LFLGCORR is PERFORM, the global count rate will be checked; a correction for global non-linearity is applied if GLINCORR is PERFORM, using the parameters GLOBAL_LIMIT, LOCAL_LIMIT, TAU, and EXPAND read from the MLINTAB reference table.

If the value of the SCI extension header keyword GLOBRATE is greater than GLOBAL_LIMIT, the keyword GLOBLIM in the SCI extension header will be set to EXCEEDED, with no change made to the data. Otherwise, GLOBLIM will be set to NOT-EXCEEDED, and a correction factor will be computed and multiplied by each pixel in the science image and error array. The correction factor is computed by iteratively solving $GLOBRATE = X * \exp(-TAU * X)$ for X , where X is the true count rate. This algorithm has not yet been updated to account for the linearity effects from the flight software data buffer management.

If LFLGCORR is PERFORM, each pixel in the science image is also compared with the product of LOCAL_LIMIT and the exposure time EXPTIME. That count rate limit is then adjusted for binning by dividing by the pixel area in high res pixels. If the science data value is larger than that product, that pixel and others within a radius of EXPAND high res pixels are flagged as nonlinear. Because our understanding of the MAMA processing electronics is currently incomplete, accurate fluxes (global linearity) at count rates exceeding 285,000 counts/sec cannot be expected from the **calstis** pipeline.

3.4.16 HELCORR: Correction to Heliocentric Reference Frame

- Reference file: none

This step is part of spectral extraction or rectification. The correction of wavelengths to a heliocentric reference frame is controlled by calibration switches HELCORR and DISPCORR — if both switches are set to PERFORM then the correction is made. The functional form of the correction (shown below) requires the calculation of the heliocentric velocity (v) of the Earth in the line of sight to the target.

$$\lambda_{\text{helio}} = \lambda_{\text{obs}} \left(1 - \frac{v}{c} \right)$$

where:

- λ_{helio} is the heliocentric vacuum wavelength.
- λ_{obs} is the wavelength observed, prior to heliocentric correction.
- v is the component of the velocity of the Earth away from the target.
- c is the speed of light.

The derivatives of low precision formulae for the Sun's coordinates described in the *Astronomical Almanac* are used to calculate the velocity vector of the Earth in the equatorial coordinate system of the epoch J2000. The algorithm does not include Earth-Moon motion, Sun-barycenter motion, nor light-time correction from the Earth to the Sun. This value for the Earth's velocity should be accurate to ~ 0.025 km/sec during the lifetime of STIS. (Note that the uncertainty of 0.025 km/s is much less than the ~ 2.6 km/s resolution obtained with the STIS high dispersion echelle gratings.) The value of heliocentric velocity, v , is written to the HISTORY record in the primary header of the output spectrum file. It is also written to the V_HELIO keyword in the SCI extension header, regardless of the value of the HELCORR keyword.

3.4.17 LORSCORR: Conversion to Native Format MAMA Pixels

- Reference file: none

This step is part of basic 2-D image reduction and is performed for MAMA data only. MAMA data are, by default, taken in high resolution mode (2048×2048 pixels), in which the individual micro-channel plate pixels are subsampled by the anode wires. This mode produces an image with improved sampling but with appreciably worse flat fielding properties (see [Chapter 11](#) of the *STIS Instrument Handbook* for more details). If LORSCORR is set to PERFORM, **calstis** simply adds the counts in pairs of adjacent pixels to produce images in the native format (or so called *reference format*) of the MAMA detectors, with 1024×1024 pixels.

The binning of the uncalibrated image is determined from the LTM1_1 and LTM2_2 keywords in the SCI extension header of the _raw data file. LTMi_i = 1 implies the reference pixel size, and LTMi_i = 2 means the pixels are subsampled into high res format. In this step, if either or both axes are high res, they will be binned down (summed) to low res.

Most MAMA raw files will be in the high resolution (2048 × 2048 pixel) format, but the default calibration settings will produce calibrated files that use the lower resolution format. Thus MAMA _flt files will normally be 1024 × 1024 pixels. Note also that MAMA auto wavecal images (_wav.fits files) will usually also be in the lower resolution format.

3.4.18 PHOTCORR: Populate Photometry Header Keywords

- Reference files: PHOTTAB, APERTAB, TDSTAB & IMPHTTAB

This step is part of basic 2-D image reduction and is applicable only for OBSTYPE=IMAGING data. For image mode, the total system throughput is calculated from the reference files. Throughputs are corrected for time dependent changes to the time of the observation using information from the TDSTAB. The IMPHTTAB reference file contains computed inverse sensitivity, reference magnitude, pivot wavelength, and RMS bandwidth; these four quantities are written to the primary header keywords PHOTFLAM, PHOTZPT, PHOTPLAM, and PHOTBW, respectively.

3.4.19 RPTCORR: Sum Repeated MAMA Observations

- Reference file: none

This step is part of secondary 2-D image reduction and is applicable only for MAMA data. If the number of repeat exposures is greater than one, then **calstis** will sum the flat-fielded data in the case of image mode data (producing an _sfl file) or the two-dimensionally rectified data (producing an _sx2 file) in the case of long slit data. RPTCORR just applies a straight pixel-to-pixel addition of the science values, bitwise ORs the data quality files, and determines the error as the square root of the sum of the squares of the errors in the individual exposures.

3.4.20 SC2DCORR: Echelle Scattered Light Correction

- Reference files: CDSTAB, ECHSCTAB, EXSTAB, RIPTAB, HALOTAB, TELTAB, SRWTAB

This step is part of spectral extraction. It can only be used with STIS echelle data. If SC2DCORR is set to PERFORM, **calstis** iteratively constructs a two-dimensional model of the scattered light present in the `_flt` image. After 3 iterations, this scattered light model is (virtually) subtracted from the `_flt` data and spectral extraction proceeds using this background-subtracted version of the `_flt` image as input to the normal **x1d** extraction with *algorithm = unweighted*, described in [Section 3.4.24](#); however, as the background has now been subtracted by the SC2DCORR algorithm, the background subtraction normally done as part of the unweighted extraction is omitted.

This scattered light correction procedure has been used since 2000-Dec-21 to process all *HST* archive requests for STIS echelle data, regardless of when the observations were performed, unless use of an unsupported mode prevents spectral extraction. Two-dimensional scattered light subtraction may be suppressed either by setting SC2DCORR to OMIT in the `_raw` file and reprocessing the entire association with **calstis**, or more directly by running the **x1d** task with the `_flt` file as input and the extraction algorithm parameter of the **x1d** task set to *unweighted* instead of *sc2d*.

Note that since the **x1d** task is used for both first order and echelle data, the default value of the *algorithm* parameter in the **x1d** task is set to *unweighted*. Users recalibrating echelle data by running the **x1d** task directly on the `_flt` image will normally want to be sure that the **x1d** *algorithm* parameter is set to *sc2d*. Alternatively, the user may run the **calstis** task using the `_flt` file as input, as **calstis** will use the value of the SC2DCORR keyword in the `_flt` file header to determine which extraction algorithm to use.

3.4.21 SGEOCORR: Small Scale Distortion Correction

- Reference file: SDSTFILE

This step would be part of spectral extraction or rectification and apply only to MAMA data, *but it is not presently implemented*. If SGEOCORR were PERFORM, a correction would be applied for the small scale geometric distortions in the MAMA detectors. The corresponding reference file, SDSTFILE, would contain the distortion offsets for each pixel in the MAMA image.

3.4.22 SHADCORR: CCD Shading Correction

- Reference file: SHADFILE

This step is part of basic 2-D image reduction and applies only to CCD data, *but it is not currently performed*. It is designed to correct for shading by the CCD shutter in very short integration time exposures. The STIS CCD shutter is specified to produce exposure non-uniformity less than or equal to 5 milliseconds for any integration time: the shortest possible STIS CCD exposure time is 100 milliseconds. Ground testing has shown that this step is not currently required. However, if SHADCORR were needed, a SHADFILE reference would need to be created to use this module.

3.4.23 WAVECORR: Wavecal Correction

- Reference files: LAMPTAB, APDESTAB, WCPTAB, DISPTAB, INANGTAB, SPTRCTAB, SDCTAB

This step is a part of wavecal processing and applies only to spectroscopic data. The purpose of wavecal processing is to determine the shift of the image on the detector along each axis owing to uncertainties in positioning by the Mode Select Mechanism (MSM) and to thermal motions. It requires one or more contemporaneous wavecal (line lamp) observations, taken without moving the MSM from the setting used for the science data.

Basic two-dimensional image reduction is first applied to the wavecal. For CCD data taken with the HITM system prior to 1998-Nov-9, the external shutter was left open during wavecal exposures, so the detector was exposed to radiation from both the science target and the line lamp. In this case, the next step is to subtract the flat-fielded science image from the wavecal, after scaling by the ratio of exposure times and by the ratio of gains.

For first order data, two-dimensional rectification is then applied to the flat-fielded (and possibly science subtracted) wavecal. The result is a temporary file that will normally be deleted after processing. For prism or echelle data, the 2-D rectification step is not done.

Because wavecal data are not CR-SPLIT, cosmic rays must be identified and eliminated by looking for outliers within columns, i.e., in the cross-dispersion direction. Because the data have been rectified, values within a single column are all at the same wavelength and hence, are fairly consistent in their brightness

for a line lamp exposure. Cosmic rays will stand out above this brightness level. The image can then be collapsed along columns to get a long slit integrated spectrum or along rows to get an outline of the slit (in the cross-dispersion direction).

In removing cosmic rays from a wavecal, a different cosmic ray rejection function has been added to *calstis4*. This function is called if the SCI extension SDQFLAGS (serious data quality flags) includes 8192. The logic here is that if SDQFLAGS does not include 8192 (DATAREJECT), the bit used to flag cosmic rays, then the cosmic rays are not considered “serious”. Therefore, when a pixel is identified by *calstis4* as being affected by a cosmic ray hit, it is flagged by including 8192 in the DQ array for that pixel. This procedure is explained in detail in [STIS ISR 98-12](#).

The shifts in the dispersion and cross-dispersion directions are determined differently for first order grating, prism, and echelle data. First-order grating data are 2-D rectified before being passed to *calstis4*. This is done so the image can be collapsed along columns or rows to make 1-D arrays that are then cross correlated with a template spectrum or a template of the slit illumination to get the shift in the dispersion or cross-dispersion direction, respectively. For a long slit, the features that are used to locate the image in the cross-dispersion direction are the occulting bars, but the cross correlation is not done directly between the slit illumination and a template. The slit illumination pattern is first normalized and inverted, so it is nominally zero where there is light, and it is unity within the occulting bars; this is then cross correlated with a template of the slit that is normalized the same way.

Prism data are handled by *calstis4* in nearly the same way as first order grating data. The differences are that the data are not rectified first: when collapsing along columns to make a 1-D spectrum, only the middle 224 pixels are used to reduce the effect of any tilt in the spectral lines, and when collapsing along rows the spectral trace (SPTRCTAB) is applied to account for spatial distortion. The reason for working with the flat-fielded but not rectified data is that the dispersion for the prism is highly nonlinear, and the shift is in pixel space, not wavelength space.

For echelle data, *calstis4* computes a 2-D cross correlation between the flat-fielded wavecal image and a template image. The offset of the peak in the cross correlation gives the shift in both axes. This works because the aperture is small in both dispersion and cross-dispersion directions.

The shifts are written to the extension header of the 2-D rectified wavecal in the keywords SHIFTA1 (the shift in pixels along AXIS1, or dispersion direction) and SHIFTA2 (the shift in pixels along AXIS2, or spatial direction) although this image is not saved unless **wavecal** is run with *save_w2d=yes*. The

SHIFTA1 and SHIFTA2 keyword values are also copied from the 2-D rectified wavecal file to the flat-fielded (`_flt` or `_crj`) science extension header. SHIFTA1 and SHIFTA2 are always given in units of unbinned CCD pixels or lo-res MAMA pixels, regardless of the binning of the CCD exposures. This is the final step performed on the science data prior to 2-D rectification or 1-D extraction of the science data in the pipeline.

Either or both the wavecal file and science file can contain multiple exposures, and the image can drift across the detector over time due to such things as thermal effects, so it is necessary to select the most appropriate wavecal exposure for each science exposure. If there are multiple wavecal exposures, the shifts are linearly interpolated at the time of a given science exposure to get the shifts that will be used for that science exposure. There is also an option to use the wavecal that is nearest in time to the given science exposure.

If it is necessary to use a wavecal exposure that differs from the default exposure in the header, this can be done either by substituting the new file name in the `WAVECAL` keyword value in the science exposure's primary data header before processing the file with `calstis`, or by using the `stistools.wavecal` task to update the SHIFTA1 and SHIFTA2 keywords in the image extension headers.

3.4.24 X1DCORR: Locate and Extract 1-D Spectrum

- Reference files: `SPTRCTAB`, `XTRACTAB`, `SDCTAB`

This step is part of spectral extraction. If X1DCORR is `PERFORM`, `calstis` will locate and extract a one-dimensional spectrum, as explained below, and in more detail in [STIS ISR 99-03](#).

Locate the Spectrum

The shapes of spectral traces are contained in the spectrum trace table, `SPTRCTAB`. For each mode (`OPT_ELEM`, `CENWAVE`) of the first order gratings, this table contains many traces at arbitrary Y positions spanning the detector. For each echelle mode, it contains one trace at a default position for every spectral order (`SPORDER`). The Y position (`A2CENTER`) of a trace on the detector at the central column (`A1CENTER`) is given in CCD or MAMA lo-res pixels. (`A1CENTER` is 513; `A2CENTER` is non-integer.) The shape of each trace is stored as an array (`A2DISPL`) consisting of offsets in pixels in the `AXIS2` direction relative to `A2CENTER`. The spectral traces of some of the first order modes have been observed to rotate slowly as a function of observation date. For the most commonly used modes, the

column DEGPERYR gives this rotation rate in degrees per year, and the column MJD gives the date for which the unrotated trace is valid. This information is used to correct the spectral traces to the observing date. (See [Section 3.5.7.](#))

For the echelle modes, an initial estimate of the location of each spectral order in the science image is obtained as the sum of the A2CENTER value in the SPTRCTAB for that order and the value of SHIFTA2 in the science data header. SHIFTA2 is the Y-offset from the nominal placement of the image on the detector due to differences in the setting of the MSM, measured as described in [Section 3.4.23.](#) For the first order modes, the entire height of the detector will be searched for the brightest spectrum, so an initial estimate of the position of the spectrum on the detector is not needed. (To extract fainter spectra at other locations, see [Section 5.5.2.](#))

The location of the spectral order or first order spectrum in the science image is determined by performing a cross-correlation between a spectral trace and the science image. For the echelle modes, the single trace for each spectral order is used in the vicinity of the initial estimate of the location of that order. The search is restricted to a few pixels along the cross-dispersion direction ($\pm n$ pixels, where n is read from the MAXSRCH column in the XTRACTAB table), in order to avoid confusion due to the simultaneous presence of many orders on the detector. For the first order modes, the shape of the lowest trace on the detector for that mode in the SPTRCTAB is used for a search of the entire detector.

The search for the spectral order or first order spectrum is conducted at integer pixel steps, starting at $A2CENTER+SHIFTA2$ for the given spectral order or for the lowest first order trace. A sum of the counts along the trace is formed by adding the value of one pixel's worth of data from each column. The "pixel" in each column generally includes a fractional contribution from two pixels, which are weighted by the fractional area. Quadratic refinement using the Y position with the highest sum and its two nearest neighbors is then used to locate the spectrum to a fraction of a pixel. For the first order modes, the shape of the trace at the initially measured position replaces the shape of the lowest trace on the detector for the quadratic refinement.

For first order spectra, the final position of the spectrum is $A2CENTER+SHIFTA2+CRSCROFF$, where A2CENTER is that of the lowest trace on the detector for that mode and CRSCROFF is the offset found during the cross correlation. If the cross correlation fails, the value of CRSCROFF is set to zero, a warning message is written to the output, and the nominal position $A2CENTER+SHIFTA2$ is used as the location of the spectrum. For echelle data, the final position of the spectral order is $A2CENTER+SHIFTA2+CRSCROFF$, where A2CENTER is the value given for that order in the SPTRCTAB. If the cross

correlation fails for an order, then the average value of `CRSCROFF` found for the other orders is used instead and that value is written in the final output header.

In rare cases, the **x1d** task will give unexpected results such that the final extracted spectrum represent the noisy background. This is due to the cross-correlation algorithm incorrectly locating the local maximum at hot pixels or cosmic rays not properly rejected by the `CRCORR` step. Detailed discussion and workaround for this issue are provided in [Chapter 5.5.2](#)

Extract the 1-D Spectrum

Once the spectrum location has been identified, the spectrum is extracted. For the first order modes, the extraction of the spectrum is performed by using a trace interpolated from the two traces in the `SPTRCTAB` with the `A2CENTER` values bracketing the final spectral position `A2CENTER+SHIFTA2+CRSCROFF`. (For some modes, the traces are rotated, as described above.) For echelle data, the final trace is simply the only trace available in the `SPTRCTAB` for that spectral order, shifted to the final position `A2CENTER+SHIFTA2+CRSCROFF`.

The extraction of the spectrum is defined by a triplet of extraction boxes found in the reference table, `XTRACTAB`; one extraction box is used for the spectrum, and the other two are used for the background. The background regions may be tilted with respect to the image axes, but the spectral region is not tilted, to avoid interpolation. For each pixel in the dispersion direction, **calstis** sums the values in the spectrum extraction box. The extraction box is one pixel wide and has a height determined from the `EXTRSIZE` column in `XTRACTAB`, centered on the spectrum. The extraction height can be overridden by the *extrsize* parameter in **x1d**. Each end point of the extraction box may include a fractional part of a pixel. In the case of a fractional pixel, **calstis** will scale the counts in the given pixel by the fraction of the pixel extracted. Thus, each pixel in the output spectrum consists of the sum of some number (or fraction) of pixels in the input image.

Calstis has been designed to allow for unweighted or optimal extraction of the spectrum, although the latter option has not been implemented. The extraction algorithm is determined by the value of the parameter `XTRACALG` in the `XTRACTAB` reference file, currently always set to *unweighted*. (This is not to be confused with setting the parameter *algorithm* to *unweighted* in **x1d**. This parameter in **x1d** is relevant to scattered light correction for echelle data. See [Section 3.4.20](#).) This parameter is written to the header of the output spectrum data file. At the end of the 1-D extraction step, a spectrum of gross counts/sec is produced.

3.4.25 X2DCORR: Produce Rectified 2-D Spectral Image

- Reference files: DISPTAB, INANGTAB, APDESTAB, SPTRCTAB

This step is part of two-dimensional rectification. If X2DCORR is PERFORM, a two-dimensional rectified spectral image will be produced for spectroscopic data. The two-dimensional rectified output image (`_x2d` or `_sx2`) will have a linear wavelength scale and uniform sampling in the spatial direction. The dispersion direction is the first image axis (AXIS1). The size of the rectified image is made somewhat larger (the increase can be substantial for sub-arrays) than the input in order to allow for variations in heliocentric correction and offsets of the spectrum on the detector. The binning of the output image will be approximately the same as the input. For each pixel in the output rectified image, the corresponding point is found in the input distorted image, and bi-linear interpolation is used on the four nearest pixels to determine the value to assign to the output.

Mapping from an output pixel back into the input image makes use of the dispersion relation and one-dimensional trace table. The dispersion relation gives the pixel number as a function of wavelength and spectral order. The one-dimensional trace is the displacement in the cross-dispersion direction at each pixel in the dispersion direction. Both of these can vary along the slit, so the dispersion coefficients and the one-dimensional trace are linearly interpolated for each image line. Corrections are applied to account for image offset, binning, and sub-array. The spectrum can be displaced from its nominal location on the detector for several reasons, including Mode Select Mechanism (MSM) uncertainty, deliberate offsets for distribution of charge extraction for MAMA data, and the aperture location relative to a reference aperture. These offsets are corrected by modifying the coefficients of the dispersion relations and by adjusting the location of the one-dimensional trace. See also DISPCORR and FLUXCORR for algorithmic details. The process of dispersion solution, spatial rectification, and wavelength calibration is similar for one-dimensional extractions and two-dimensional spectral images. However, the flux calibration and error estimates are somewhat different for the two cases (see [STIS ISR 98-13](#)).

¹The rationale for maintaining three types of flat field reference files rather than a single integrated reference file is described in detail in [STIS ISR 95-07](#).

3.5 Recalibration of STIS Data

- 3.5.1 Mechanics of Full Recalibration
- 3.5.2 Rerunning Subsets of the Calibration Pipeline
- 3.5.3 Improving the Treatment of Hot Pixels
- 3.5.4 Improving Cosmic Ray Rejection
- 3.5.5 Removing Fringes from Near-IR Spectral Data
- 3.5.6 Using GO Wavecals
- 3.5.7 Correcting the Orientation of Spectral Traces

Sometimes the default pipeline calibration, performed shortly after the data were obtained from the telescope, is not the best possible calibration for your science program. There are a number of reasons why it may be desirable to recalibrate your data. The most likely reasons include:

- More appropriate reference files have become available since the data were taken. CCD darks and biases are examples of reference files that are updated frequently, but they require some time to be installed in the pipeline. Further refinement of the dark files can be achieved by using daily dark exposures.
- Contemporaneous CCD flat fields were obtained with the science data for G750L or G750M NIR observations to remove fringing.
- Some steps need to be repeated with different input parameters. For example, you may wish to re-perform the cosmic ray rejection or the 1-D spectral extraction after adjusting the input parameters. The best target and background extraction regions for extracting 1-D spectra can depend on the science goals of the program.
- Integer pixel dithers were performed along the slit to move hot pixels in a series of CCD spectroscopic exposures. These exposures are not associated and are thus not combined in pipeline processing. The `_flt` images must be aligned before they can be combined with `ocrreject`.
- Spectral extractions will be made with heights less than the default size to isolate targets with small separations along the slit, or individual rows in a rectified spectral image of an extended target will be analyzed. More accurate spectral traces are needed to improve the extraction or rectification.



Be sure you are using the latest version of the calstis software. See <https://astroconda.readthedocs.io/> for information about the latest release, and also see [Table 3.5](#) of this chapter.

The simplest way to re-calibrate your data with the most appropriate reference files is to request the data from the archive again. However, to tailor the calibration to your individual preferences, it may be beneficial to run **calstis** yourself on your local machine, or to use tasks that improve the reference files or allow customized treatment of the data. **Calstis**, its constituent programs, and other STIS-specific tasks are available in the **stistools** package in **AstroConda**.

The STIS calibration pipeline was designed to accommodate the need for full or partial recalibration. As mentioned at the beginning of this chapter, **calstis** is re-entrant, so that certain calibration steps can be performed outside of the pipeline, and others can be executed multiple times, depending upon the science goals.

Generally, the calibration switches in the header control the operations that **calstis** performs on the data. There are two basic ways to select which operations are performed during calibration:

- Edit the calibration switches and run the **calstis** task.
- Use one or more of the pipeline subset tasks or other STIS-specific tasks described below, managing the calibration through task parameters.

This section describes the first two methods. In the end, the calibration switches in the headers of the calibrated data files will reflect the operations performed on the calibrated data and the reference files used.

3.5.1 Mechanics of Full Recalibration

If you choose to fully recalibrate your STIS data, there is a certain amount of set up required for **calstis** to run properly. The operations mentioned in the checklist below will be described in detail in the following subsections:

- Set up a directory with the required reference files.
- Determine which reference files are needed and retrieve them from the Archive.
- Set the environment variable **oref** to point to your reference file directory.
- Set the calibration switches to perform the needed steps.

- Run **calstis** or a subset of its constituent tasks.

The **stistools** package in **AstroConda** requires the use of a Bash or Bash-compatible shell. Users are referred to: https://astroconda.readthedocs.io/en/latest/getting_started.html for tips on getting started with the **AstroConda** environment.

Before running **calstis**, you will need to define an environment variable to indicate the location of the directory containing the required calibration reference files. The names of the calibration files are preceded with the logical path name “oref\$” in the STIS science headers. In a Bash shell, you may set the path with this command:

```
$ export oref = "/data/calibration/oref/"
```

Note the inclusion of the trailing slash (/) above. If you plan to run **calstis** inside a **Python**, **iPython**, or **Jupyter Notebook** session, you may instead set the environment by doing:

```
>>> import os
>>> os.environ['oref'] = "/data/calibration/oref/"
```

An alternative to using the oref\$ variable is specifying the full pathnames to the reference files in the science headers.

Retrieve Reference Files

To recalibrate your data, you will need to retrieve the reference files used by the difference calibration steps to be performed. The names of the reference files to be used during calibration must be specified in the primary header of the input files, under the section “CALIBRATION REFERENCE FILES.” Note that the data headers will be populated already with the names of the reference files used during pipeline calibration at STScI.

To retrieve the best reference files for a given exposure via the MAST, check “Best Reference Files” in the “Reference Files” section of the Retrieval Options form. Alternatively, the reference files may be retrieved with a tool developed by the Calibration Reference Data System (CRDS) that offers the advantage of retrieving the most recent reference files for observations in a working directory as well as updating the names of the reference files in the primary data headers of the files. In a BASH shell execute the following commands:

```
$ export CRDS_PATH="$HOME/crds_cache"
$ export CRDS_SERVER_URL=https://hst-crds.stsci.edu
$ export oref="{CRDS_PATH}/references/hst/oref/"
```

The above syntax define where your personal copies of CRDS reference files will be stored and the CRDS server that is used. Then the following command may be used to assign and obtain the best references files:

```
$ crds bestrefs --update-bestrefs --sync-references=1 --files *.fits
```

The STIS reference files are all in FITS format, and can be in either IMAGE or BINTABLE extensions. The names of these files along with their corresponding primary header keywords, extensions, and format (image or table), are listed in [Chapter 2](#). The (somewhat obscure) rootname of a reference file is based on the time that the file was delivered to the CRDS.

Edit the Calibration Header Keywords

To edit file headers in preparation for recalibration, use the `astropy.io.fits` package. The following syntax illustrates how to turn on the bias correction switch and update the name of the bias image reference file for a given STIS `_raw` image in the current directory:

```
>>> from astropy.io import fits
>>> hdu = fits.open('<name_raw.fits>', mode='update')
>>> header = hdu[0].header
>>> header['BIASCORR'] = "PERFORM"
>>> header['BIASFILE'] = "oref$new_bias.fits"
>>> hdu.close()
```

The flags listed in [Table 3.4](#) as controlling the basic calibration will usually be set to PERFORM, whether or not the data is fully calibrated. For data not fully calibrated by the pipeline, some or all of the flags in the last column of [Table 3.4](#) will be set to OMIT. To fully calibrate such data, the user can reset these flags in the primary extension header of the `_raw` file to PERFORM, and then run the `calstis` task with this `_raw` file as input. It is also possible to reset the necessary flags in the `_flt` or `_crj` file and then run `calstis` with this file as input to complete the steps that were omitted by the original calibration.

Table 3.4: STIS calibration switches commonly set to PERFORM

| Modes | For Basic Calibrations | Added for Full Calibrations |
|-----------------|------------------------|-----------------------------|
| First-order CCD | | |

| | | |
|--------------------------|--|--|
| | DQICORR, BLEVCORR, BIASCORR, CRCORR, EXPSCORR, DARKCORR, FLATCORR | WAVECORR, X1DCORR BACKCORR, HELCORR, DISPCORR, FLUXCORR, CTECORR, X2DCORR |
| First-order MAMA L modes | DQICORR, LORSCORR, GLINCORR, LFLGCORR, DARKCORR, FLATCORR | WAVECORR, X1DCORR, BACKCORR, HELCORR, DISPCORR, FLUXCORR, X2DCORR |
| First-order MAMA M modes | DQICORR, DOPPCORR, LORSCORR, GLINCORR, LFLGCORR, DARKCORR, FLATCORR | WAVECORR, X1DCORR, BACKCORR, HELCORR, DISPCORR, FLUXCORR, X2DCORR |
| MAMA echelle modes | DQICORR, DOPPCORR, LORSCORR, GLINCORR, LFLGCORR, DARKCORR, FLATCORR | WAVECORR, X1DCORR, BACKCORR, HELCORR, DISPCORR, FLUXCORR, SC2DCORR |
| NUV-PRISM | DQICORR, LORSCORR, GLINCORR, LFLGCORR, DARKCORR, FLATCORR | WAVECORR, X1DCORR, BACKCORR, HELCORR, DISPCORR, FLUXCORR |

If WAVECORR is set to PERFORM, an appropriate STIS line lamp image should be named in the WAVECAL header keyword. This can be either the _wav file supplied with the dataset, or if a GO specified wavecal is used, the file name of the raw wavelength calibration lamp image should be put into this keyword.

The default calibration assumes that the target was centered in the aperture along the dispersion direction. If this is not correct, the wavelength scale will be incorrect, and this offset will apply the wrong sensitivity calibration at each wavelength. In such a case it may be better to perform only the basic 2-D calibrations

using the **calstis** task, and to then perform the spectral extraction or rectification by running the **x1d** or **x2d** tasks independently, and taking the offset in the dispersion direction into account when running those tasks (see [Section 5.5.2](#)).

It is also possible to impose a wavelength offset by setting the `WAVECORR` keyword in the primary extension header to `COMPLETE`, and then setting the desired values for the `SHIFTA1` and `SHIFTA2` keywords in all science extension headers of the input image before running `calstis`. See the description of the `WAVECORR` task ([Section 3.4.23](#)) for an explanation of the `SHIFTA1` and `SHIFTA2` keywords. However, in the absence of a valid wavecal exposure, there is no straightforward way to determine what these values should be. In general they will be non-zero even in the absence of target offsets.

When running the **calstis** task itself, the calibration steps are controlled by setting the values of the calibration step keywords discussed in [Section 3.4](#). These are set in the input data file's primary extension header. However, when running the individual standalone tasks (e.g., **basic2d** or **x1d**), the calibration steps need to be turned on or off using the input parameters of each of the standalone tasks. The values of the calibration keywords in the data file's header are usually ignored, unless they are set to `COMPLETE`. Most standalone tasks will not apply a correction if the header marks it in this way as already done.

However, regardless of whether **calstis** or one of the stand alone tasks is being used, all reference file names must be appropriately specified in the corresponding header keywords in the input data file's primary extension header.

3.5.2 Rerunning Subsets of the Calibration Pipeline

Selected portions of the pipeline can be executed with special tasks in the **stistools** package. The tasks that can be simply used in this fashion are listed in [Table 3.5](#) below. See also [Table 3.1](#) for the association between **basic2d**, **ocrreject**, **wavecal**, **x1d**, and **x2d** and the components of the **calstis** pipeline. See [Chapter 5](#) for further information about some of these tasks. When you run these tasks individually, the calibration parameters usually read from the reference file *must* be entered as command line arguments, however most corrections will not be applied if the corresponding header keyword is already set to `COMPLETE` (see the Appendix of [STIS ISR 98-26](#) and Section 6 of [STIS ISR 98-10](#) for details).

The **inttag** task for TIME-TAG data will accumulate selected events from the raw event table, writing the results as one or more image sets (imsets) in a single, output FITS file. You can optionally specify an explicit starting time, time interval, and number of intervals over which to integrate, and the collection of

imsets will be written to the output file, simulating a REPEATOBS ACCUM observation. Breaking the data into multiple, short exposures can be useful not only for variables but also to improve the flat fielding when the Doppler shift is significant. Once the new raw images have been created, it is straightforward to process them with **calstis** and to analyze the output image or spectra, as appropriate.

Table 3.5: stistools Calibration Tasks

| Task | Description |
|------------------|---|
| inttag | Integrate TIME-TAG event list to form one or more raw images. |
| basic2d | Perform basic 2-D calibration on a raw image. |
| ocrreject | Combine images, rejecting cosmic rays. |
| wavecal | Process wavecal images. |
| x1d | Extract 1-D spectrum. |
| x2d | Rectify 2-D spectral images. |

3.5.3 Improving the Treatment of Hot Pixels

Radiation damage creates hot pixels in the STIS CCD Detector. Some of these hot pixels recover spontaneously. Many more have been repaired monthly by warming the CCD from its normal operating temperature to the ambient instrument temperature for several hours. Despite this annealing procedure, the number of permanently hot pixels has been increasing with time. The development of hot pixels is documented at: http://www.stsci.edu/files/live/mounts/STIS%20Monitors/anneals/pre_post.pdf.

Because the set of hot pixels changes continually, it is important to use the dark reference file prepared for the week of your observation. You should use the corresponding bias reference file, which corrects hot columns. If you requested your data close to the time of the observation, you should check whether new reference files applicable to your data have been made available since. If so, you may want to request your data from the archive again for automatic recalibration with the current reference files, since dark and bias correction occur so early in the calibration sequence.

The standard dark file subtracted from STIS data is based on a combination of several long dark files taken over an entire week. They usually don't do a perfect job of subtracting hot pixels, both because the hot pixels can change on short time scales, and because some of the hotter pixels may have been saturated in the long dark images. It will therefore often be useful to construct a customized dark image for that particular day using short darks taken on the same day as your science image. Procedures for doing this are described at: <https://refstis.readthedocs.io/en/latest/api/weekdark.html>.

After you create your new daydark file, you should set the `DARKFILE` keyword in the primary header of the `_raw` files to reference this new dark file and then reprocess the data through **calstis**.

Even using a daydark will not give perfect removal of all bad pixels. There is no routine available that will automatically find and fix the bad pixels. If a more customized removal of bad pixels is required, it will be necessary to identify them by hand and interpolate over them using neighboring good pixels. The **NumPy** module `numpy.interp` may be useful for the latter task.

3.5.4 Improving Cosmic Ray Rejection

For CCD datasets, **calstis** first runs the equivalent of **basic2d** with `DQICORR`, `BLEVCORR`, and `BIASCORR` set to `PERFORM` to initialize the `ERR` and `DQ` arrays, to trim the overscan regions and subtract the bias level measured there, and to subtract the bias image. It then performs cosmic ray rejection by running the equivalent of **ocrreject**. Next, the equivalent of **basic2d** is run with `DARKCORR` and `FLATCORR` set to `PERFORM` to perform dark subtraction and flat fielding. You can instead run **basic2d** just once on the raw data to perform all of its relevant tasks, then run **ocrreject** on the resulting `_flt` file, but this ordering of the tasks does not provide the optimum rejection of cosmic rays. The cosmic ray rejection is based on a "noise model." Part of that model is that the detected number of photons will follow a Poisson distribution. In order to compute the expected variation in detected photons at a pixel, i.e. to evaluate the noise model, you need a reasonable value for the number of electrons at that pixel. That estimate could be based on the median (for example) of the counts at that pixel in all the images that are to be combined. Because that value should reflect the number of detected photons, the bias level and bias image must first be subtracted from the images, because the electronic bias is an arbitrary offset. The data should not be corrected for dark counts or flat field, however. Dark counts do contribute to Poisson noise. The number of electrons to use for computing the Poisson distribution is the number that were actually

detected, not the number corrected for variations in sensitivity. See [STIS ISR 98-22](#) for further information on cosmic ray rejection. (**Calstis** was changed to perform the tasks in the order described here in July 1998, after the ISR was published.)

In cosmic ray rejection, one wants to strike a balance between failing to identify cosmic rays and clipping real flux from the target. The former lets spurious flux into the `_crj` image; the latter depresses the flux by systematically excluding values that are relatively high for that pixel because of noise fluctuations or small shifts of the target on the detector. Default values of cosmic ray rejection parameters to be used by **calstis**, or its component task **ocrreject**, are taken from the `CRREJTAB` reference file. If your `_crj` images still have many pixels affected by unrejected cosmic rays, you may want to try running **ocrreject** on the `_flt` files with different values for the rejection parameters, which will override the values taken from the `CRREJTAB`. Use `crmask=yes` to flag CRs in the input DQ images.

The optimum values of the cosmic ray rejection parameters depend on many factors, including the number of exposures to be combined, exposure time, signal-to-noise level, source structure, and the magnitude of the misalignment of the exposures due to drift of the target on the detector. (See [STIS ISR 98-22](#).) For example, a small spatial misalignment of two exposures made with very high signal-to-noise may require one to increase the value of the parameter `crsigmas` (for a higher rejection threshold in sigmas) to avoid the systematic rejection of real flux. For a direct image or spectral image with only gradual spatial or spectral changes in flux from pixel to pixel, it may be possible to lower the rejection threshold to catch more cosmic rays without rejecting real flux. One may also need to change the value of `crthresh`, which sets a more stringent rejection level for the pixels surrounding a pixel that failed the `crsigmas` test. (e.g., for `crthresh=0.5` and `crsigmas=7`, rejection occurs for surrounding pixels at a level of $0.5 * 7 \text{ sigma} = 3.5 \text{ sigma}$ out to a radius of `crradius`.)

To see if real flux is being rejected by **ocrreject**, one can compare the `_crj` image to a summed image and look for systematically lower fluxes in the `_crj` image. Problems will tend to occur where the pixel-to-pixel flux changes are the greatest. For a direct image, examine the pixels near the centers of point sources. For a spectral image, examine the peak rows in the spectral image. One can also examine the DQ extensions of the `_flt` files after they have been flagged by **ocrreject** (`crmask = yes`). Systematic problems due to spatial misalignment are especially conspicuous in the DQ extensions of the `_flt` files of spectral images. Improperly flagged spectral images will have strings of `DQ=8192` running along a row near the spatial peak of the spectrum, since that row will be less well centered on the target in one exposure than in

another. Remember to examine the DQ extension of the `_flt` files instead of the `_crj` file, since pixels in the latter will not be flagged for cosmic rays if their flux was computed from cosmic-ray-free pixels in any of the input exposures.

3.5.5 Removing Fringes from Near-IR Spectral Data

The **Python** version of the IR fringe-removal package is in development. Until we release this, users are advised to use the relevant **IRAF** tasks and follow the instructions illustrated below.

Detailed descriptions of the **IRAF STIS** tasks (**normspflat**, **mkfringeflat**, **defringe**, and **prepspec**) for using contemporaneous flat field images to remove IR fringing from STIS G750L and G750M spectra are given in [STIS ISR 98-29](#). Note that this ISR was written before pixel-to-pixel flats were routinely subtracted from STIS spectroscopic data in the OTFR pipeline, and, as a result, includes some steps that are no longer always necessary.

Here we give a simplified and updated subset of these instructions for the most common case: a point source observed with the G750L.

The IR fringe flats may be taken with a variety of apertures. For point source fringe flats taken at or near a standard aperture position near the center of the detector, the best alignment between science image and fringe flat will usually be for fringe flats taken using the 0.3X0.09 aperture. For extended targets, or point sources located elsewhere along the slit, e.g., at the E1 aperture location near row 900, it will be necessary to use a long slit fringe flat, e.g, 52X0.1.

For G750L data, the defringing will usually be applied to the `_crj` image. In this example, the rootname of the fringe flat image is `o8u201070`, and the science image of the external target is `o8u201060`.

The **normspflat** task is used to prepare the fringe flat image and remove the low order lamp vignetting.

```
cl> normspflat o8u201070_raw.fits o8u201070_nsp.fits do_cal='yes'
```

Fringe flat images taken with G750L include not only the IR fringing at wavelengths greater than 7500 Angstroms, but also some fringes at wavelengths less than 6000 Angstroms due to an order-sorter filter. Since these order-sorter fringes are already included in the sensitivity function, they should not be included in the fringe flat, and so these columns should be set to unity in the normalized fringe flat. This

can easily be done by using the **IRAF imcalc** task to create a temporary array, and to then use the **imcopy** task to replace the appropriate columns in the fringe flat.

```
cl> imcalc o8u201070_nsp.fits temp_nsp.fits "if(x .lt. 250) then 1 else im1"  
cl> imcopy temp_nsp.fits[1][1:250,*] o8u201070_nsp.fits[1][1:250,*]
```

The next task is to align and scale the IR fringes in the normalized flat to match those in the science image by using the **mkfringeflat** task.

```
cl> mkfringeflat o8u201060_crj.fits o8u201070_nsp.fits o8u201070_frr.fits
```

It may be necessary to adjust a number of the input parameters of the **mkfringeflat** task to get proper alignment of the fringe flat and science image. See [STIS ISR 98-29](#) for further details. Then, to actually apply the fringe flat to remove the fringes from the science image:

```
cl> defringe o8u201060_crj.fits o8u201070_frr.fits o8u201060_drj.fits
```

The final output file will be the equivalent of the `_crj` file with the fringes removed. This file may be used as input to the **x1d** task to produce a final, fringe-subtracted 1-D spectrum.

3.5.6 Using GO Wavecals

To use an exposure other than the default wavecal, the user can either (1) put the name of the raw exposure file of the lamp image to be used into the `WAVECAL` keyword in the primary header of the `_raw` science image, make sure that the `WAVECORR` keyword is set to `PERFORM`, and then run **calstis** as normal, or (2) use the **stistools** task **wavecal**, to measure the offset of the wavelength calibration image and populate the `SHIFTA1` and `SHIFTA2` keywords in the science file's extension headers. For example, if `o8mi02010` is the science observation and `o8mi02ovq` a corresponding wavelength lamp calibration image, the command would be

```
>>> stistools.wavecal.wavecal('o8mi02010flt.fits','o8mi02ovq_raw.fits')
```

This will update the `SHIFTA1` and `SHIFTA2` keywords and set `WAVECORR` to `complete`. The modified science image file can then be processed with **calstis** and/or one or more of the stand alone STIS tasks, e.g.,

```
>>> stistools.x1d.x1d('o8mi02010flt.fits')
```

Note that the **wavecal** task is meant to update the headers of spectral images, prior to running the **x1d** or **x2d** tasks. It should not be used on images or tables (e.g., `_sx1`, `_sx2`, `_x1d`, or `_x2d` files) that have already had wavelengths assigned to individual pixels.

3.5.7 Correcting the Orientation of Spectral Traces

The orientation of spectral traces on the STIS detectors has been found to rotate slowly over time. Additionally, there is a small random offset in the orientation each time the MSM is positioned. The time-dependent component of the orientation has been calibrated for the most commonly used grating/central-wavelength combinations: G140L/1425, G230L/2376, G230LB/2375, G430L/4300, G750L/7751, G750M/6581, G750M/6768, and G750M/8561. **Calstis** was modified to apply time-dependent rotation to spectral traces, and the evolutionary parameters for these modes are included in `SPTRCTAB` reference files. For other L and M modes with uncalibrated trace rotation, the **mktrace** task can be used to generate a `SPTRCTAB` with accurately rotated traces for a specific science image. The task can also be applied to data taken with the calibrated modes to correct for the random offset in orientation due to the positioning of the MSM.

The **mktrace** task computes the trace of the science target using the default aperture location or accepting an input location. A linear fit is made to this trace. The user can choose to exclude portions of the trace from the fit because of velocity structure, low signal-to-noise, etc. A calibration trace is interpolated from the traces at the nearest rows in the `SPTRCTAB`, and a linear fit is made using the same ranges of columns selected for the fitting of the science trace. Image files of the target trace and calibration trace and of the linear fits are generated to assist the user in selecting the portions of the spectrum to include in the fits. The difference in the angle of the two linear fits is the correction that must be applied to the `SPTRCTAB` traces. A new `SPTRCTAB` is generated, applying this correction to all of the traces for that grating /cenwave combination, thus covering the entire detector. The keyword `SPTRCTAB` in the primary header of the science image is changed to the name of the new trace file, so that subsequent processing by **calstis**, **x1d**, or **x2d** will use the new file.

3.6 Updates to calstis

The **calstis** modules evolve and improve with time, as we understand and characterize more fully the on-orbit performance of STIS. It is possible, even likely, that improvements in the **calstis** software will improve the calibration of your data. To determine the version of the software used to calibrate your data, note the value of the `CAL_VER` keyword in the primary header. The following example uses **astropy.io.fits** to print the rootname, the optical element, and the version of **calstis** for all `_flt` files in the current directory:

```
>>> from astropy.io.fits import fits
>>> hdr = fits.getheader('odbue5040_x1d.fits',0)
>>> print(hdr['ROOTNAME'], hdr['OPT_ELEM'], hdr['CAL_VER'])
```

Watch the STScI Analysis Newsletters (STANs) or consult the STIS WWW pages for any announcement of enhancements to **calstis**.

If you are uncertain whether a given enhancement to **calstis** merits recalibrating your data, contact the Help Desk. Often, it is instructive to re-calibrate (or simply re-request your data from the archive) and to determine empirically whether the revised calibration files or software affect the scientific interpretation of your data. If you need to upgrade your version of the **stistools** package, please refer to <https://astroconda.readthedocs.io/en/latest/updating.html>.

Chapter 4: STIS Error Sources

4.1 Error Sources Associated with Pipeline Calibration Steps

4.1.1 Readout Noise and A-to-D Conversion

4.1.2 Bias Subtraction (only relevant for CCD observations)

4.1.3 Dark Current and Hot Pixels

4.1.4 Flat Fields

In this section, we discuss sources of error that are associated with major steps in the STIS calibration pipeline (**calstis**). Note that these steps themselves were already described in [Chapter 3](#) and will not be repeated here; this section will only describe specific issues related to the error budget of the resulting data which were not described before.

4.1.1 Readout Noise and A-to-D Conversion

Readout Noise (only relevant for CCD observations)

The readout noise is an unavoidable contribution to the total error budget of CCD observations. (MAMA observations do not suffer from readout noise.) It is linked to the readout process and there are no reduction steps that can minimize or remove it. The effect of the read noise on science measurements can however be minimized by keeping the number of pixels where signal is measured small and by minimizing the number of CCD readouts (while still allowing for good cosmic ray and hot pixel removal). The read noise is independent of position on the CCD, but it does vary with the gain setting. Furthermore, the read noise of the STIS CCD has been found to vary with time. The main changes occurred after Servicing Mission 3a (January 2000) and after the switch to the Side-2 electronics (July 2001). A table of read noise values of the STIS CCD as a function of time and gain setting can be found at the following URL: <http://www.stsci.edu/~STIS/monitors/readnoise/>.

A-to-D Conversion (only relevant for CCD observations)

The analog information (electrons) accumulated in the CCD are converted into data numbers (DN) by an analog-to-digital converter (ADC). The STIS CCD camera employs a 16-bit ADC, which can produce a maximum of $2^{16} = 65,535$ DN. However, this is not a limitation for STIS CCD operations, because other factors set the maximum observable DN to lower levels in both supported gain settings. (For the

CCDGAIN = 1 setting, the gain amplifier already saturates at ~33,000 e⁻/pixel, while the full well of the CCD occurs at 144,000 e⁻/pixel, which is before digital saturation would occur in the CCDGAIN = 4 setting.) The ADC produces only discrete output levels. This means that a range of analog inputs can produce the same digital output. This round-off error is called *quantization noise* (QN). It can be shown (Janesick, 2001, Scientific Charge Coupled Devices, SPIE Press) that the quantization noise is constant for a given gain setting when expressed in DN: $QN(\text{DN}) = 12^{-1/2}$. The quantization noise can be converted into noise electrons as follows: $QN(e^-) = 0.288675 \times g$, where g is the ATODGAIN (from the CCDTAB). The total noise (TRN) associated with CCD readout noise (RN) and quantization noise is obtained by adding the two figures in quadrature: $TRN = \sqrt{RN^2 + (0.288675 \times g)^2}$.

4.1.2 Bias Subtraction (only relevant for CCD observations)

CCD bias frames are acquired daily for scientific calibration purposes and for monitoring detector performance. Every week multiple CCD bias frames are combined together into a reference superbias image. The combination removes the cosmic rays accumulated during the readout time and reduces the noise associated with the bias subtraction procedure to a level that is insignificant relative to the read noise associated with any single image.

The **calstis** calibration pipeline performs the bias correction in two steps (see [Section 3.4](#)): BLEVCORR subtracts the bias level from the overscan regions in two steps: it first measures the level and slope in part of the 19 pixel wide leading physical overscan region and then does the same in a 20 row wide virtual overscan region. After the BLEVCORR procedure, some structure remains in the bias frames. This structure includes real bias signal (“spurious charge”) and also some dark current accumulated during the time required to read out the detector. However, this structure is stable on timescales of a few weeks. To remove this structure a superbias frame with high signal-to-noise ratio is subtracted from each science image in the BIASCORR step.

This process has been found to be highly stable and reliable. Details can be found in [STIS ISR 97-09](#) and [STIS ISR 98-31](#).

4.1.3 Dark Current and Hot Pixels

CCD Dark Current and Hot Pixels

Similar to the case of CCD bias frames, CCD dark frames are acquired on a daily basis, and combined together every week for use in the *calstis* calibration pipeline. The creation procedure of the CCD dark reference files involves two main steps:

1. Every month, a high signal-to-noise superdark frame is created from a combination of typically 40-60 “long” darks (dark frames with exposure time > 900 s). For Side-2 electronics, the “long” darks are first scaled to a reference temperature. These monthly superdark frames are not actually delivered to the calibration data base, but used as “baseline” dark for the next steps.
2. All “long” darks taken during a given week are combined together (rejecting cosmic rays in the process), and normalized to intensity units of e^-/s . After that, the hot pixels in the monthly baseline dark (created as described above) are replaced by those of the normalized weekly superdark. These new ‘hot’ pixels have a value higher than “median dark current + 5 of the normalized weekly superdark.” Previously hot pixels that have fully annealed out between the observing dates of the baseline and the new dark are assigned a value equal to that in a median filtered version of the baseline dark. The resulting dark has the high signal-to-noise ratio of the monthly baseline superdark, updated with the hot pixels of the current week. These “weekly darks” are the STIS CCD dark reference files used in the *calstis* pipeline (and are retrievable from the *HST* Archive).

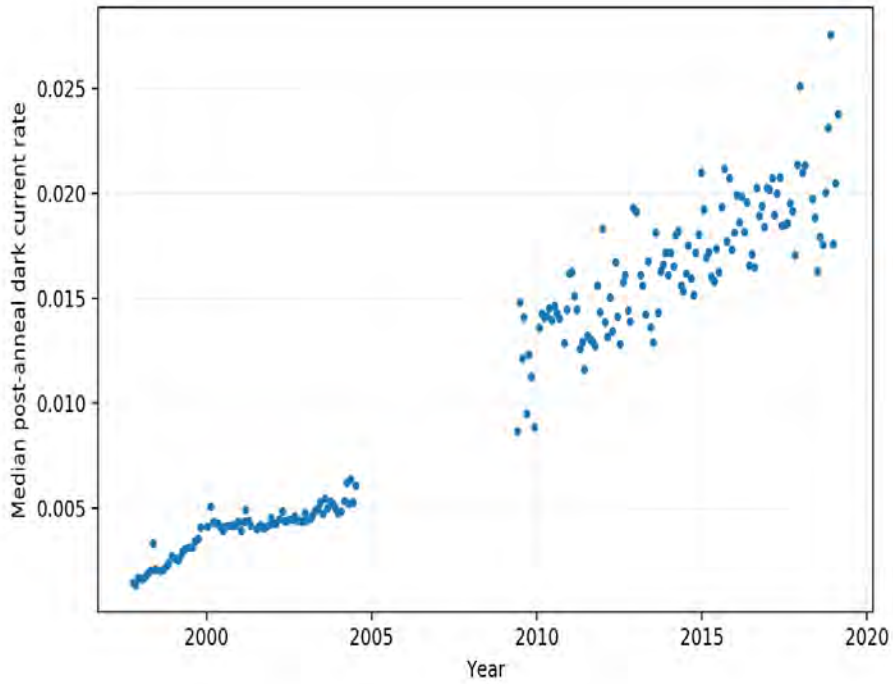
We emphasize that the use of the correct dark reference file is important for most science applications. An incorrect dark reference file will likely introduce a poor dark correction. It will either leave too many hot pixels uncorrected and unflagged, or create many negative “holes” caused by the correction of hot pixels which were not actually hot in the science data (e.g., if the CCD was annealed in the meantime).

Finally, observers have the option to create “daily darks” for their CCD observations, i.e., CCD dark files for which the hot pixels have been optimized for any given date. These “daily darks” are not created within the automatic *calstis* pipeline, but observers have been provided with the **Python** script **weekdark** within the **refstis** package as well as detailed instructions to create such files by themselves. Details are described on the following web page: <https://refstis.readthedocs.io/en/latest/api/weekdark.html>.

In terms of long term trends of the CCD dark current rate, it is relevant to recall that the STIS CCD temperature was stabilized at -83 °C between its installation onto HST on 1997-Feb-14 and the failure of the Side-1 electronics on 2001-May-16. During the Side-1 era, the CCD median dark rate rose from 0.0013 to 0.0043 $e^-/s/pixel$. CCD temperature cannot be stabilized with the Side-2 electronics, so thermal fluctuations perturbed the dark rate during the Side-2 era. These fluctuations are discussed in [STIS ISR 2001-03](#) and [2018-05](#).

The **calstis** pipeline uses EPC files to scale the CCD superdark according to temperature. When recalibrating locally with calstis, it is important to run the correction from within the directory containing the EPC files so they can be found. [Figure 4.1](#) shows the measured median CCD dark current as a function of time.

Figure 4.1: Median CCD Dark Current vs. Time



MAMA Dark Current

NUV-MAMA Dark Current

Most of the dark current in the NUV-MAMA detector is caused by phosphorescence of impurities in the MgF_2 detector faceplate. A simple model of the phenomenon has been developed by Jenkins and Kimble (private communication) that envisions a population of impurity sites each having three levels: (1) a ground state, (2) an excited energy level which can decay immediately to the ground state, and (3) a metastable level that is at an energy slightly below the one that can emit radiation. The metastable state can be thermally excited to the upper level, and this excitation rate is proportional to $\exp(-E/kT)$, where E is the energy difference between the levels. The behavior of the count rate versus temperature leads to an estimate of 1.1 eV for E . At a fixed detector temperature of 30 °C, the time constant for the dark current to

reach an equilibrium value is about 8 days. However, since the MAMA high voltage power supplies have to be shut down during orbits impacted by the South Atlantic Anomaly (SAA), the detector temperature varies from about 27 °C to 40 °C, and the dark current never actually reaches equilibrium.

MAMA temperatures cycle on a roughly daily time scale, being lowest just after the high voltage is turned on after an SAA passage. The dark current can be predicted with about 5% to 10% accuracy using the contemporaneous temperature of the NUV-MAMA charge amplifier recorded in the OM2CAT keyword in the _raw science file that is part of the standard data products. Originally the NUV-MAMA dark current was fit with the curve $darkrate = 9.012 \times 1020 \times \exp(-12710/T)$. This worked well for the first two years of STIS operations, but as the mean time-averaged temperature of the detector increased with time, this formula started to predict too high a dark current. Once this was realized, a more flexible fitting formula was implemented in the calstis pipeline. This updated formula for the dark current was

$$darkrate = norm \times 1.805 \times 1020 \times \exp[-12211.8/\max(T, T_{min})],$$

where both *norm* and *T_{min}* are slowly varying functions of time that are empirically adjusted to give a good match to the observed dark rate, and which are tabulated in the temperature dependent dark correction table (_tdc) reference file. The uncertainty related to the application of the updated NUV-MAMA dark rate is 5% rms. Note however that this doesn't translate to any significant photometric uncertainty, since any residue of the dark subtraction process gets subtracted out during the extraction of imaging photometry or spectroscopic flux.

Right after SM4, the dark count rate for NUV-MAMA was found to be as high as 0.0160 counts/pix/s, significantly higher than expected from the detector's pre-SM4 behavior. However, over a time scale of a year, the count rate decreased exponentially with time down to a level of ~0.0035 counts/pix/s, until the STIS detectors were turned off on October 2010 due to issues with HST's control and data handling electronics. When the NUV-MAMA was turned back on a month later on Nov 2010, the dark rate was measured to be at an increased level of 0.006 counts/pix/s. As before, the dark rate followed an exponential decrease with time eventually reaching a median rate of ~0.0015 counts/pix/s and staying at that level for several years. In [STIS ISR 2013-01](#), the dark rate formula has been updated for post-SM4 data to include both the short-term variation due to detector temperature and the long-term variation due to the exponential decay with time. Details of this formula can be found in [Section 3.4.7](#) and in [STIS ISR 2013-01](#).

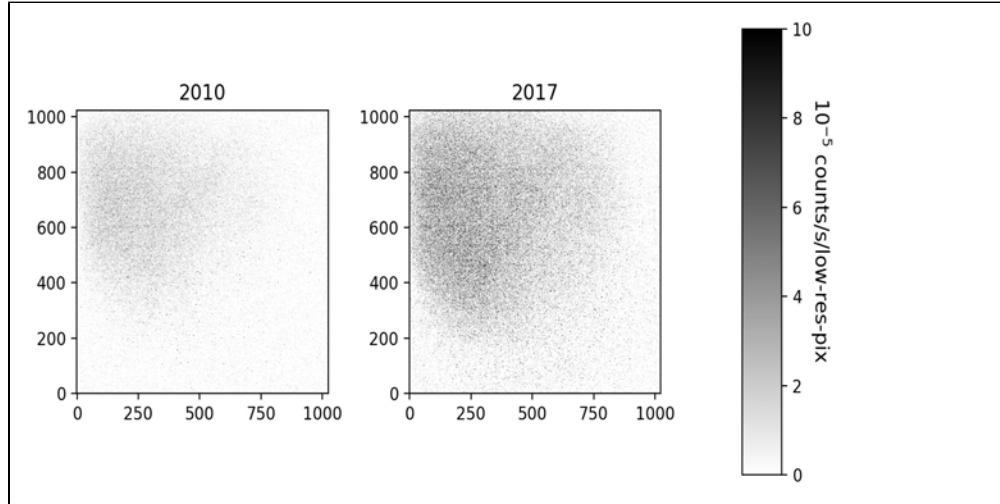
HST entered safe mode on October 5, 2018 due to a gyro failure, and came back online on Oct 27, 2018. After this, the STIS NUV-MAMA dark count rate was measured to be as high as 0.0038 counts/pix/s, but

it quickly declined back to normal levels. As of January 2019, the dark count rate is at ~ 0.0020 counts/pix/s. The STIS team plans to update the parameters in the TDCTAB as necessary for observations obtained after October 27, 2018 once the number of data points become sufficient for deriving a solution. The long-term time variation of NUV-MAMA dark count rate can be found at: <http://www.stsci.edu/files/live/mounts/STIS%20Monitors/nuv/STIS-NUV-MAMA.png>.

FUV-MAMA Dark Current

The FUV-MAMA dark current is very low compared to that of the NUV-MAMA. In the early years of STIS operations, dark current values as low as 7 counts/s integrated over the whole detector were routinely encountered. However, there is also an intermittent glow that covers a large fraction of the detector (see [Figure 4.2](#)). The source of the dark current is not phosphorescence but is intrinsic to the micro-channel plate array. This glow can substantially increase the dark current over a large fraction of the detector, and this leads to count rates of up to 100 counts/s integrated across the face of the detector (which is of course still very low). During the first two years of STIS operations, this glow was only present intermittently, but since mid-1999 it showed up more often than not. This extra glow appears to be a function of both the detector temperature, and the length of time the detector has been on. (The STIS MAMA detectors were turned off daily during *HST*'s passages through the South Atlantic Anomaly.) However, the strength and frequency with which this glow appears increased throughout the lifetime of STIS. At later epochs, only the first non-SAA-impacted orbit each day could be reliably expected to be free of the extra glow.

Figure 4.2: Dark Current Variation Across FUV-MAMA Detector.



Examples of the FUV-MAMA dark current variation across the detector can be seen in [Figure 4.2](#), which are the sums of a number of 1380 second dark frames taken during periods of high dark current in 2010 (left) and in 2017 (right). The dark current in the lower right quadrant varies with time and temperature. The total dark current can be approximated by the sum of a constant dark current plus a “glow” image, scaled to the net rate in the upper left quadrant. No reliable method has been found to predict the brightness of the glow with sufficient accuracy to subtract it from pipeline processed FUV-MAMA images, and so FUV-MAMA dark images provided by archive contain only the base dark current plus the mean values for any pixels flagged as hot pixels. For the FUV-MAMA, hot pixels are defined to be those that show an average dark current of more than 1×10^{-4} counts/hi-res-pixel/s as measured over several months of dark monitor observations. In 1997, only 97 out of the more than 4 million pixels had a dark rate of more than 1×10^{-4} counts/s. By the time of the Side-2 failure, more than 3,000 pixels were at this level; by 2018, over 13,000 pixels were at this level.

Subtracting the extra glow requires identifying a region on the detector where the glow is strong while the intrinsic target flux is weak, and then using this region to scale and subtract a smoothed image of the glow. For long slit spectroscopic observations, the region of the detector occulted by one of the aperture bars may sometimes be useful for this purpose. Mean glow images for different epochs can be obtained upon request by contacting the help desk and can be used for off-line data reduction if appropriate.

However, it is good to keep in mind that the FUV-MAMA dark current is so low that a typical STIS FUV-MAMA observation will have less than one count per pixel from the dark, so that many science projects will not require special data reduction efforts in this respect. Also, various standard measures of background (the median for example) are not good estimates of the dark when the data are quantized into just a few values. The best way to estimate the background is to identify hot pixels using the dark reference files, and then use an unclipped mean for the remaining pixels in a source-free region of the image.

4.1.4 Flat Fields

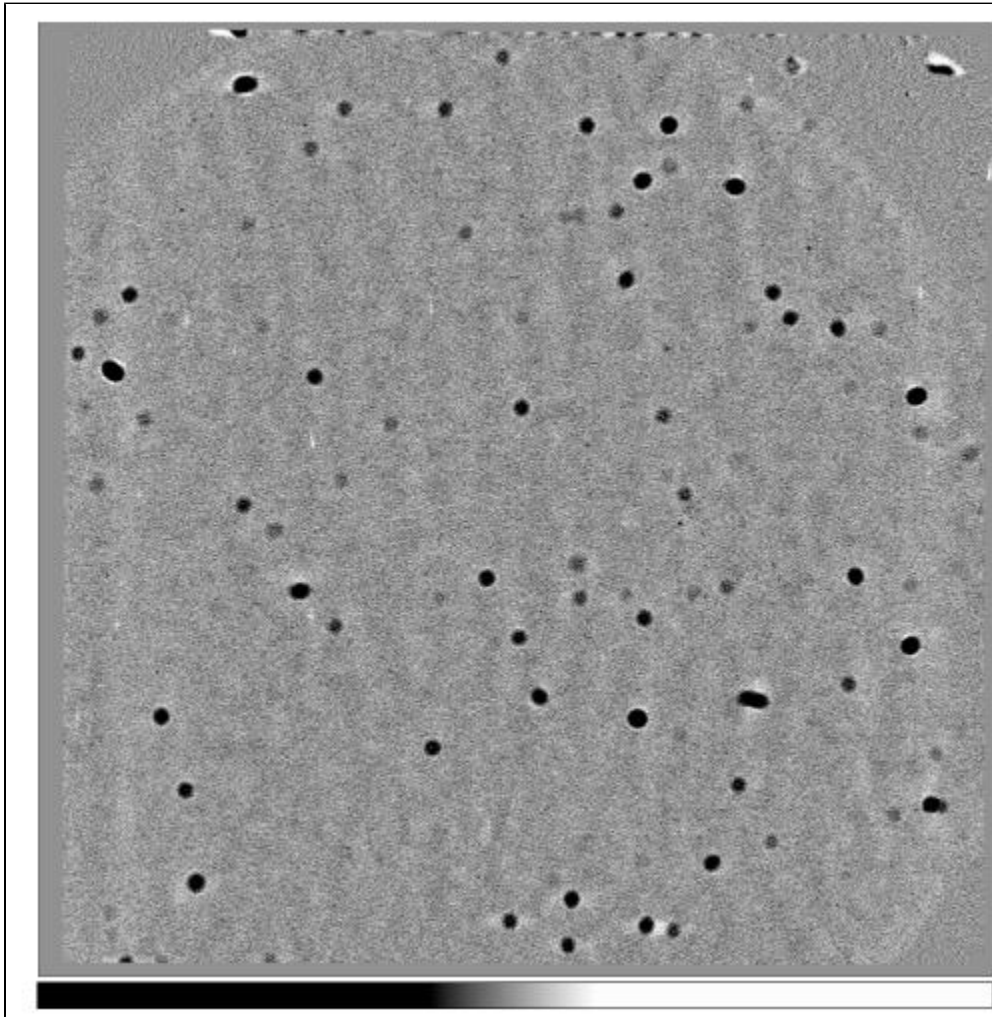
The flat field reference files currently in use by the **calstis** calibration pipeline were derived by several different methods, depending on the detector, the observing mode (imaging vs. spectroscopy), and (for some modes) the optical elements used. For many observing modes, there are two types of flat fields involved in the calibration: *p-flats* (the *_pfl.fits reference files) which correct for the pixel-to-pixel sensitivity variations, and *l-flats* (*_lfl.fits) which model the low-frequency variations in sensitivity over the field of view of the observing mode in question. Important features regarding the accuracy of the flat fields for different observing modes are described in the following sections.

CCD Imaging Flat Fields

- **p-flat:** The p-flat reference file for CCD imaging was created from several exposures of the internal tungsten lamp during ground calibration. The total accumulated intensity was at least 100,000 electrons/pixel, except for the borders of the image which are partially vignetted by the mode select mechanism (MSM). After image combination, the lamp illumination function was removed through division by a median-filtered version of the image (using a 55×55 pixel kernel). The vignetted borders of the image were flagged during this procedure (note that due to the intrinsic non-repeatability of the MSM, the exact vignetting of the borders of the image is different every time the MSM is moved to the CCD imaging mode). The structure of the CCD p-flat is shown in [Figure 4.3](#). The most obvious features are circular dark patterns with typical diameters of ~ 20 pixels. These artifacts are shadows of dust on the CCD window, often called "dust motes". They are removed by the p-flat to well within 1%. On-orbit testing of CCD imaging p-flat images has shown that the p-flat is stable to within about 0.2% after correction for Poisson noise.
- **l-flat:** The low-order flat-field reference file for CCD imaging was created from numerous images taken during the Hubble Deep Field South (HDF-S) campaign in October 1998. After bias

subtraction and dark subtraction using dedicated high-signal-to-noise combinations of bias and dark files, the images were masked for cosmic rays and heavily masked around all sources detected in the individual images. The combined image was then fit by a 5-piece cubic spline function. The main purpose of this l-flat is a correction of the 5-10% sensitivity roll off near the edges of the 50CCD aperture which remains after application of the CCD imaging p-flat described above.

Figure 4.3: Pixel-to-pixel flat field for the STIS CCD with a stretch from 0.90 (black) to 1.10 (white). The intensity transfer table is shown in the bar at the bottom. The numerous ~20 pixel size dark circles in the field are caused by dust particles on the CCD window.



CCD Spectroscopic Flat Fields

- **p-flats:** P-flat reference files for the CCD spectroscopic modes were originally created from high S/N spectra of deuterium and tungsten lamps during ground calibration of STIS. They were first updated by in-flight data on 1999-Sep-20 (and several updates followed afterwards). Flat field data

were taken in flight on a regular schedule and in every supported observation mode in order to enable one to identify any dependence on in-flight epoch and/or the grating used. Details of the flat field file creation procedure and analysis are published in [STIS ISR 99-06](#). The main results of this analysis were:

- (a) The pixel-to-pixel flat field for the CCD has been found to be independent (to within the limits set by Poisson statistics) of wavelength, CCD gain setting, and signal level.
- (b) The structure of the L-mode flat fields is different from that of the M modes, due to the different optical magnification of the two sets of modes. Hence, flat fields have been derived separately for L- and M-modes.
- (c) A time dependence of the structure of the flat field was identified. The systematic (non-Poisson) effect is of order 0.3% per year. To keep this effect within 1%, spectroscopic CCD flat fields have been delivered for all spectroscopic CCD modes with `USEAFTER` dates of April 1997, July 1999, August 2000, and October 2001.

- **l-flats:** To probe the sensitivity as a two-dimensional function of wavelength and position along the slit, a number of calibration programs were performed in which a bright star was dithered up and down the length of the 52X2 slit. In addition, CCD sensitivity monitor measurements made after April 2002 routinely included measurements at both the central and E1 aperture positions on the slit (see [Section 7.2.7](#) of the *STIS Instrument Handbook*). The ratio of sensitivities at the E1 position to the central row is therefore very well measured, while more limited data is available at other positions along the slit. The latter measurements feature 1 to 4 arcsec spacing along the cross-dispersion direction.

L-flats were produced for the G140L, G230LB, G430L, and G750L gratings. The medium-resolution gratings lack sufficient data at most central wavelengths, while the G230L mode was found not to require a low-order flat field correction. The l-flats are defined to be unity at the row where the absolute sensitivity calibration is determined. The typical effect of applying the l-flats is of order 1-2% in sensitivity along the dispersion (depending on the grating in question) and 2-3% perpendicular to the dispersion. It should be kept in mind that the l-flat corrections are only strictly applicable to targets positioned along the center line of the slits. Targets that are significantly offset in the dispersion direction will not be corrected with the same degree of accuracy, especially near the extremes of the wavelength coverage of the grating used. More details are available in Proffitt ([2006](#)).

MAMA Flat Fields

- **p-flats:** The MAMA flat fields are dominated by a fixed pattern that is a combination of several effects including "beating" between the micro-channel plate array and the anode pixel array and variations in the charge cloud structure at the anode. For this reason, the flat field correction for MAMA data is applied to the data in unbinned format (2048×2048 pixel²). Intrinsic pixel-to-pixel variations are 3.9% rms for the FUV-MAMA and 2.8% rms for the NUV-MAMA, respectively, in the format delivered by the **calstis** pipeline ("low-resolution pixels", 1024×1024 pixel²).

The creation of high-signal-to-noise-ratio p-flats with the STIS MAMA detectors is done using the internal Krypton (for the FUV-MAMA) and Deuterium (for the NUV-MAMA) lamps. It is a rather long and tedious process, since individual exposures have to adhere to the global count rate linearity limit for MAMA detectors^[1] One also has to take exposures at several slit locations in order to illuminate regions of the detector that are normally occulted by the slit fiducial bars (see *STIS Instrument Handbook*, Chapter 13.2.6) and other scheduling limitations, it takes several HST cycles to achieve this.

The current MAMA p-flat reference files have been in use by the calstis pipeline since 2002-Nov-20, and have a signal-to-noise ratio of ~ 200 per pixel. A detailed analysis of the quality of the MAMA p-flats using well-illuminated spectra of flux standard stars (white dwarfs) shows that the rms of extracted spectra (summing 11 MAMA rows) is of order 1%. This is larger than the rms of the p-flats due to Poisson statistics, and it represents the current limit of the quality of flux calibration of individual targets from individual exposures (imaging or spectra). STIS users whose science requires higher signal-to-noise ratios have been directed to use multiple exposures using FP-SPLIT slits or spatial dithering along the slit (see *STIS Instrument Handbook*, Chapter 12.5).

- **Spectroscopic l-flats:** The need for L-flats was considered for the low-resolution spectral modes G140L and G230L, as described in detail above for the CCD spectral modes. It was eventually determined that an l-flat correction was only required for the G140L mode.
- **Imaging l-flat:** MAMA imaging l-flats were determined from observations of the Galactic globular cluster NGC 6681 obtained at a large number of offset pointing positions (144 for the NUV-MAMA, 207 for the FUV-MAMA) using the "CLEAR" (25MAMA) filter. The l-flat consists of a two-dimensional, second-order polynomial surface fit to the ratios of large-aperture fluxes obtained

for the same stars, normalized to unity in the inner 400×400 pixel² region. The results showed that an imaging l-flat is only needed for the FUV-MAMA, which features a significant ~22% peak-to-peak variation in sensitivity over the field of view (mainly due to variations towards the upper right corner and near the left-hand edge of the detector). The l-flat corrects this to 2% rms. In contrast, the sensitivity variations of the NUV-MAMA stay below 1% rms even without the l-flat correction.

¹200,000 counts/s; given the lamp brightness, this can only be achieved with the G140M and G230M gratings and a narrow slit. Hence these p-flats are applied to both imaging and spectroscopic MAMA data.

4.2 Summary of Accuracies

In [Table 4.1](#) through [Table 4.5](#), the accuracies are listed for each basic observation mode of the STIS: CCD spectroscopy, MAMA spectroscopy, CCD imaging, MAMA imaging, and target acquisition. The MAMA pixels in these tables are low resolution pixels. All accuracies quoted are 2 limits, and reflect our current understanding of STIS calibration. Any updates to these accuracies will be documented in [Chapter 16.1](#) of the *STIS Instrument Handbook*. The main sources of inaccuracy are discussed in some detail in the next subsections.

We remind you that calibration data are, and have always been, made non-proprietary immediately after they are (or were) taken. Should you have a need for higher accuracy or urgent results, you may wish to consider direct analysis of the calibration data for your particular observing mode (see also [Chapter 17](#) of the *STIS Instrument Handbook* for a description of our on-orbit calibration program).

Table 4.1: CCD Spectroscopic Accuracies

| Attribute | | Accuracy | Limiting Factors |
|--|---------|---------------|--|
| Relative wavelength ^[1] | | 0.1–0.4 pixel | Stability of optical distortion Accuracy of dispersion solutions |
| Absolute wavelength ^a (across exposures) | | 0.2–0.5 pixel | Thermal stability Derivation of wavecal zero point Accuracy of dispersion solutions |
| Absolute photometry ^[2] | | | Instrument stability Correction of charge transfer efficiency Time dependent photometric calibration Fringe correction (for > 7500 Å) |
| | L modes | 5% | |
| | M modes | 5% | |
| Relative photometry ^[2] (within an exposure) | | | Instrument stability Correction of charge transfer efficiency Time dependent photometric calibration Fringe correction (for > 7500 Å) |
| | L modes | 2% | |
| | M modes | 2% | |

¹ For more recent analyses of wavelength accuracy, see [STIS ISR 2011-01](#) and [STIS ISR 2015-02](#). Note that the wavelength accuracies will also depend on the accuracies of the rest wavelengths used in calculating the dispersion relations

² Assumes star is well centered in slit, and use of a 2 arcseconds wide photometric slit. This accuracy excludes the G230LB and G230MB modes when used with red targets, for which grating scatter can cause large inaccuracies in the flux calibration; see Gregg et al., (2006). Photometric accuracies referenced are for continuum sources; equivalent width and line profile measures are subject to other uncertainties (such as spectral purity and background subtraction).

Table 4.2: MAMA Spectroscopic Accuracies

| Attribute | | Accuracy | Limiting Factors |
|--|---------------------------------|-------------------------------|---|
| Relative wavelength ^[1] (within an exposure) | | 0.25–0.5 pixel ^[2] | Stability of small scale geometric distortion Optical distortion Accuracy of dispersion solutions |
| Absolute wavelengths ^[1] (across exposures) | | 0.5–1.0 pixel ^[2] | Thermal stability Derivation of wavecal zero point Accuracy of dispersion solutions |
| Absolute photometry ^[3] | | | Instrument stability Time dependent photometric calibration |
| | L modes | 4% | |
| | M modes | 5% | |
| | Echelle modes ^[4] | 8% | |
| Relative photometry (within an exposure) ^d | | | Instrument stability Flat fields Echelle modes: Blaze shift correction accuracy Scattered light subtraction |
| | L modes | 2% | |
| | M modes | 2% | |
| | Echelle modes ^{d, [5]} | 5% | |

¹ For more recent analyses of wavelength accuracy, see [STIS ISR 2011-01](#) and [STIS ISR 2015-02](#). Note that the wavelength accuracies will also depend on the accuracies of the rest wavelengths used in calculating the dispersion relations

² A pixel for the MAMA refers to 1024×1024 native format pixels.

³ Assumes star is well centered in slit, and use of a wide photometric slit.

⁴ For 0.2X0.2 arcsecond slit. These are typical accuracies which can be 2 to 3 times better or worse as a function of wavelength (see [STIS ISR 1998-18](#) for details).

⁵ Quoted relative flux accuracies of echelle spectra assume that the time dependent shifts in the echelle blaze function are properly corrected. Recent improvements to the blaze shift correction yield agreement in the order overlap regions to better than 5% for E140H (see [August 2017 STAN](#)).

Table 4.3: CCD Imaging Accuracies

| Attribute | Accuracy | Limiting Factors |
|-------------------------------------|-----------|---------------------------------|
| Relative astrometry within an image | 0.1 pixel | Stability of optical distortion |
| Absolute photometry | 5% | Instrument stability |
| Relative photometry within an image | 5% | External illumination pattern |

Table 4.4: MAMA Imaging Accuracies

| Attribute | Accuracy | Limiting Factors |
|-------------------------------------|-------------------------------|---------------------------------------|
| Relative astrometry within an image | 0.25 pixel ^{[1],[2]} | Small scale distortion stability |
| Absolute photometry | 5% | Instrument stability and calibration |
| Relative photometry within an image | 5% | Flat-fields and external illumination |

¹ A pixel for the MAMA refers to 1024×1024 native format pixels.

² A recent re-analysis of the FUV-MAMA geometric distortion has yielded rms residuals of 4mas (0.16 pix) in each coordinate, compared to the positions in an astrometric standard catalog based on WFC3

/UVIS imaging data (see [STIS ISR 2018-02](#)).

Table 4.5: Target Acquisition Accuracies

| Attribute | Accuracy | Limiting Factors |
|---------------------------------------|----------------------|--|
| Guide star acquisition | 1-2 0.2-0.3 | GSCI catalog uncertainties GSCII catalog uncertainties See Section 1.2.1 |
| Following target acquisition exposure | | Signal to noise Source structure |
| Point sources Diffuse sources | 0.01 0.01–0.1 | Centering accuracy plus plate scale accuracy to convert pixels to arcseconds See Chapter 8 of the <i>STIS Instrument Handbook</i> |
| Following pickup acquisition exposure | 5% of the slit width | Signal to noise Source structure Number of steps in scan and PSF |

4.3 Factors Limiting Flux and Wavelength Accuracy

4.3.1 Flux Accuracy

4.3.2 Wavelength and Spatial Accuracies

4.3.1 Flux Accuracy

The accuracy to which you can trust the absolute flux calibration of your STIS spectroscopic data at slit center is limited by several factors including:

- The accuracy of the absolute sensitivity calibration of the grating and central wavelength setting. The on-orbit absolute sensitivity calibration is determined by observing a standard star, with known absolute flux calibration, well centered in both wavelength and cross dispersion in a large slit. The STIS spectrum of this star is then extracted over a standard aperture extraction box and the sensitivity required to return the known flux from the star is determined as a function of wavelength. The standard aperture extraction box is large enough to be relatively insensitive to spacecraft jitter and breathing but small enough that the signal-to-noise of a typical stellar spectrum will not be degraded. STIS calibration accuracies are defined for the standard aperture extraction box; the standard boxes are mode dependent and are given in the XTRACTAB reference file.
- The accuracy of the calibration of the time dependence of the sensitivity of the grating and wavelength region you are using. This calibration is typically accurate to within 1% rms (see [STIS ISR 2004-04](#), [STIS ISR 2006-04](#), [STIS ISR 2014-02](#) and [STIS STAN April, 2004](#) for details).
- The accuracy of the calibration of the aperture throughput for the aperture you are using for your science relative to the aperture that was used for the absolute sensitivity calibration.
- The accuracy to which your source is centered in the slit.
- The size of the extraction aperture you use to measure your flux and the accuracy to which the cross dispersion profile is known in the mode in which you are observing. Because the corrections for the aperture extraction can be large (e.g., 30% in the near-infrared and the far-UV) this effect can be important.
- Bias and background subtraction can add considerable additional uncertainty for faint sources or spectra with significant variations in flux, particularly for the echelle modes.

- Grating scatter, which can play an important role, particularly for the G230LB and G230MB gratings when used with red targets (see footnote to [Table 4.1](#)).
- For Echelle modes: the accuracy of the correction of the behavior of the echelle blaze function with time and location of the spectra on the detector and the accuracy of the scattered light correction (see [STIS ISR 2002-01](#) and [2018-01](#)).

Additional uncertainties arise for flux measurements not at slit- and field-center. These uncertainties are relevant when, for example, you wish to determine relative fluxes in an extended source along the long slit or when you have used POS-TARGs to move a target along the long slit. They include:

- The variation in slit throughput along the slit. The slits have 5 micron variations along their widths (corresponding to ~ 0.02 arcsecond), which for a 0.1 arcsecond wide slit on a diffuse source, would produce a 20% variation in flux. For a point source the variation would be more in the 5% range for that same slit. There are also dust specks with appreciably higher opacity along some places in some slits.
- The accuracy to which the vignetting along the cross-dispersion direction is known for your grating and central wavelength.
- The accuracy to which the low order flat field along the dispersion direction is known off of field center for your grating and central wavelength.

4.3.2 Wavelength and Spatial Accuracies

The accuracy with which the wavelength scale is known in your calibrated STIS spectrum will depend on several factors:

- The accuracy of the dispersion solutions, which governs the accuracy to which relative wavelengths are known in a given spectrum.
- The accuracy of the wavelength zero point, which governs the accuracy to which relative wavelengths are known across spectra.
- The accuracy to which your source is centered in the science slit (a pixel of miscentering corresponds to a pixel in absolute wavelength space).

The dispersion solutions used to calibrate STIS on-orbit data were derived on the ground during thermal vacuum testing. On-orbit tests confirm the applicability and accuracy of the ground dispersion solutions for on-orbit data, producing relative wavelength accuracies of 0.2 pixels across the spectrum for first-order

gratings at the prime settings and appreciably better in some instances. For the echelle modes, at the prime settings, the accuracies are roughly 0.2 pixels for wavelengths in the same order and approximately 0.5 pixels for the entire format. The intermediate wavelength settings have roughly twice these errors. The accuracy of the dispersion solutions is well maintained across the spatial extent covered by the first-order modes. However, the illumination of the CCD detector by the line lamp used for wavecal exposures suffers somewhat from vignetting at the top and bottom of the detector. Fortunately, the effect of this at the location of the E1 pseudo apertures, has been found to be insignificant, although a few observing modes may have a slightly lower accuracy (details are presented in [STIS ISR 2005-03](#)).

Due to the lack of repeatability of the Mode Select Mechanism (STIS's grating wheel), the projection of your spectrum onto the detector in both wavelength and space will vary slightly (1 to 10 pixels) from observation to observation if the grating wheel is moved between observations. In addition, thermally induced motions can also affect the centering of your spectrum. The **calstis** pipeline removes the zero point offsets using the contemporaneous wavecals (see [Section 3.4.23](#)). The wavelength zero point in your calibrated data (the `_sx2`, `_x2d`, `_x1d`, and `_sx1` files) is corrected for these offsets and should have a wavelength zero point accuracy of ~0.1–0.2 pixels (better when the wavecal is taken through small slits, worse for those taken through wider slits). This accuracy should be achieved, so long as contemporaneous wavecals were taken along with the science data, distributed at roughly one hour intervals among the science exposures, and assuming the target was centered in the slit to this accuracy or better.

The accuracy of the zero point pipeline calibration in the spatial direction is slightly less, roughly 0.2–0.5 pixels. This is because the finding algorithm, which must locate the edges of the aperture for short slits and the edges of the fiducial bars on the slits for the long slits, is less robust. Observers need to be aware of possible offsets between spectra in the spatial direction, particularly when deriving line ratios for long slit observations of extended targets taken with different gratings.

A source can lie off-center in an aperture because of errors in the ACQ or ACQ/PEAK procedure, because of errors in the defined displacement from the acquisition aperture to the science aperture, and because of drift of the target over time. The component of error in the AXIS1 direction produces an uncalibrated shift in wavelength. The ACQ for a point source is generally accurate to 0.01 arcsec. An ACQ/PEAK can improve the accuracy, but can also degrade it if, for example, the signal to noise is poor. See [Section 5.2.6](#) for a guide to the interpretation of acquisition data, and [Chapter 8](#) in the *STIS Instrument Handbook*, for a full discussion of acquisition procedures. The error in the defined displacement from the acquisition aperture to the science aperture has generally been insignificant, except for errors in the original definition of the E1 apertures. These long-slit pseudo-apertures, which place the target high on the detector near the

readout amplifier to minimize CTE effects, were introduced on 2000-Jul-03 and revised on 2003-Aug-04. The defined AXIS1 positions of apertures 52X0.2E1, 52X0.5E1, and 52X2E1 were revised by shifting them -0.73 pixels; those of the 52X0.05E1 and 52X0.1E1 were revised by shifting them -0.55 and -0.70 pixels, respectively. Before the revision, E1 aperture exposures made after an ACQ or after an ACQ /PEAK at the center of the detector were systematically miscentered by the full amount of these shifts, causing spectral features to appear at longer wavelengths. Exposures made after an ACQ/PEAK with the same E1 aperture were free of the error, and exposures made after an ACQ/PEAK with a different E1 aperture were off-centered by the relative error, which is usually ~ 0 . Target drift is generally insignificant over the course of an orbit when two guide stars are used, but is larger and variable when one guide star is used. See [Section 5.2.6](#) and [Section 8.1.4](#) in the *STIS Instrument Handbook*.

Chapter 5: STIS Data Analysis

5.1 Data Reduction and Analysis Applications

5.1.1 STIS-Specific Python Tasks

5.1.2 Handling FITS Tables

5.1.3 General Spectral Display and Analysis Tasks

5.1.4 AstroDrizzle for Image Combination

Most of the software tools for operating on STIS FITS files are contained in the **stistools** package.

Stistools is a package that provides **Python**-based data processing tools for working with STIS data. It contains **calstis**, the full STIS calibration pipeline, as well as its individual components (e.g., **basic2d**, **ocreject**, **wavecal**, **x1d**, **x2d**). Many of these tasks are described in [Chapter 3](#). In addition, **stistools** features a selection of analysis tools independent from the pipeline. The following website provides documentation including example usages for individual tasks in the **stistools** package: <https://stistools.readthedocs.io/>

As of early 2019, the transition from older **IRAF/PyRAF** routines to **Python**-based routines is still in progress, and there remains a few tools from the **IRAF/PyRAF** version of the package that are still in development in the Python package. In this transitional period, users are encouraged to use **IRAF/PyRAF** for the tools/tasks currently unavailable in **Python**., e.g., tasks for removing IR fringes (see [Section 3.5.5](#)). In the meantime, we plan to keep the [stistools web documentation](#) up to date, so users are aware of any update to its components.

5.1.1 STIS-Specific Python Tasks

In [Chapter 3](#), we gave detailed discussions of the use of the data reduction pipeline **calstis**, the **calstis** component tasks, and auxiliary tasks that were developed to create customized reference files and to facilitate the combination of unassociated images. Most of these tasks are contained in the **stistools** package. Other tasks useful for reducing and analyzing STIS data are contained in this package as well. A complete listing and brief description of these tasks can be found at <https://stistools.readthedocs.io/>.

The function **stistools.stisnoise** was implemented to deal with the increase in pattern noise with the shift of STIS operations to Side-2 electronics in July 2001. The function **stistools.mktrace** was created to correct the orientation of spectral traces for application to a given image when it was discovered that the

traces have gradually rotated over time. (The average rotation rates have been incorporated into the trace reference files for the L gratings and for the most commonly used M modes: G750M (CENWAVEs 6581, 6768, 8561). See [Section 3.5.7](#).) The function `stistools.wx2d` is being offered as an alternative to the bilinear interpolation performed by `stistools.x2d`. It produces an image that is iteratively subsampled in the cross-dispersion direction, then rectified in that dimension and summed back into pixels. The final image can then be processed by `stistools.x2d` for photometric calibration.

5.1.2 Handling FITS Tables

STIS spectral extractions, TIME-TAG data, and most STIS reference files are stored in FITS tables (see [Section 2.3.2](#) for a description of the structure of the table extension files for spectral extractions and TIME-TAG data). The `Table` module in `astropy.table` is designed to read in data contained in FITS tables. Below, we provide several examples of using the `Table` module with STIS data files. A sample output is given after each command.

Find out what information is given in the columns of a FITS table (the parameters listed here are discussed in depth in [Section 5.4](#)):

```
>>> from astropy.table import Table
>>> ex_table = Table.read('obc410010_x1d.fits')
>>> print(ex_table.info)
```

| <Table masked=True length=1> | | | | | |
|------------------------------|---------|---------|------------------------|-----------|--|
| name | dtype | shape | unit | format | |
| SPORDER | int16 | | | {:11d} | |
| NELEM | int16 | | | {:11d} | |
| WAVELENGTH | float64 | (1024,) | Angstroms | {:25.16g} | |
| GROSS | float32 | (1024,) | Counts/s | {:15.7g} | |
| BACKGROUND | float32 | (1024,) | Counts/s | {:15.7g} | |
| NET | float32 | (1024,) | Counts/s | {:15.7g} | |
| FLUX | float32 | (1024,) | erg / (Angstrom cm2 s) | {:15.7g} | |
| ERROR | float32 | (1024,) | erg / (Angstrom cm2 s) | {:15.7g} | |
| NET_ERROR | float32 | (1024,) | Counts/s | {:15.7g} | |
| DQ | int16 | (1024,) | | {:11d} | |
| A2CENTER | float32 | | pix | {:15.7g} | |
| EXTRSIZE | float32 | | pix | {:15.7g} | |
| MAXSRCH | int16 | | pix | {:11d} | |
| BK1SIZE | float32 | | pix | {:15.7g} | |
| BK2SIZE | float32 | | pix | {:15.7g} | |
| BK1OFFST | float32 | | pix | {:15.7g} | |
| BK2OFFST | float32 | | pix | {:15.7g} | |
| EXTRLOCY | float32 | (1024,) | pix | {:15.7g} | |
| OFFSET | float32 | | pix | {:15.7g} | |

To look at the contents of the table:

```
>>> print(ex_table)
```

| SPORDER | NELEM | ... | EXTRLOCY [1024] | ... | OFFSET |
|---------|-------|-------|-----------------|----------|----------|
| | | ... | pix | | pix |
| ----- | ----- | ----- | ----- | ----- | ----- |
| 1 | 1024 | ... | 378.1119 .. | 381.7816 | 332.1185 |

Note that the number of columns displayed is limited by the width of the window that you are working in when using `print()`. To see more columns, you can simply adjust the width of the window and rerun the command above. If you want to view specific columns:

```
>>> print(ex_table['BK1SIZE', 'BK2SIZE', 'BK1OFFST'])
```

| BK1SIZE | BK2SIZE | BK1OFFST |
|---------|---------|----------|
| pix | pix | pix |
| ----- | ----- | ----- |
| 5 | 5 | -300 |

Reference file FITS tables generally have many rows, with each row characterizing a specific operating mode, location on the detector, value of a parameter to be used in the reduction, etc. To display specific rows in the table:

```
>>> from astropy.table import Table
>>> ref_table = Table.read('q541740qo_pct.fits')
>>> columns = ['CENWAVE', 'APERTURE', 'EXTRHEIGHT', 'NELEM', 'WAVELENGTH']
>>> print(ref_table[columns])
```

| CENWAVE | APERTURE | EXTRHEIGHT | NELEM | WAVELENGTH [8] |
|------------|----------|------------|-------|----------------|
| Angstrom | | pix | | Angstrom |
| ----- | ----- | ----- | ----- | ----- |
| -1 52X0.05 | | 3 | 8 | 5812 .. 9696 |
| -1 52X0.05 | | 5 | 8 | 5812 .. 9696 |
| -1 52X0.05 | | 7 | 8 | 5812 .. 9696 |
| -1 52X0.05 | | 9 | 8 | 5812 .. 9696 |
| -1 52X0.05 | | 11 | 8 | 5812 .. 9696 |
| -1 52X0.05 | | 15 | 8 | 5812 .. 9696 |
| -1 52X0.05 | | 21 | 8 | 5812 .. 9696 |
| -1 52X0.05 | | 200 | 8 | 5812 .. 9696 |
| -1 52X0.05 | | 600 | 8 | 5812 .. 9696 |
| -1 52X0.1 | | 3 | 8 | 5813 .. 9697 |
| -1 52X0.1 | | 5 | 8 | 5813 .. 9697 |
| -1 52X0.1 | | 7 | 8 | 5813 .. 9697 |
| -1 52X0.1 | | 9 | 8 | 5813 .. 9697 |
| -1 52X0.1 | | 11 | 8 | 5813 .. 9697 |
| -1 52X0.1 | | 15 | 8 | 5813 .. 9697 |
| -1 52X0.1 | | 21 | 8 | 5813 .. 9697 |
| -1 52X0.1 | | 200 | 8 | 5813 .. 9697 |
| -1 52X0.1 | | 600 | 8 | 5813 .. 9697 |
| -1 52X0.2 | | 3 | 8 | 5807 .. 9692 |
| -1 52X0.2 | | 5 | 8 | 5807 .. 9692 |
| -1 52X0.2 | | 7 | 8 | 5807 .. 9692 |
| -1 52X0.2 | | 9 | 8 | 5807 .. 9692 |
| -1 52X0.2 | | 11 | 8 | 5807 .. 9692 |
| -1 52X0.2 | | 15 | 8 | 5807 .. 9692 |

```

...
-1 52X0.1F1      ...      7      8      5813 ..      9697
-1 52X0.1F1      ...      9      8      5813 ..      9697
-1 52X0.1F1      ...     11      8      5813 ..      9697
-1 52X0.1F1      ...     15      8      5813 ..      9697
-1 52X0.1F1      ...     21      8      5813 ..      9697
-1 52X0.1F1      ...    200      8      5813 ..      9697
-1 52X0.1F1      ...    600      8      5813 ..      9697
-1 52X0.1F2      ...      3      8      5813 ..      9697
-1 52X0.1F2      ...      5      8      5813 ..      9697
-1 52X0.1F2      ...      7      8      5813 ..      9697
-1 52X0.1F2      ...      9      8      5813 ..      9697
-1 52X0.1F2      ...     11      8      5813 ..      9697
-1 52X0.1F2      ...     15      8      5813 ..      9697
-1 52X0.1F2      ...     21      8      5813 ..      9697
-1 52X0.1F2      ...    200      8      5813 ..      9697
-1 52X0.1F2      ...    600      8      5813 ..      9697
-1 52X0.2F2      ...      3      8      5807 ..      9692
-1 52X0.2F2      ...      5      8      5807 ..      9692
-1 52X0.2F2      ...      7      8      5807 ..      9692
-1 52X0.2F2      ...      9      8      5807 ..      9692
-1 52X0.2F2      ...     11      8      5807 ..      9692
-1 52X0.2F2      ...     15      8      5807 ..      9692
-1 52X0.2F2      ...     21      8      5807 ..      9692
-1 52X0.2F2      ...    200      8      5807 ..      9692
-1 52X0.2F2      ...    600      8      5807 ..      9692
Length = 198 rows

```

5.1.3 General Spectral Display and Analysis Tasks

The astropy package **specutils** provides a basic interface for loading, manipulating, and common forms of analysis of spectroscopic data. Documentation for **specutils** can be found at <https://specutils.readthedocs.io>. **SpecViz** is an interactive tool for visualization and quick-look analysis of 1-D astronomical spectra written in the **Python** language. Documentation for **SpecViz** can be found at <https://specviz.readthedocs.io>. Note that these packages are currently in active development and may lack some functions for detailed analyses. For these cases, users can utilize the older **PyRAF/IRAF/STSDAS** applications for displaying and analyzing STIS spectral data. such as those listed in [Table 5.1](#).

Table 5.1: Spectral Analysis Tasks

| Task | Input Formats | Purpose |
|------------------------------------|-----------------------------|--|
| stsdas.hst_calib.stis. echplot | 3-D tables | Plots multiple STIS echelle spectral orders. |
| stsdas.analysis.fitting. nfit1d | 2-D & 3-D tables, images | General 1-D feature fitting; part of the STSDAS fitting package. |

| | | |
|----------------------------------|-----------------------------|--|
| stdas.graphics.stplot. igi | 2-D & 3-D tables, images | General presentation graphics; supports world coordinates. |
| stdas.graphics.stplot. sgraph | 2-D & 3-D tables, images | General 1-D plotting; supports world coordinates. |
| stdas.contrib.sffit. specfit | 1-D images, ASCII tables | General 1-D spectrum modelling package. |
| noao.onedspec.splot | multispec images | General 1-D spectral analysis. |

5.1.4 AstroDrizzle for Image Combination

AstroDrizzle is a **Python** script that automates the detection of cosmic rays and the combination of dithered images. A user guide for DrizzlePac, which includes AstroDrizzle, can be found at <http://www.stsci.edu/scientific-community/software/drizzlepac.html>.

AstroDrizzle has been adapted to STIS imaging as well as ACS, WFC3, and COS imaging. It can be used to combine STIS CRSPLIT or REPEATOBS image sets as well as dithered images and images made with the same aperture and optical elements but with different target centering or orientation. It uses cosmic ray rejection algorithms which often gives superior results to **calstis** for CRSPLIT and REPEATOBS exposures, especially for images of unresolved targets with high signal-to-noise.

5.2 Evaluating Target Acquisitions and Guiding

[5.2.1 Target Acquisition Basics](#)

[5.2.2 ACQ Data](#)

[5.2.3 ACQ/Peak Data](#)

[5.2.4 The tastis Task](#)

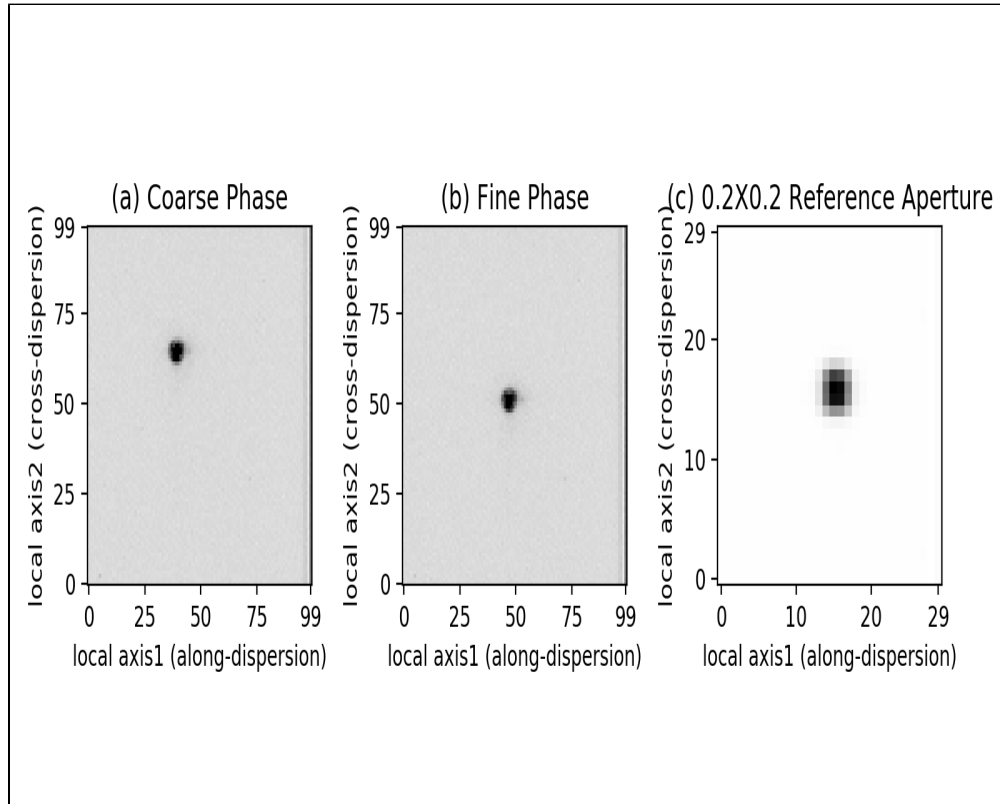
[5.2.5 The STISstarg Package](#)

[5.2.6 Guiding Error for Single Guide Star Mode](#)

5.2.1 Target Acquisition Basics

There are two types of STIS target acquisition: ACQ and ACQ/PEAK; for more details on target acquisition, see [STIS ISR 97-03](#). For ACQ observations, there are three parts to the target acquisition data that you receive. The first is an image of the target in the target acquisition sub-array (100×100 pixels for point sources, scaling linearly for diffuse sources) based on the initial pointing (see [Figure 5.1a](#), `_raw.fits['sci',1]`). The software then determines the position of the target with a flux weighted pointing algorithm and calculates the slew needed to place the target at a reference point in the target acquisition sub-array; for diffuse sources, an option to perform a geometric centroiding is available. An image of the target at this corrected position is then obtained (see [Figure 5.1b](#), `_raw.fits['sci',2]`)—this is the coarse centering. To perform the fine centering (i.e., to place the object precisely in a slit), a 32×32 pixel image of the lamp-illuminated 0.2X0.2 aperture (the "reference aperture") is obtained (see [Figure 5.1c](#) `_raw.fits['sci',3]`), and the location of the aperture on the detector is determined. A fine slew is then performed to center the target in the reference aperture, which should be accurate to 0.2 pixels (0.01 arcsec). A final slew to center the target in the science aperture is performed at the start of the following science observation.

Figure 5.1: The three components of an ACQ observation. All coordinates are given in the appropriate sub-array frame.



If a narrow aperture is used for the science exposures, an ACQ/PEAK acquisition may have been performed to refine the centering of the ACQ. An aperture (often the science aperture) is stepped across the object with a pattern determined by the aperture selected. The flux measured at each step is saved, but the image is not. The telescope is then slewed to center the target in the aperture, and a "confirmation" image (a 32×32 pixel grid for imaging mode) of the target viewed through the aperture is obtained and saved. The pattern of fluxes and the confirmation image are delivered in a `_raw` file. The accuracy of the ACQ/PEAK is 5% of the slit width for a point source with adequate signal-to-noise. See [Section 8.3](#) in the *STIS Instrument Handbook*.

5.2.2 ACQ Data

The ACQ_raw.fits file contains the initial image of the target, the image of the target after the coarse slew, and the image of the lamp viewed through the 0.2X0.2 aperture:

```
>>> from astropy.io import fits
>>> fits.info('ocyw0lzeq_raw.fits')

Filename: ocyw0lzeq_raw.fits
No.      Name      Ver  Type      Cards  Dimensions  Format
  0  PRIMARY      1  PrimaryHDU  208    ()
  1  SCI          1  ImageHDU   105    (100, 100)  int16 (rescales to uint16)
  2  ERR          1  ImageHDU   54     ()
  3  DQ           1  ImageHDU   37     ()
  4  SCI          2  ImageHDU  105    (100, 100)  int16 (rescales to uint16)
  5  ERR          2  ImageHDU   54     ()
  6  DQ           2  ImageHDU   37     ()
  7  SCI          3  ImageHDU  105    (30, 30)   int16 (rescales to uint16)
  8  ERR          3  ImageHDU   54     ()
  9  DQ           3  ImageHDU   39     ()
```

Note that target acquisition data are always uncalibrated; the ERR and DQ images are unpopulated. An examination of the target images will allow you to detect gross errors in the centering of your target. A comparison of the initial image (extension ['sci',1] or [1]) and post coarse slew image (extension ['sci',2] or [4]) should show the object moving close to the center of the acquisition sub-array, as in [Figure 5.1a](#) and [Figure 5.1b](#). It will not be precisely centered, as the MSM's centering is non-repeatable and measured with the HITM lamp image.

You can also verify that the maximum flux in a checkbox is consistent in the two images, either by running **tastis** ([Section 5.2.4](#)) or by using **Python** to find this flux in the keyword MAXCHCNT in the science extension headers:

```
>>> with fits.open('ocyw0lzeq_raw.fits') as f:
    print ("Coarse stage -- ext['SCI',1] = ext[1]: ", f['SCI',1].header['MAXCHCNT'])
    print ("Fine stage   -- ext['SCI',2] = ext[4]: ", f['SCI',2].header['MAXCHCNT'])

Coarse stage -- ext['SCI',1] = ext[1]:      6434.0
Fine stage   -- ext['SCI',2] = ext[4]:      6514.0
```

If the fluxes are not consistent, or if the object did not move closer to the center of the array, there is likely a problem with your acquisition. A more extensive analysis of the ACQ data is performed by **tastis** ([Section 5.2.4](#)).

5.2.3 ACQ/Peak Data

The ACQ/PEAK_raw.fits file contains the final "confirmation" image of the target viewed through the aperture in the first extension and the fluxes measured in the stepping pattern in the fourth extension:

```
>>> fits.info('od6n05ikq_raw.fits')

Filename: od6n05ikq_raw.fits
No.    Name      Ver  Type      Cards  Dimensions  Format
 0  PRIMARY    1  PrimaryHDU  207    ()
 1  SCI        1  ImageHDU   99     (32, 32)   int16 (rescales to uint16)
 2  ERR        1  ImageHDU   54     ()
 3  DQ         1  ImageHDU   37     ()
 4  PEAKUP    1  ImageHDU   97     (7, 1)     int32
```

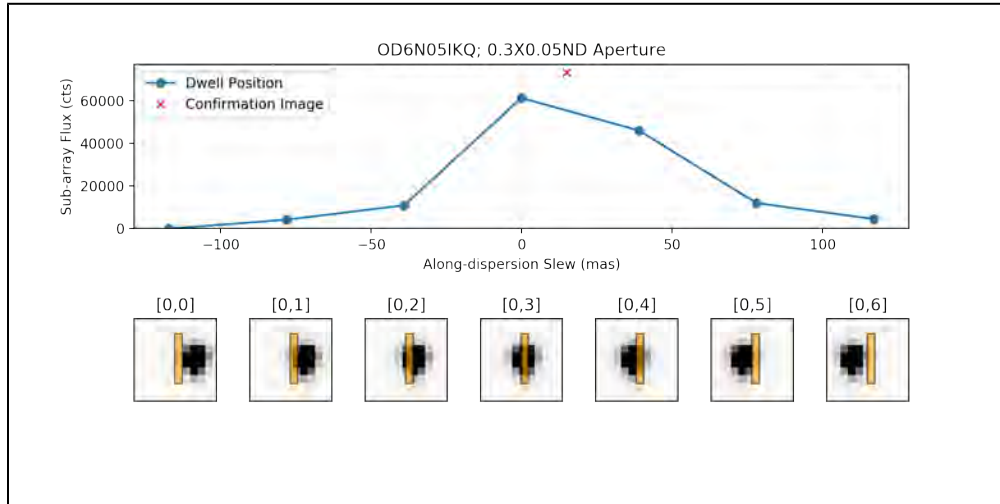
To verify that the ACQ/PEAK worked, you can use **tastis** ([Section 5.2.4](#)) to analyze this data. Here we describe other ways to examine the data.

You can see the flux values at each stage of the peakup relative to the minimum value, which is set to zero, by examining the ext=4 data with the **fits** module in [astropy.io](#), e.g.,

```
>>> fits.getdata('od6n05ikq_raw.fits', ext=4)
array([[ 0, 4236, 10970, 61423, 46167, 12072, 4531]], dtype=int32)
```

For a 7-step along-dispersion linear peakup, the pixel [0,0] is the leftmost scan position, [0,3] is the middle position, and [0,6] is the rightmost position. See [Figure 5.2](#) for a cross-dispersion linear peakup, the dimensions are reversed.

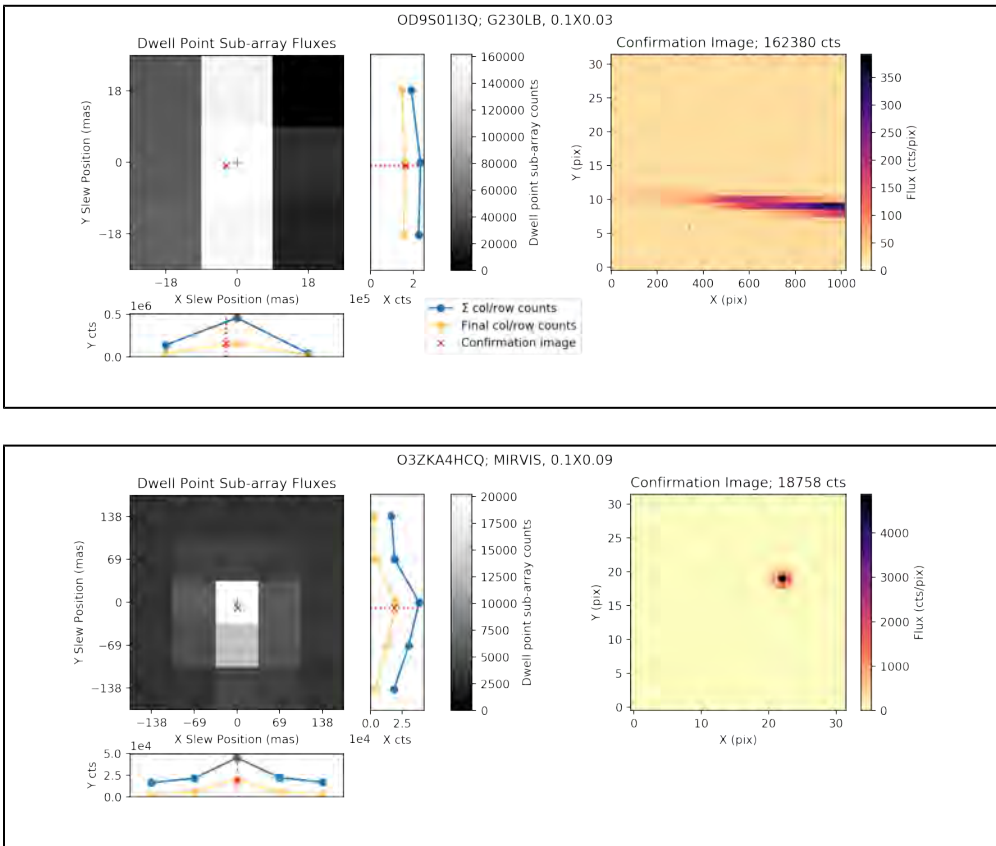
Figure 5.2: Flux values at each stage in an ACQ/PEAK. The individual dwell points are not downlinked from HST, so copies of the confirmation image are shown here for demonstration purpose only. This approximation does not show changes to the PSF with sub-pixel shifts.



For a 9-step spiral pattern, pixels [0,:] is the lower row of the pattern, [1,:] is the middle row, and [2,:] is the upper row.

When examining the confirmation image (`_raw.fits[4]`), note that the slit will be illuminated by the sky even if no target is present. See [Figure 5.3](#) for examples of successful and failed acquisitions.

Figure 5.3: Displaying the total sub-array flux at each dwell point for a 9-point and a 25-point spiral ACQ/PEAK (left). The zero-point is determined from the flux at the lowest dwell point and the X- and Y-centroids are calculated by summing along the orthogonal axis. The red dotted lines and 'X' mark the calculated centroid position where the confirmation image (right) was taken



To determine the flux in the confirmation image, do the following inPython:

```
>>> fits.getdata('od6n05ikq_raw.fits', ext=1).sum()
106798
```

The total counts in the image is 106798 in this example. Note that you will need to perform one correction to the total value prior to your comparison. Since the flux values in the peakup have been adjusted by

subtracting the minimum value in the sequence, this value needs to be subtracted from the counts in the confirmation image to do a proper comparison. The value can be found in the `_raw.fits` file `ext=0` `PEDESTAL` keyword as shown in the example below.

```
>>> fits.getval('od6n05ikq_raw.fits', ext=0, keyword='PEDESTAL')
33233.0
```

In the example, the `PEDESTAL` value was 33233 which means the corrected number of counts in the confirmation image is 73565. Comparison of the maximum flux value during the peakup sequence (61423) with the adjusted flux in the confirmation image (73565) should show that the flux in the confirmation image was greater than or equal to the maximum flux in the peakup grid. If this is not the case, then there could be a problem with your peakup acquisition. A more extensive analysis, taking into account the distribution of fluxes across the `ACQ/PEAK` steps and the magnitude of the fluxes, is performed by `tastis` ([Section 5.2.4](#)).

5.2.4 The `tastis` Task

The `stistools` package contains a task, `tastis`, that will print general information about each input target acquisition image, and will analyze both types of STIS target acquisitions: `ACQs` and `ACQ/PEAKs`. For an `ACQ`, target positions, in global and local (sub-array) coordinates, and the total flux of the target in the maximum checkbox during both acquisition phases (coarse and fine) are displayed; the location of the reference aperture (used during the fine locate phase) is also displayed. For an `ACQ/PEAK`, the flux values at each step during the peakup, the total flux in the post-slew confirmation image, and the pedestal value subtracted from each dwell point are displayed. For each procedure, diagnostics are performed and the user will either be informed that the procedure appears to have succeeded or will be warned of an apparent problem.

For an `ACQ`, `tastis` examines the flux of the brightest object in the original image of the target, the flux of the brightest object in the recentered image of the target, and the flux of the lamp viewed through the reference aperture. It also examines the slews made to recenter the target and to place it at the position of the reference aperture, and the status of the `DATAFLAG` in the `_spt` file, which can indicate that an exposure was not performed. For an `ACQ/PEAK`, `tastis` analyzes the sequence of fluxes measured in the stepping pattern, compares the peak flux in the stepping pattern to the flux in the confirmation image, and checks the status of the `DATAFLAG`. If any unexpected values are encountered, a diagnostic message is

given to the user. For example, the user is warned if the brightest measured flux in the first and second ACQ images is significantly different, since the same target and flux would normally be dominant in each image. A warning is given if the expected lamp flux is not detected, since failure to illuminate and locate the reference aperture on the detector would result in a misplacement of the target in the slit. An ACQ /PEAK triggers a warning if the flux is too low for good signal-to-noise, the most common cause of poor ACQ/PEAKs. Other diagnostics are documented in the task's documentation. An example run of `tastis` is shown below.

```
>>> stistools.tastis.tastis('ocyw01zeq_raw.fits')

=====
ocyw01zeq      HST/STIS      MIRVIS      F25ND3      ACQ/POINT
prop: 14084      visit: 01      line: 1      target: GJ3323
obs date, time: 2016-09-22 03:37:22      exposure time: 30.90
dom GS/FGS: S1NF000373F2      sub-dom GS/FGS: S1ND000111F1
ACQ params:      bias sub: 1510      checkbox: 3      method: FLUX CENTROID
subarray (axis1,axis2):      size=(100,100)      corner=(487,466)
-----
Coarse locate phase:      Target flux in max checkbox (DN): 6434

                global                local
                axis1 axis2            axis1 axis2
Target location:  525.2  529.3          39.2  64.3

                axis1 axis2            axis1 axis2            V2      V3
                (pixels)              (arcsec)              (arcsec)
Estimated slew:  -10.5  13.3          -0.536  0.676          0.099 -0.857
-----
Fine locate phase:      Target flux in max checkbox (DN): 6514

                global                local
                axis1 axis2            axis1 axis2
Target location:  533.1  516.0          47.1  51.0
Ref ap location:  536.5  515.5          18.5  15.5

                axis1 axis2            axis1 axis2            V2      V3
                (pixels)              (arcsec)              (arcsec)
Estimated slew:  -2.2   0.5           -0.109  0.025          -0.059 -0.095
-----
Total est. slew:  -12.7  13.8          -0.645  0.701          0.039 -0.952
-----
Your ACQ appears to have succeeded, as the fluxes in the coarse
and fine stages agree within 25% and the fine slews were less than
4 pixels as expected

All coordinates are zero-indexed.
=====
```

5.2.5 The STIStarg Package

The STIS target acquisition simulator, or **stistarg**, is a **Python** package that allows users to simulate and visualize the behavior of the STIS flight software (FSW) on an input image while varying the APT acquisition optional parameters. Inputs are assumed to be in the native STIS plate scale and detector format, so users should scale and trim images from other instruments accordingly. Note that differences in the filter throughputs convolved with the source's SED may affect the flux distribution of extended sources. The **stistarg** can be run as follows.

```
>>> import stistarg
>>> st = stistarg.stistarg('ocyw01zeq_raw.fits', display=True)

-----

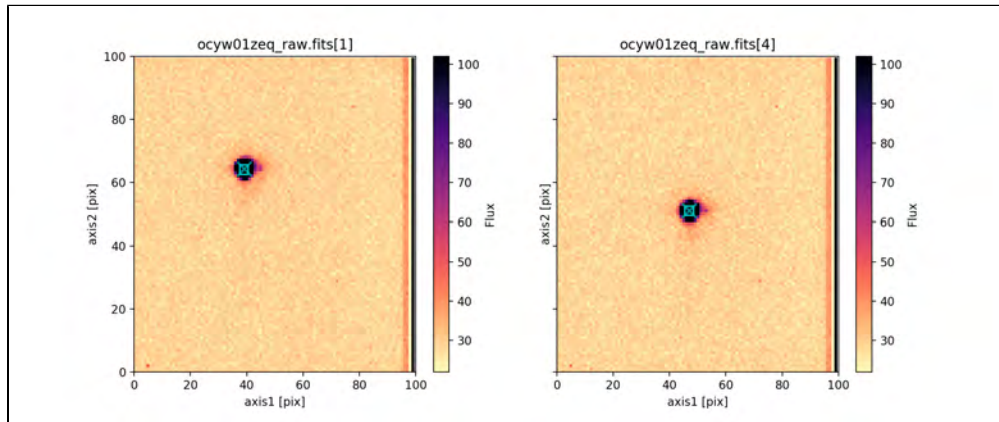
STIS Target Acquisition Simulator
stistarg.py v2.4
Python v3.6.3
Run time: 2018-11-09 22:58:52
Input Options:  point source, checkbox size = 3

Input File:      ocyw01zeq_raw.fits[1]
Image Subarray: (95, 100)
Brightest checkbox flux: 6434
Flux center:      axis1 = 39.2 ; axis2 = 64.3 [cyan X]

Input File:      ocyw01zeq_raw.fits[4]
Image Subarray: (95, 100)
Brightest checkbox flux: 6514
Flux center:      axis1 = 47.1 ; axis2 = 51.0 [cyan X]

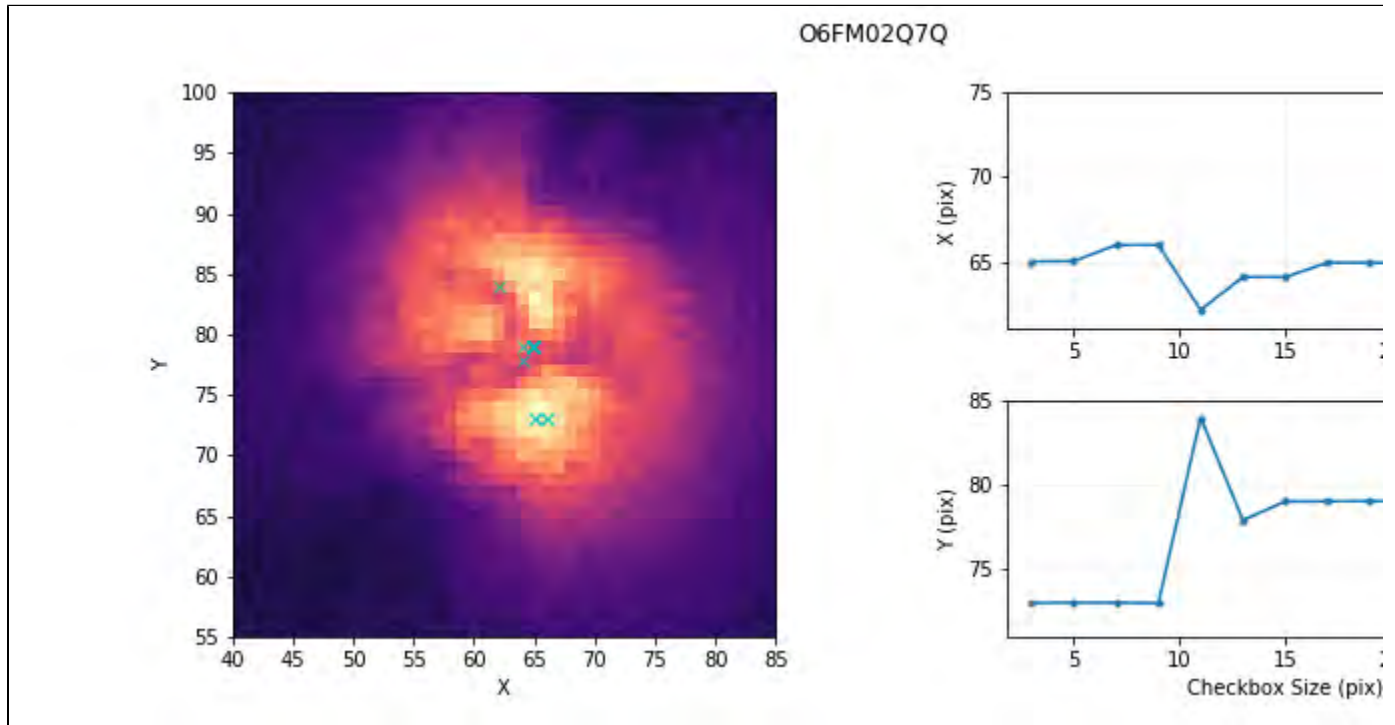
(All coordinates are zero-indexed.)
-----
```

Figure 5.4: Output images from the stistarg example.



By adding random noise or varying the size of the diffuse target acquisition checkbox size, one may estimate the stability of the FWS's solution. For example, [Figure 5.5](#) shows that as the checkbox size increases, an ACQ on M51 centers on different blobs or the whole galaxy. Unstable centering results should be avoided.

Figure 5.5: Output images from the `stistarg` example.



For more details, see the `stistarg` documentation at <https://stistarg.readthedocs.io>.

5.2.6 Guiding Error for Single Guide Star Mode

Tracking on two guide stars has generally provided pointing accuracy sufficient to keep targets well centered in the narrow STIS apertures for several orbits. However, in some cases, observations have been made using only a single guide star instead of the usual two. Either the Principal Investigator has consented to this in consultation with the Program Coordinator when two suitable guide stars could not be found, or one Fine Guidance Sensor failed to acquire its guide star during the guide star acquisition /reacquisition. See Sections 6.3.1 and 6.3.2 in the *Introduction to the HST Data Handbooks* for keywords to check for the status of the guide star acquisition. In this situation, the roll of the telescope is under GYRO control, which may allow a slow drift of the target on a circular arc centered on the single guide star.

The rate of the drift of the radiant of this circle is unknown for any particular observation, but typically is expected to be in the range of 1.0 to 1.5 milliarcsec/sec (possibly, but very rarely, as large as 5 milliarcsec/sec).

To calculate the approximate magnitude of the drift of the target on the detector, you will need to find the distance of the target from the acquired guide star. The primary header of the observation log file `_jif` identifies the acquired guide star (`GSD_ID`) and gives its right ascension (`GSD_RA`) and declination (`GSD_DEC`) in degrees. For example, for a target 10 arcmin from the guide star, a drift of the guide-star-to-target radiant of 1 milliarcsec/sec during a 1,000 second exposure would cause the target to move 0.0029 arcsec on the detector. The direction of the motion on the detector can be deduced from header keywords in the science data describing the position angle of the detector (e.g., `PA_APER`), in combination with the direction perpendicular to the radiant. In many cases, the drift will be a small fraction of a pixel or slit width, although in some cases an image exposure may appear smeared or the target may drift from the slit of a spectroscopic exposure.

Elongation of point sources in direct images can be assessed by examination of the image or contour plots. If a series of spectroscopic images has been made, it may be possible to measure increments in position along the slit or increments in wavelength (due to motion in the dispersion direction) on `_x2d` images or in `_x1d` extractions. For example, the values of the parameter `A2CENTER` in the `_x1d` file (adjusted for any changes in `SHIFTA2`) will reveal shifts along the slit. Wavelength shifts may be found by cross-correlation of the spectra. Once a shift has been found in either dimension, the geometry of the drift can be used with the spectroscopic dispersion to find the shift in the other dimension. Compensating adjustments can then be made to `SHIFTA1` and `SHIFTA2` to make `_x1d` or `_x2d` files that can be combined or compared, as discussed in [Section 5.4.3](#).

5.3 Working with Imaging Data

5.3.1 Sensitivity Units and Conversions

5.3.2 Spatial Information

5.3.3 Combining Images

5.3.1 Sensitivity Units and Conversions

Your calibrated image (`_flt` or `_crj` file) has units of counts. The conversion to flux ($\text{erg cm}^{-2} \text{sec}^{-1} \text{\AA}^{-1}$) for a flat spectrum is:

$$f_{\lambda} = \frac{\text{counts} \cdot \text{PHOTFLAM}}{\text{EXPTIME}}$$

where *PHOTFLAM* is the sensitivity for the observing mode in units of $\text{erg cm}^{-2} \text{sec}^{-1} \text{\AA}^{-1}$, and *EXPTIME* is the exposure time in seconds. Both of these parameters are given in the science header. These fluxes can be converted to magnitudes in the STMAG system by the relation $\text{STMAG} = -2.5 \log_{10} f_{\lambda} - 21.1$.

5.3.2 Spatial Information

Several tasks in the **astropy.wcs** package can be used to convert between pixels and celestial coordinates, provided that the images have already been corrected for geometric distortion. This correction should have been performed already if `GEOCORR=COMPLETE` (default for all STIS images) in the primary header of the image. Details on the conversion process can be found in the **astropy.wcs** documentation at <http://docs.astropy.org/en/stable/wcs/>.

5.3.3 Combining Images

Multiple imaging exposures made with `CR-SPLIT` or `REPEATOBS` can be combined using **calstis** or its components, described in [Table 3.1](#). By running the component tasks, you can select different options or adjust the values of the task parameters to override the values provided by the reference files. For example, you can change the values of the parameters which control cosmic ray processing in **ocrreject** to strike a balance between missing cosmic rays and clipping real flux from point sources. You may also

want to generate improved reference files and run the component tasks to apply them to your data. See [Section 3.5](#) for detailed discussions of improvements that can be made by recalibrating the data.

The **AstroDrizzle** can be used to combine dithered images or images made with the same aperture and optical elements but with different target centering or orientation, as well as multiple imset (CR-SPLIT or REPEATOBS) exposures. See the **DrizzlePac** website (<http://www.stsci.edu/scientific-community/software/drizzlepac.html>) for more on **AstroDrizzle**.

5.4 Working with Spectral Images

- 5.4.1 Sensitivity Units and Conversions
- 5.4.2 Wavelength and Spatial Information
- 5.4.3 Improving the Rectification of Spectral Images
- 5.4.4 Combining Undithered Spectral Images
- 5.4.5 Combining Dithered Spectral Images
- 5.4.6 Producing Rectified Spectral Images for Long-Slit Echelle Data

5.4.1 Sensitivity Units and Conversions

The calstis pipeline software produces a rectified two-dimensional spectral image when `X2DCORR` is set to `PERFORM` (see [Section 3.4.25](#)). The image is flux-calibrated (see [Section 3.4.13](#)). At each pixel i , this image contains the surface brightness per Angstrom, B_i , in $\text{erg cm}^{-2} \text{sec}^{-1} \text{\AA}^{-1} \text{arcsec}^{-2}$. The image has a linear wavelength scale and uniform sampling in the spatial direction. Here we review how the image is calculated by the pipeline, and how to convert the data in this image to other quantities.

The flux detected by pixel i in a two-dimensional spectral image is:

$$F_i = \frac{10^8 \cdot C_\lambda \cdot g \cdot h \cdot c}{R_\lambda \cdot A_{HST} \cdot \lambda \cdot f_{TDS} \cdot f_T}$$

in $\text{erg cm}^{-2} \text{sec}^{-1}$, where:

- C_λ is the wavelength dependent count rate, which is the ratio of the total counts to the exposure time. The exposure time is given in the `EXPTIME` header keyword.
- g is the detector gain, which is unity for MAMA observations. For the CCD, this is the conversion from counts to electrons, the value for which is given in the header keyword `ATODGAIN`.
- $h = 6.626e^{-27} \text{ erg s}$ is Planck's constant.
- $c = 2.9979e10 \text{ cm s}^{-1}$ is the speed of light.
- R_λ is the wavelength dependent integrated system throughput, given in the `PHOTTAB` for individual optical elements.
- $A_{HST} = 45238.93416 \text{ cm}^2$ is the area of the unobstructed *HST* mirror.
- λ is the wavelength in Angstroms, which is converted to cm by the factor of 10^8 in the numerator.

- f_{TDS} is the correction for time-dependent sensitivity computed from the TDSTAB (e.g., [STIS ISR 2017-06](#)).
- f_{T} is the correction for temperature-dependent sensitivity, also computed from the TDSTAB.

The flux per Angstrom is:

$$F_{\lambda i} = \frac{F_i}{d}$$

in $\text{erg cm}^{-2} \text{sec}^{-1} \text{\AA}^{-1}$, where: d is the dispersion in $\text{\AA}/\text{pixel}$, derived from the CD1_1 header keyword.

The surface brightness detected by that pixel is:

$$B_i = \frac{F_i}{W \cdot m_s}$$

in $\text{erg cm}^{-2} \text{sec}^{-1} \text{arcsec}^{-2}$, where:

- m_s is the plate scale in $\text{arcsec}/\text{pixel}$ in the cross-dispersion direction (i.e., spatial direction). This corresponds to the CD2_2 header keyword value multiplied by 3600 -arcsec/degree.
- W is the slit width in arcsec.

The surface brightness per Angstrom, $B_{\lambda i}$, given in the flux calibrated, rectified, two-dimensional spectral image (_sx2 or _x2d file) is thus:

$$B_{\lambda i} = \frac{F_i}{d \cdot W \cdot m_s}$$

in $\text{erg cm}^{-2} \text{sec}^{-1} \text{\AA}^{-1} \text{arcsec}^{-2}$. So, starting from the rectified two-dimensional spectral image (_sx2 or _x2d file), F_i , $F_{\lambda i}$, and B_i can be computed from $B_{\lambda i}$ as:

$$F_i = B_{\lambda i} \cdot d \cdot W \cdot m_s$$

$$F_{\lambda i} = B_{\lambda i} \cdot W \cdot m_s$$

$$B_i = B_{\lambda i} \cdot d$$

Similarly, fluxes can be summed over regions in the _sx2 and _x2d files and used to compute the flux or surface brightness per Angstrom for the continuum, or flux or surface brightness of a spectral feature (after subtracting off the continuum). For a rectangular region in the spectral image spanning N_p pixels in

the dispersion direction (N_λ is proportional to Angstroms) and N_s pixels in the spatial direction ($N_s m_s$ arcsec along the slit):

$$F = \sum_i F_i = N_\lambda \cdot N_s \cdot \langle F_i \rangle = N_\lambda \cdot N_s \cdot \langle B_{\lambda i} \rangle \cdot d \cdot W \cdot m_s$$

$$F_\lambda = \frac{\sum_i F_i}{N_\lambda \cdot d} = N_s \cdot \langle B_{\lambda i} \rangle \cdot W \cdot m_s$$

$$B = \frac{\sum_i F_i}{W \cdot N_s \cdot m_s} = N_\lambda \cdot \langle B_{\lambda i} \rangle \cdot d$$

$$B_\lambda = \frac{\sum_i F_i}{N_\lambda \cdot d \cdot W \cdot N_s \cdot m_s} = \langle B_{\lambda i} \rangle$$

where F is in $\text{erg cm}^{-2} \text{sec}^{-1}$, F_λ is in $\text{erg cm}^{-2} \text{sec}^{-1} \text{\AA}^{-1}$, B is in $\text{erg cm}^{-2} \text{sec}^{-1} \text{arcsec}^{-2}$, and B_λ is in $\text{erg cm}^{-2} \text{sec}^{-1} \text{\AA}^{-1} \text{arcsec}^{-2}$.

No slit loss corrections have been made above. This is correct in the limiting case of spatially uniform surface brightness. For a point source, the flux can be corrected for slit loss by using the data header keyword `DIFF2PT`. This keyword is calculated as:

$$DIFF2PT = \frac{W \cdot m_s \cdot H}{T^{\text{ap}}}$$

$$DIFF2PT = \frac{W \cdot m_s \cdot H}{T^{\text{ap}}}$$

where W and m_s are as above, T^{ap} is the wavelength-averaged point source aperture throughput for the science aperture (which is determined from the reference table specified by the keyword `APERTAB`), and H is the wavelength-averaged correction for the extraction slit of height H to a slit of infinite height, which is obtained from the reference table specified by the keyword `PCTAB`. That is, to derive the flux from a point source, integrate the `_x2d` or `_sx2` file over the default extraction slit height (from the `PCTAB`) and multiply the result by `DIFF2PT`. The default extraction slit height for first order modes is at present 11 pixels for the MAMAs and 7 pixels for the CCD. If the desired extraction slit height differs from the default, the `PCTAB` has a set of wavelength-dependent corrections for selected alternative apertures that

must also be applied. See [STIS ISR 98-01](#) for further details. Of course, point source observers are better advised to use the `x1d` task to extract a one-dimensional spectrum from their long slit first order data, which will then apply the wavelength-dependent aperture throughput and extraction height corrections and the `GACTAB` correction, as well as perform background subtraction. For the narrowest apertures and for some gratings and wavelength settings, the wavelength-dependent corrections can vary substantially across the detector.

In general we note that the cross dispersion profiles can be quite extended (particularly in the far-UV and in the near-IR). Fluxes derived for extended sources from the `_x2d` files, as above, assume that the sources are extended on scales that contain the bulk of the cross dispersion flux from a point source. Encircled energies for the first order modes can be found in [STIS ISR 97-13](#).

See also [Chapter 6](#) of the *STIS Instrument Handbook* for a more detailed discussion of units and conversions for different source types.

5.4.2 Wavelength and Spatial Information

Two-dimensional spectral images have been wavelength calibrated and rectified to linear wavelength and spatial scales. Reading the `_sx2` and `_x2d` files (e.g., with [astropy.io.fits](#)) makes the wavelength header information stored in the standard FITS CD matrix keywords available for inspection and/or modification, and one can use those keywords directly to determine the wavelength or distance along the slit at any pixel as:

$$\begin{aligned}\lambda(x) &= \text{CRVAL1} + (x - \text{CRPIX1}) \times \text{CD1_1} \\ s(y) &= (y - \text{CRPIX2}) \times \text{CD2_2}\end{aligned}$$

where $\lambda(x)$ is the wavelength at any given x pixel, and $s(y)$ is the distance along the slit from slit center for any given y pixel, in units of degrees.

5.4.3 Improving the Rectification of Spectral Images

Systematic errors are introduced into the rectification of spectral images by the use of inaccurate spectral traces and by interpolation of undersampled data. CTE errors in `CCDflt` or `crj` images are also propagated into the rectified image; i.e., in columns (wavelength regions) with low flux levels in the target and background, the observed flux of the target will be diminished and the target will appear to be centered slightly further away from the readout amplifier, the more so for targets more distant from the

readout amplifier. For the case of a point source on a spatially uniform background, one can obtain a CTE-corrected extracted spectrum ([Section 3.4.6](#)). No CTE correction is made in the much more general (and much less tractable) case of rectifying and flux-calibrating a spectral image. However, CTE effects should generally be small for targets placed at the E1 pseudo-aperture positions, implemented in July 2000.

To improve rectification, one must first ensure that accurate traces are applied to the input image. The orientation of spectral traces on the STIS detectors has been found to rotate slowly over time for the L and M modes (e.g., [STIS ISR 2007-03](#)). The rotation rate is most consequential for the later observations made with the CCD. For exposures taken just before the suspension of operations in August 2004, the Y-range of the CCD traces differed from that of the reference file traces by about half a pixel. This is sufficient to introduce tilts and curvatures into row-by-row spectra taken from the rectified image, and to cause a discrepancy in the physical centers of rotation curves measured from widely separated spectral lines. New trace files were delivered with time-dependent orientations for the most commonly used first order modes, and the **stistools** task **mktrace** was developed to produce an improved trace reference file for any L or M mode image, as discussed in [Section 3.5.7](#). If needed, new trace reference files should thus be retrieved from the archive or generated with **mktrace**.

The greatest problem in the rectification of STIS spectral images, especially CCD images, is that the point spread function (PSF) is undersampled along the slit. The bi-linear interpolation employed by **calstis**, and by its constituent script **stistools** task **x2d**, produces artifacts in the rows of spectra in the rectified image when a point source is present. For gratings with spectral traces that drop by several rows as they cross the detector, the artifacts take the form of periodic scallops in the flux which change phase from one row to the next. For gratings with a trace that is confined to a height of less than one pixel, the flux in each row is modulated by a broad irregular shape. See [Figure 11.9](#) in [Section 11.3.5](#) of the *STIS Instrument Handbook*.

Interpolation artifacts can be reduced in rows near the center of a point source by using the wavelet method of interpolation described by Barrett and Dressel (2005, *The HST Calibration Workshop*). This method uses average interpolation (instead of point interpolation) and iterative refinement. The pixels in each column are repeatedly subdivided into pairs of subpixels, and the flux is distributed among the subpixels using polynomial fits to the flux profile. The subpixels are then reassembled into pixels centered on the trace, thus producing an image that has been rectified in the spatial dimension. (Quantization effects are removed by taking the appropriate fractions of subpixels at the edges of the new pixel boundaries.)

Wavelet interpolation has been implemented in the **stistools** task **wx2d** (STIS ISR 2007-04). The task takes an `_flt`, `_sfl`, or `_crj` image as input and produces an array that has been rectified in the spatial direction and, optionally, a corresponding array of wavelengths. (As for input to **x2d**, the input image should already have `SHIFTA1` and `SHIFTA2` populated by the **stistools** task **wavecal**.) The user can select the order of the polynomial used to fit the flux profile, the number of subpixels to create, and the range of rows in the image to be processed. Convolution with a model PSF can be performed; this reduces the magnitude of the artifacts at the expense of resolution along the slit. The task optionally outputs the subpixelated image, with and/or without convolution. The interpolated image can be processed by **x2d** to linearize wavelengths and provide flux calibration. **X2d** automatically turns off interpolation along columns for a **wx2d** image, signified by `WX2DCORR= 'COMPLETE'`.

5.4.4 Combining Undithered Spectral Images

A set of undithered flat-fielded spectral images can easily be combined in the usual ways (outlined below) if the images are well aligned. This will be the case if the optical path has not changed appreciably and if the target has not drifted due to errors in tracking or reacquisition. The optical path is generally very stable once the grating has been positioned, and a series of science exposures is usually taken without repositioning the grating. Nearly all spectral images have associated wavecals, which were taken with the same grating positioning. To determine shifts in the optical path, `calstis` or its constituent task **stistools** task **wavecal** measures the positioning of the wavecal image(s) on the detector and computes the values `SHIFTA1` and `SHIFTA2` (shifts from the nominal x, y positions) as described in [Section 3.4.23](#). You can check the values for the corresponding header keywords `SHIFTA1` and `SHIFTA2` to see if the changes are small for the series of `_flt` images that you want to combine.

To check for target drift, you should first check whether the exposures were made in single guide star mode, as discussed in [Section 5.2.6](#). If so, the roll angle of the telescope will be less well controlled, and drift may be significant for long exposures or exposures with large time separations. Even if two guide stars are used, target drift can build up over many orbits to a significant fraction of the aperture width unless a new ACQ/PEAK was performed. To check for drift, you can use any method that compares the wavelength scale or position along the slit. For example, for MAMA exposures that include a point source, you can check the values of `A2CENTER` ([Section 3.4.24](#)) in the `_x1d` table extensions to look for drift along the slit in excess of the optical path shift measured by `SHIFTA2`. For CCD images, you can check whether **ocrreject** systematically rejected long strings of pixels along a row in a `_flt` image because

a shift along the slit caused a mismatch in flux ([Section 3.5.4](#)). If there is a mismatch, you will need to measure the shift along the slit with a method that gives robust results for images that are undersampled in the spatial direction and that have not been cleaned of cosmic rays. e.g., you can run the **stistools** task **mktrace** on the `_flt` images to look for differences in the reported central row. For either detector, you can use a spectral modelling routine such as **SpecViz** to look for differences in the central wavelengths of spectral features in individual `_x1d` images or rows of `_x2d` images. A shift in wavelength can be converted to a shift in pixels using the dispersion relation.

If you find measurable misalignments of the individual exposures that you want to combine, you will need to decide how much misalignment is acceptable in your final data products. If the resulting degradation in spatial and spectral resolution is insignificant, you can combine the `_flt` images in the usual ways with appropriate consideration of cleaning/masking (bad pixels, cosmic rays) and weighting the individual images and generation of a suitable error array for the combined image:

1. For associated images, one can use **calstis** (if the default parameters are acceptable)
2. For MAMA images, one can use either the **IRAF msartih** and **mstools** or the basic array manipulation capabilities of **Python numpy** and **astropy.io.fits**.
3. For CCD images, one can use the **stistools** task **ocrreject**, relaxing the rejection parameters to accommodate the misalignment ([Section 3.5.4](#)).

If the misalignment of the `_flt` exposures is unacceptable, you can combine individual `_x2d` images instead. If the misalignment is due primarily to shifts in the optical path, you can simply average the default `_x2d` images, since those images have all been shifted to the nominal position. For example, generate an individual `_x2d` file for each CCD `_flt` imset, or split a MAMA `_x2d` file into imsets with **astropy.io.fits**. Then combine the individual `_x2d` images, using the capabilities of **Python numpy** or **astropy.io.fits**, masking, cleaning, and weighting as necessary. If there is substantial target drift, you will need to adjust `SHIFTA1` and `SHIFTA2` in the `_flt` data extension headers ([Section 2.3.1](#)) to include the increments due to the drift. If the target has drifted too close to the edge of the slit in an exposure, the flux will not be properly corrected for slit losses, and you may choose to reject that exposure.

5.4.5 Combining Dithered Spectral Images

Dithering by a few pixels along Y (the spatial dimension in a spectroscopic image) is recommended to allow removal of hot pixels when CCD images are combined. To prepare dithered images for combination, first perform bias, flat, and dark correction of the raw images with the **stistools** task **basic2d** to produce

_flt images. Some of the _flt images must then be shifted up or down to align them with each other. This shifting can be accomplished with the **stistools** task **sshift** task. The cosmic ray rejection routine **ocrreject** can be applied to the set of shifted images to combine them into a _crj image. Hot pixels will be rejected along with the cosmic rays. The _crj images can then be reduced in the usual way applying **calstis** or its components. See [Section 3.5.4](#) for a discussion of the use of this task in the broader context of improving cosmic ray rejection. If the shifted _flt images are not well aligned, they should be handled like the _flt images in [Section 5.4.4](#).

5.4.6 Producing Rectified Spectral Images for Long-Slit Echelle Data

An entire input echelle image cannot be 2-D rectified all at once because the dispersion relation is different for each spectral order. The **stistools** task **x2d** task is thus not normally run by the STScI pipeline on echelle data, and users do not get an _x2d file as a normal data product. Nonetheless, this task can be used (with care) on echelle spectra. In this case, **x2d** will generate a single output FITS file with a 2-D image set (imset) for each spectral order in the input _flt file – i.e., each order is corrected and written separately.

Several problems may arise in the 2-D rectification of long-slit echelle spectra with the **x2d** task. One problem is that, e.g., while the 6X0.2 slit is so long that it overlaps several spectral orders, the height of the output images is small enough that they cover only one spectral order per image. If the feature the user is interested in is, say, at 50 pixels from the center in the cross-dispersion direction, but the output _x2d images are only 71 pixels high, the features will not fall within the output image (though it might appear in an image for a different spectral order). A work around for this problem is to edit the SDCTAB and change the values in the NPIX2 and CRPIX2 columns for the OPT_ELEM and CENWAVE that were used for the observation. More than one row may need to be changed, depending on which spectral orders (SPORDER) contain data for which a full slit length should be corrected. Set NPIX2 to a large enough value to cover as much of the slit as you need, and set CRPIX2 to $(NPIX2 + 1) / 2$ to center the spectrum.

For the 2-D rectification of long-slit echelle spectra there are two possible sources of tilt error. The first is the "physical" tilt, due to the fact that the slit is rotated by a small angle from its nominal orientation. The slits are mounted in the aperture wheel, and the nominal orientation is that the slit be perpendicular to the line from the center of the slit to the center of the aperture wheel. This physical tilt from the nominal orientation is a fraction of a degree for most apertures; it is stored in the ANGLE column in the aperture description table (APDESTAB) for the aperture in use. The second source of tilt error is due to an optical

distortion, in which the slit image on the detector is curved and tilted. For first order data this "slit to detector" tilt appears to be quite small, but for echelle data it is much larger than the physical tilt and can be several degrees. It depends strongly on the particular echelle grating in use and varies across the detector. While this has not been thoroughly investigated, it looks as if the tilt of the slit images changes systematically across the image in the sense that the slit images have a center of rotation well off the detector, i.e., lines drawn from the rotation point to the center of the slit images are perpendicular to the slit images, and the slit images are quasi-circular arcs. If this model is correct, it should be possible to measure the tilts of the bright emission lines in calibration data and predict the behavior of the tilt as a function of the position on the detector. However, not enough calibration data are available in the archive to do this for all locations on all gratings.

For echelle data, running the **stistools** task **x2d** with default parameters takes into account only the physical tilt, but not the optical distortion, for echelle data. For first order spectral data, the optical distortion is corrected for by the dispersion relation, which varies with the Y coordinate in the image. In the case of echelle data, the dispersion relation used in **calstis** and its components depends on spectral order but not on Y coordinate for a given order. Consequently, the spectral lines in the 2-D echelle output image will still be tilted with an angle that varies across the detector. One can use the following procedure to correct for the "slit to detector" tilt as well as the physical tilt of the slit in a long-slit echelle **_x2d** image. First, measure the tilt of strong lines in the **wavecal** in the neighborhood of the emission lines of interest in the science data (i.e., same spectral order and wavelength region). Enter the value of this tilt, expressed in degrees measured clockwise from the Y axis, into the parameter *angle* in the **wavecal** task parameter list and into the column **ANGLE** in the **APDESTAB** table in the row for that aperture. Run **wavecal** and then run **x2d**. Since a single value of the tilt is not representative of the entire image, regions with different tilts should be calibrated separately.

5.5 Working with Extracted Spectra

[5.5.1 Working With _x1d Files](#)

[5.5.2 Using the stistools Task x1d to Recalibrate Data](#)

[5.5.3 Splicing Extracted Spectra](#)

Here we discuss ways of customizing the extraction of spectra from `_flt`, `_sfl`, or `_crj` images. It is assumed that you have already performed any of the recommended recalibration described in [Section 3.5](#).

5.5.1 Working With _x1d Files

When used to calculate one-dimensional extracted spectra, the `calstis` pipeline and the `stistools` task `x1d` task puts the output into an `_x1d` file with a name like `“o5jj01010_x1d.fits”`. Note that when the input spectral image is a combination of multiple subexposures, such as a combined cosmic ray rejected image, the file name will contain the string `“sx1”` in place of `“x1d”`, e.g., `“o5ja06050_sx1.fits”`. When `x1d` is used as a standalone task, the default output file’s name will always end in `“_x1d.fits”`.

The `_x1d` file will be a multi-extension FITS file. As with other STIS data files, the primary [0] extension will contain only header information, but no data. The extracted spectra will be stored in the [SCI] extension(s). There will be one [SCI] extension in the `_x1d` file for each separate [SCI] extension in the input image. The science extensions of the `_x1d` file are multidimensional FITS tables. STIS spectra are stored as binary arrays in FITS table cells. [Section 2.3.2](#) discusses this format and describes the selectors syntax used to specify these data arrays. Each row of the table contains the extracted spectrum for a single spectral order. For first order spectra, there is only a single row.

Each row of each of the science extensions in an `_x1d` file will contain the columns listed in [Table 5.2](#); a similar table, including array dimensions, can be displayed by using the `astropy.table` (see [Section 5.1.2](#)). The `SPORDER` column lists the spectral order number. For first order spectra, this is of course always 1. The `NELEM` column lists the number of elements in each of the data arrays. This will most commonly be 1024, although it may be less in the case of CCD data binned along the dispersion direction, or more in the rare situations when the user opts not to bin MAMA high-res pixels down to the native pixel scale. The `WAVELENGTH` column will be an array of `NELEM` values giving the calibrated wavelength vector for the spectral extraction in units of Angstroms. The `GROSS` column gives the summed counts within the

extraction region for each pixel along the dispersion direction. The BACKGROUND gives the background vector that was found during the BACKCORR step of the processing, and NET=GROSS BACKGROUND.

The FLUX column is an array that gives the extracted flux for the point source spectrum. The units are erg /s/cm²Å. The ERROR array gives the propagated error vector, including Poisson noise, dark noise and readnoise, and includes the propagated error due to the noise in the background. It normally has the same units as the flux array; however, if for some reason, the FLUXCORR step of the processing did not run, the FLUX values will all be zero, and the ERROR array will be in units of counts/s rather than erg/s/cm²Å.

The A2CENTER value gives the row number in the y direction at which the spectral trace is centered. The EXTRLOCY column is an array that gives the location of the center of the spectral trace for each pixel along the dispersion direction. The BK1SIZE, BK2SIZE, BK1OFFST, and BK2OFFST columns give the sizes of the background extraction regions, and the amount by which the centers of the background regions were offset from the spectral trace. EXTRSIZE give the height of the extraction box in the cross dispersion direction. MAXSRCH gives the range that was allowed for the cross correlation search that located the spectral location, while OFFSET gives the difference between the starting position of the search and the A2CENTER value where the spectrum was actually found.

The nominal size of a pixel in the cross dispersion direction in units of arcsec can be found in the PLATESC keyword in the primary header of any STIS data file. For example, for the file o5jj01010_x1d.fits, typing the following command, will give the result 0.024600023:

```
>>> from astropy.io import fits
>>> hdu = fits.open("o5jj01010_x1d.fits")
>>> print(hdu[0].header['PLATESC'])
>>> hdu.close()
```

Note that the plate scale of a geometrically corrected output image is given in the SCALE column of the IDCTAB.

For most first order STIS modes, the plate scale in the dispersion direction is very close to that in the cross dispersion direction. The differences are largest for the medium resolution CCD first order modes. Results for these are detailed in [STIS ISR 98-23](#).

Table 5.2: Science Extension Binary Table Columns

| | | |
|--|--|--|
| | | |
|--|--|--|

| Column name | Format | Units |
|--------------------|---------------------|---------------------------------|
| SPORDER | short integer | dimensionless |
| NELEM | short integer | dimensionless |
| WAVELENGTH | double array | Angstroms |
| GROSS | real array | Counts/s |
| BACKGROUND | real array | Counts/s |
| NET | real array | Counts/s |
| FLUX | real array | erg/s/cm ² /Angstrom |
| ERROR | real array | erg/s/cm ² /Angstrom |
| DQ | short integer array | dimensionless |
| A2CENTER | real | pixel |
| EXTRSIZE | real | pixel |
| MAXSRCH | short integer | pixel |
| BK1SIZE | real | pixel |
| BK2SIZE | real | pixel |
| BK1OFFST | real | pixel |
| BK2OFFST | real | pixel |
| EXTRLOCY | real array | pixel |
| OFFSET | real | pixel |

When working with the `_x1d` files in the **Python** environment, it is important to be aware that the spectral data for a given column (e.g., wavelength) is contained in rows, even when the number of rows is only one, as it is for first order spectra. For example, the command `len(data['WAVELENGTH'])` returns 1 for first order spectra indicating the number of rows, whereas `len(data['WAVELENGTH'][0])` returns 1024 which is the length of the wavelength array for that row. Below is an example for plotting flux vs. wavelength for the first spectral order included in an `_x1d` file with commonly used **Python** libraries.

```
>>> from astropy.io import fits
>>> from matplotlib import pyplot as plt

# Grab data from the science extension of a fits file
>>> hdulist = fits.open('obc410010_x1d.fits')
>>> sci_data = hdulist['SCI'].data

# For an x1d file, extract the wavelength and flux separately using keywords
>>> wavelength = sci_data['Wavelength'][0]
>>> flux = sci_data['Flux'][0]

# Plot Wavelength vs Flux
>>> plt.plot(wavelength,flux)

>>> hdulist.close
```

The following example shows one way of plotting flux vs. wavelength for an echelle spectrum in an `_x1d` file:

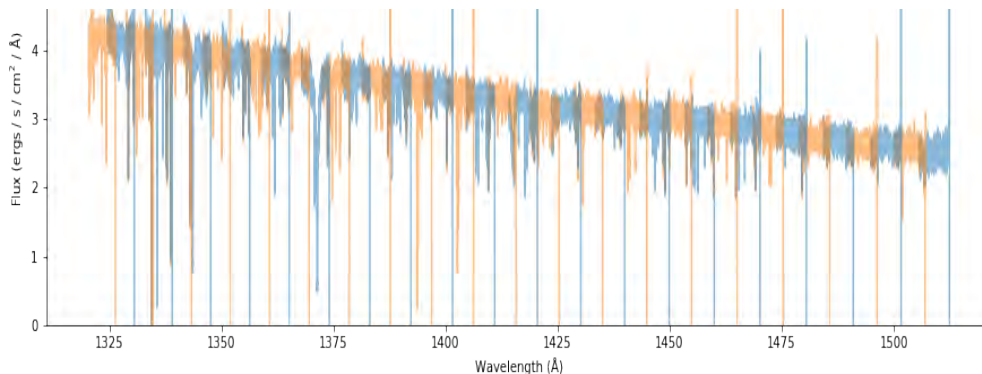
```
>>> from astropy.io import fits
>>> from matplotlib import pyplot as plt

>>> d = fits.getdata('odpce4050_x1d.fits', ext=1)

>>> fig, ax = plt.subplots(1,1)
>>> fig.set_size_inches(15,5)

>>> for i, order in enumerate(d):
    ax.plot(order['WAVELENGTH'], order['FLUX'], alpha=0.5, color='C{}'.format(i % 2))
    ax.set_xlabel('Wavelength (Å)')
    ax.set_ylabel('Flux (ergs / s / cm$^{2}$ / Å)')
    ax.set_ylim(0, 0.6e-10)
```





5.5.2 Using the `stistools` Task `x1d` to Recalibrate Data

The `stistools` task `x1d` is designed to extract flux calibrated 1-D spectra from unrectified STIS spectral images (`_flt`, `_crj`, or `_sfl` files). It serves as a front end to the `calstis6` routine used in pipeline extraction. The original implementation of this code and the algorithms used are described in [STIS ISR 99-03](#).

The `x1d` task is not intended for use with rectified files (`_x2d` or `_sx2` files), or files that have been processed by the `wx2d` task. It can be used for either echelle or first order STIS spectra; `x1d` will extract a single spectrum when used with first order spectral images and a spectrum for each order when used with echelle spectral data. This task is called by `calstis` as part of standard pipeline processing; its functioning in that role is described in [Section 3.4.24](#).

Users should remember that the default parameters for the `x1d` task will not always match the default calibration flags set in the header keywords. When running `x1d` as a stand alone task, the task parameters will control which options execute, while when running `calstis`, the header keywords will control which steps execute. This may result in different results when using the same file as input for `x1d` vs. `calstis`. For example, STIS echelle files retrieved from the OTFR pipeline have `SC2DCORR` set to 'PERFORM', but the `x1d` default of `algorithm = unweighted` is equivalent to setting `SC2DCORR` to 'OMIT'. It would be necessary to set `algorithm = sc2d` in `stistools.x1d` to reproduce the pipeline default.

The `x1d` task can be run to recalibrate spectra by using the following command:

```
>>> from stistools import x1d
>>> x1d.x1d('o5ja03030_flt.fits')
```

The output spectrum will be written in the file "o5ja03030_x1d.fits". For echelle data, the user will usually want to set the *algorithm* parameter of the **x1d** task to *sc2d* to select the deconvolution algorithm for computing and subtracting scattered light in echelle observations. Recall that **calstis** instead uses the value of the keyword SC2DCORR (PERFORM or OMIT) to turn the scattered light correction on or off. (see [Section 3.4.20.](#))

We will not attempt to describe all of the options of the **x1d** task here. Instead we will concentrate on the options that users are likely to want to adjust to customize the extraction of their data.

Correcting for Shifts Along the Dispersion Direction

Properly aligning the spectrum along the dispersion direction is important not only for obtaining the correct wavelength solution, but also for properly applying the flux calibration. Incorrect registration of the spectrum will result in the wrong sensitivity being applied at each wavelength. This is especially important for low resolution & echelle spectra, for which the sensitivity changes rapidly with wavelength.

Auto-wavecal exposures are generally used to determine the location of both the wavecal image and the corresponding science image on the detector. The location varies somewhat because of non-repeatability of the STIS grating positions and flexures of the STIS optical bench. Science exposures and their auto-wavecals are taken close in time and without intervening changes in the grating position to keep them at approximately the same location. If either an auto-wavecal or a user-inserted wavecal has been taken, the **stistools** task **wavecal** should be run to measure the shifts in the wavecal spectrum. This populates the SHIFTA1 and SHIFTA2 keywords in each SCI extension header of the science image. The **x1d** task then takes these shifts into account when calculating the dispersion relation. If there is no wavecal exposure, or if the shift calculated from the wavecal has not been applied, the spectrum may be offset in wavelength by as much as several pixels.

Shifts of the spectrum along the dispersion direction can result from spatial offsets of the target from the center line of the aperture, repositioning the grating, and thermal flexures. Users can change the adopted shift along the dispersion direction by either editing the value of the SHIFTA1 keyword in the SCI extension of the file used as input to the **x1d** task, or by using the *xoffset* parameter in the **x1d** task to add an additional shift. Increasing the SHIFTA1 value or specifying a positive value for the *xoffset* parameter, will result in a smaller wavelength value being assigned to each pixel. Applying a positive correction will cause the spectrum plotted as a function of wavelength to shift to the left. So if the target is

offset by two pixels to the right of the aperture center line, then specifying *xoffset=2* would correct for this offset, i.e.,

```
>>> from stistools import x1d
>>> x1d.x1d('o5ja03030flt.fits')
```

Note that when using a non-zero *xoffset* parameter, the value of the `SHIFTA1` keyword in the output table is not changed, although a text message is printed to standard output, and placed in a `HISTORY` keyword in the primary header of the output `x1d` file. e.g., “Offset of 10 low-res pixels added in dispersion direction”. `SHIFTA1` and *xoffset* are always specified in units of unbinned pixels for the STIS CCD, and low-res pixels for the MAMA detectors.

Locating the Spectrum in the Cross-Dispersion (Spatial) Direction

The default procedure for finding the location in the cross-dispersion direction at which a spectrum will be extracted is described in the “locate the spectrum” part of [Section 3.4.24](#). Normally this procedure will correctly locate the brightest spectrum in the desired search range. However, occasionally this cross-correlation procedure will find a noise spike instead of the true spectrum, or the true spectrum may be faint enough that the cross correlation does not find it. In addition, some first order spectral images may contain point-source spectra of multiple objects; the default cross correlation will only find the brightest one. Also, for echelle data the spectrum of the wrong order can be extracted if multiple orders end up falling within the search region of a given order. The region searched for a spectrum can be controlled by using the *a2center* and *maxsrch* parameters of the **x1d** task. When both these parameters are specified, the cross-correlation search will extend from row *a2centermaxsrch* to row *a2center+maxsrch*. If *maxsrch* is set to zero, the cross correlation will be turned off and a spectral extraction will be done at *a2center*. In the case of echelle spectral images, it is also possible to extract a single order at a time. In this case, it is possible to control the order that will be extracted at a certain position by using the *sporder* parameter together with the *a2center* and *maxsrch* parameters.

If several individual first order spectra are to be extracted from a single long slit STIS image, the **x1d** task should be run once for each extraction, with *a2center* set each time to approximately the mean row at which that spectrum appears, and *maxsrch* set to a value that is large enough to allow the cross-correlation algorithm to find the best centroid but small enough that the algorithm does not find the wrong spectrum. If individual targets are also offset from the aperture center in the dispersion direction, it will be useful to

specify the appropriate *xoffset* values to obtain the correct dispersion relations. A different output file name should also be specified for each extraction. For example to extract the spectra of two closely spaced stars, one might do:

```
>>> from stistools import x1d
>>> x1d.x1d('o5ja06030flt.fits', output='ngc6681_e.fits', xoffset=12.43, a2center=424.5, maxsrch=3)
>>> x1d.x1d('o5ja06030flt.fits', output='ngc6681_f.fits', xoffset=16.16, a2center=436.2, maxsrch=3)
```

Changing the Default Extraction Box Height

For each pixel in the dispersion direction, **calstis** sums the values over the height of the spectral extraction box. Each endpoint of the extraction box may include a fractional part of a pixel; **calstis** scales the counts in the given pixel by the fraction of the pixel extracted. The default full height of the extraction box is taken from the EXTRSIZE column of the XTRACTAB table. For CCD first order spectra and echelle spectra, this default height is 7 pixels, while for MAMA first order and PRISM spectra, the default height is 11 pixels. This default value can be overridden by specifying a value for the extrsize parameter of the **x1d** task.

The default extraction box heights were chosen so that roughly 85% of the total flux at a given wavelength is contained in the default extraction box. For observations of point source targets with good signal-to-noise, there will normally be little reason to change these default values. However, for very faint spectra, the signal-to-noise may sometimes be improved by using a smaller extraction box that includes less background noise. Similarly, when working with first order spectral images of a crowded field, a smaller than default extraction box might be needed to minimize contamination from adjacent sources. If the total flux of an extended object is being measured, it may be desirable to use an *extrsize* larger than the default, in order to include flux from the entire object.

There are some issues the user should take into account when using a non-standard extraction box height:

1. STIS CCD spectral modes are significantly undersampled in the spatial direction. This, combined with the tilt of the spectral trace on the detector, can lead to substantial undulations of the extracted spectrum if a single row is extracted. The undulations are out of phase from one row to the next, so they become increasingly insignificant as more rows are combined in the extraction. (See [Section 5.4.3](#).)
2. Throughputs for each mode are based on measurements made using the standard extraction box height and a standard aperture (52X2 for first order modes and 0.2X0.2 for echelle modes) for each

mode. Fluxes derived for different apertures or extraction box heights also depend on the accuracy of the PCTAB and aperture throughput corrections.

- When converting from counts/s in the extraction box to total point source flux, a correction for the fraction of encircled energy in the extraction box at each wavelength is applied using information tabulated in the PCTAB. This correction depends on the grating, the aperture, and the central wavelength. However, for each grating, there are values in the PCTAB for only selected extraction box sizes. If the selected *extrsize* does not match one of these pre-tabulated values, the correction that most nearly matches the specified *extrsize* is applied; no attempt is made to interpolate the PCTAB correction to an intermediate extraction box size. It is therefore best to only choose extraction box sizes that match the pre-tabulated correction vectors in the PCTAB. For all gratings, PCTAB vectors are supplied for the eight extraction height values of 3, 5, 7, 9, 11, 15, 21, and 600 pixels, where the 600 pixel high extraction box is intended to represent the estimated “infinite aperture” encircled energy. For most gratings, an additional *ninth* PCTAB row is included, the height of which depends on the grating (see [Table 5.3](#) and [STIS ISR 98-01](#)). These second-largest extraction boxes contain 99% of the signal and in some instances provide a more robust estimate of the total signal. Note that these encircled energy fractions were, for the most part, measured using only low dispersion spectra, which were then used to estimate the corrections for other modes.

Table 5.3: 9th PCTAB Row Extraction Box Size

| Grating | Extraction Box Height |
|----------------------------------|-----------------------|
| FUV MAMA modes | 140 |
| NUV MAMA modes (except PRISM) | 110 |
| G230LB/MB | 80 |
| G430L/M | 64 |
| G750L/M | 200 |

- The spectral purity declines significantly at increasing distances from the central trace of the spectrum. Using a larger than standard extraction box may therefore significantly degrade the spectral resolution.

5. The observed flux is corrected to the total flux assuming that all of the observed flux originates in a point source. If the aperture width and/or the extraction box height are large enough to include a significant amount of extended flux after background subtraction, the correction will be inaccurate.

Adjusting the Background Subtraction

For first order spectra, two background regions offset from the extraction region are used to determine the background. A number of the parameters defining the way the background is derived can be adjusted by changing parameters of the **x1d** task. Note that for echelle data, when the background subtraction is done using the *sd2c* scattered light correction algorithm, most of these parameters do not affect the final background (see [Section 3.4.20](#)).

Changing the Background Smoothing Algorithm

The algorithm used for smoothing the background can be changed by adjusting the *bksmode* and *bksorder* parameters. The default value for the *bksorder* parameter is 3. Allowed values for *bksmode* are *median* (the default), *average*, and *off*. If set to *off*, no smoothing takes place. If set to either *median* or *average*, then background smoothing will be done. The detailed behavior depends on the mode for which the background smoothing is being done:

- For CCD data, the raw background, after 1-D extraction, is smoothed by a running window low-pass filter (i.e. boxcar smoothing) with a 9 pixel window, then fitted by an *n*th degree polynomial. The value of the *bksmode* parameter defines the boxcar smoothing function to be either a *median* or *average* within the running window. The polynomial degree is defined by the *bksorder* task parameter. The default value for the *bksorder* parameter is 3.
- For MAMA first order data, the 1-D extracted background is fitted by an *n*th degree polynomial, and the background is replaced by the fitted curve. The data is not filtered before the polynomial fit, and so for MAMA first order data, the result is the same whether *bksmode* is set to *median* or *average*. The polynomial degree is defined by the *bksorder* task parameter. For the G140L/M first order gratings, the regions around Lyman and the 1300 Angstrom O I line are not smoothed.
- For MAMA echelle when *SC2DCORR* is set to *OMIT*, the 1-D extracted background is smoothed twice by a running average with a 31 pixel window. This is equivalent to smoothing with a triangular filter.

Changing the Default Background Regions

The details of how the background regions are specified are described in [Section 3.4.2](#). Two background regions are offset by amounts that are tabulated in the 1-D extraction table. This file also specifies the angle by which regions of constant wavelength are shifted as a function of offset. These values can be changed by adjusting parameters of the **x1d** task. The *bk1size* and *bk2size* parameters give the width of each background region, *bk1offst* and *bk2offst* give the offset from the center of the extraction region, and the *bktilt* parameter specifies the angle by which the background region at a given wavelength is offset. Leaving any of these parameters at the default *INDEF* value will cause the task to use the appropriate defaults from the 1-D extraction table. Note that users should rarely if ever have a reason to change the *bktilt* parameter.

Changing the Interpolation of the Background Values

The default of *backord=0* which is implemented in the XTRACTAB for all modes, averages the values measured in the two background regions at each wavelength. In some cases, (e.g., other objects or detector artifacts contaminate one or both background regions), it might be desirable to chose asymmetrical offsets for the two background regions (*bk1offst* *bk2offst*). Setting *backord=1* would then interpolate between those two regions rather than taking a simple average. However, if both background regions were offset in the same direction, (this is the default for the E1 and E2 aperture positions where *bk1offst=-300* and *bk2offst=-320*), setting *backord=1* would extrapolate the measured values. In such a case it may usually be better to leave *backord=0*, and just average the two regions.

TDS, CTE, and BZS Corrections

The FLUXCORR step, which converts net counts to flux units, now includes three additional corrections not envisaged in the original version of **x1d**. These are the corrections for time and temperature dependent sensitivity (TDS) changes applied to all spectroscopic modes, the correction for charge transfer efficiency (CTE) losses applied to CCD spectroscopic observations, and the blaze shift (BZS) correction applied to echelle spectroscopic data.

The TDS correction is calculated as a function of wavelength using coefficients taken from the TDSTAB. There is no flag for turning off the TDS correction, although if the TDSTAB keyword in the dataset header is set to a null value, the TDS correction will be skipped.

For the CTE correction, there is a parameter of the **x1d** task, *ctecorr*, which can be used to turn the CTE correction on or off. Note that the empirical CTE correction is not valid for data taken using sub-arrays, and so the correction is turned off by default for data processed with the full **calstis** pipeline, although it will be turned on by default when running **x1d** as a stand-alone task.

The CTE algorithm used for correcting STIS CCD spectra is described in [STIS ISR 2006-01](#), [STIS ISR 2006-03](#), as well as in the paper Goudfrooij et al. (2006, PASP, 118,1455). The BZS correction is calculated as a function of grating, order, and side of STIS operations (Side-1 or Side-2). It is based on the values of SHIFTA1 and SHIFTA2, as well as the day of observation as expressed in Modified Julian Days (MJD). Coefficients taken from the PHOTTAB are used for this purpose. There is no flag for turning off the BZS correction. However, **x1d** can be run with the value of the *blazesh* parameter equal to zero in order to skip this correction. In addition, the BZS correction can be customized (and the default BZS correction value applied can be overwritten) by setting *blazesh* to a certain number of pixels when running **x1d** as a stand-alone task. Only one value of *blazesh* can be specified at one time. In this case, all extracted orders will have the same BZS correction applied. We recommend the extraction of a single order at a time if a different value of *blazesh* is desired for every echelle spectral order.

5.5.3 Splicing Extracted Spectra

Users wishing to combine multiple spectra together to create a single one-dimensional spectrum (e.g., combining first-order spectra from observations using different gratings or combining echelle orders from a single observation) may do so with the **IRAF** task **splice**. Such task currently does not exist in **Python**, but work is being done to create a task similar to **IRAF splice**.

The task **splice** can be applied to both first order and echelle data. It takes into account the error (ERR) array as well as the data quality (DQ) array. Handling of the DQ array is important as it helps **splice** perform the combination properly and avoid bad or noisy data in the output file arising from the large changes in throughput at the edges of the detector. In order to use **splice** correctly, one has to manually mark these edges in the DQ array as “bad pixels” and tell **splice** to ignore these by setting the *sdqflags* parameter to the appropriate value (refer to [Table 2.9](#) for the data quality values). A flag value of 4 or 8 will work fine. The reason this does not work by default in **splice** at the moment is that the vignetted regions of the MAMA detectors change over time, and new bad pixel maps showing these regions as a function of time have not been produced. So at the moment, users need to modify the DQ arrays

themselves. A simple way to do this is to edit the DQ array in the `_flt` image, flagging the edges as bad pixels, then re-extracting the 1-D spectrum using the `x1d` task in the `stis` package. For example, to set a 10-pixel border to a value of 4 (“bad detector pixel”) in the 1024×1024 image:

```
>>> import numpy as np
>>> from astropy.io import fits

>>> hdu = fits.open('obmj01050_crj.fits') # Pick your file
>>> dqdata = hdu['DQ',1].data # Pick your header layer

# Set a 10-pixel border to a value of 4
>>> dqdata[:10,:] = dqdata[-10:,:] = dqdata[:,10] = dqdata[:, -10:] = 4

# To save these changes in a new fits file
>>> hdu.writeto('temp_nsp.fits', overwrite=True)
>>> hdu.close
```

```
cl> imcalc o4qx04010_flt.fits[dq,1] o4qx04010_flt.fits[dq,1] \
"if x <= 10 || x >= (1024-10) || y <= 10 || y >= (1024-10) then 4 else im1"
```

Users are encouraged to visually compare the 2-D science spectrum and the DQ arrays to determine the optimal size of the order for other data. Once you have followed the steps above, you can rerun `x1d` on the `_flt` file and get a new `_x1d` spectrum, which will have the updated DQ values. Then you can run `splice`, specifying that you want to ignore those vignetted regions that you just marked with DQ values when you do the splicing together of the spectrum, i.e., by making sure the `sdqflags` parameter in the `splice` task is set to an appropriate value.

```
cl> splice obs1_x1d.fits,obs2_x1d.fits output_splice.fits sdqflags=4
```

Splice will then only use data that has not been marked by the specified DQ flags when splicing together the spectrum. Please refer to the `splice` task help file for more useful information.

5.6 Working with TIME-TAG Data

[5.6.1 Heliocentric and Barycentric Time Correction](#)

[5.6.2 Converting TIME-TAG Data to an Image](#)

[5.6.3 Echelle TIME-TAG Data](#)

STIS MAMA detectors can be used in ACCUM or TIME-TAG modes, as described in [Chapter 11](#) of the *STIS Instrument Handbook*. In TIME-TAG mode, the position and detection time of every photon is recorded in an event list. Detection times are recorded with 125 microsecond precision, although events from bright sources may be buffered for as long as 128 milliseconds prior to assignment of a detection time.

For TIME-TAG datasets, the *HST* archive returns all normal data products and also an event list in a file with a `_tag` suffix. The `_tag` file is a FITS file with two binary table extensions. The first FITS extension is a binary table named EVENTS, and contains four columns named TIME, AXIS1, AXIS2, and DETAXIS1. The last FITS extension is a binary table named GTI (good time intervals), and indicates time intervals when events could have been detected.

An event list in a `_tag` file is a FITS binary table extension named EVENTS, containing four columns named TIME, AXIS1, AXIS2, and DETAXIS1.

The TIME column in the EVENTS extension of a `_tag` file contains the time when each event was recorded, relative to the start time (MJD) of the exposure given in the `TEXPSTRT` keyword of the primary FITS header. Each relative time is stored as an integer number of 125 microsecond hardware clock ticks, but application of the column SCALE FACTOR converts relative times to seconds. Application of the column SCALE FACTOR is automatic when using **astropy.table** task to read `_tag` files.

The AXIS1 column in the EVENTS extension of a `_tag` file contains the pixel coordinate along the spectral axis where each event was recorded plus a correction term to remove Doppler shifts introduced by the orbital motion of *HST*. The correction term depends on optical element and the projected orbital velocity of *HST*, which varies over the course of an observation. In ACCUM mode, this Doppler compensation is applied during an observation, but in TIME-TAG mode raw positions are downlinked and Doppler compensation is applied during ground processing.

The `AXIS2` column in the `EVENTS` extension of a `_tag` file contains the pixel coordinate along the spatial or cross-dispersion axis. No Doppler compensation is applied.

The `DETAXIS1` column in the `EVENTS` extension of a `_tag` file contains the pixel coordinate along the spectral axis where each event was recorded with no correction for Doppler shifts introduced by the orbital motion of *HST*. In general, `AXIS1` coordinates are the ones users will more likely use than `DETAXIS1` coordinates.

After all `EVENTS` extensions in a `_tag` file, there will be one final binary table extension named `GTI`, containing columns named `START` and `STOP`. There will be associated start and stop times for every uninterrupted observing interval during a planned exposure. For most datasets, there will be only one `START` and one `STOP` time encompassing all buffer dumps in an exposure. Multiple good time intervals are possible, however - for example, if guide star lock is lost. Times in `START` and `STOP` are expressed in seconds since the start time (MJD) of the exposure given in the `TEXPSTRT` keyword of the primary FITS header. Good time intervals can be examined as follows, where `rootname` must be replaced by the root name of the `_tag` file being examined:

```
>>> from astropy.table import Table
>>> ex_table = Table.read('rootname_tag.fits', hdu='GTI')
>>> print(ex_table)
```

5.6.1 Heliocentric and Barycentric Time Correction

`TIME-TAG` observations with `STIS` have a temporal resolution of 125 microseconds. The effects on the observed times of both the orbital motion of the Earth and the *HST* may need to be corrected relative to the solar system barycenter. The **IRAF `odelaytime`** task creates a file of observation time events corrected for light delay from three sources: 1) general relativistic effects (up to 2 milliseconds), 2) displacement of the telescope from the center of the Earth (up to 20 milliseconds), and 3) displacement of the Earth from the solar system barycenter (up to 500 sec). The inputs to **`odelaytime`** are the `TIME-TAG` data and the ephemeris files. For details regarding the **`odelaytime`** task and parameters, the reader is referred to [STIS ISR 2000-02](#).

To find and retrieve the orbital ephemeris file(s) required for the `odelaytime` task, visit http://www.stsci.edu/~STIS/monitors/ephemeris_files.html and follow the instructions.

5.6.2 Converting TIME-TAG Data to an Image

The `stistools` task `inttag` was developed to convert the TIME-TAG table (EVENTS tables) into one or more sub-exposures using a user specified time increment. The result is similar to the ACCUM mode data. The default start time here is the first value in the GTI table. The time increment value can be adjusted so that each sub-exposure has reasonable signal-to-noise. Details regarding the `inttag` task and its parameters can be found at <https://stistools.readthedocs.io/en/latest/inttag.html>.

5.6.3 Echelle TIME-TAG Data

STIS echelle TIME-TAG data that are converted to images and calibrated, will require longer processing and calibration time because they consist of many orders, especially if multiple sub-exposures are created with `inttag`. After converting the TIME-TAG data into an image and calibrating it, one can be used to extract wavelength dependent data for a single order from the `_x1d` file as shown in the example below:

```
>>> from astropy.table import Table
>>> from astropy.io import fits

>>> hdu = fits.open('o57904050_x1d.fits')
>>> sci_data = hdu['SCI'].data

>>> order_mask = sci_data['SPORDER'] == 116
>>> columns = ['WAVELENGTH', 'FLUX']
>>> order_column_data = [sci_data[column][order_mask][0] for column in columns]
>>> order_table = Table(order_column_data, names=columns)
>>> order_table.pprint()

>>> hdu.close()
```

5.6.4 Further TIME-TAG Data Analyses

Users who wish to further analyze TIME-TAG data are encouraged to consult the [STIS ISR 2000-02](#). This ISR provides instructions on how to carry out various tasks such as converting TIME-TAG FITS data into a different format (QPOE) for timing analysis, merging separate event tables into a single table, and performing Doppler and spatial resolution corrections. We note, however, that the **IRAF** tools discussed in [STIS ISR 2000-02](#) will soon be deprecated and not supported by STScI.